



The
University
Of
Sheffield.

The behaviour of clay surrounding pile foundation heat exchangers

By:

Nicola Lazenby

A thesis submitted in partial fulfilment of the requirements for the degree of
Doctor of Philosophy

The University of Sheffield
Faculty of Engineering
Department of Civil and Structural Engineering

31st October 2017

Contents

1	Introduction	8
1.1	Pile foundation heat exchangers	8
1.2	Low carbon heating and cooling	9
1.3	Temperature profiles	9
1.4	Construction	11
1.5	Research scope	11
1.6	Thesis organisation	12
2	Impact of pile foundation heat exchangers	14
2.1	Understanding clay microstructure	14
2.1.1	Clay microstructure at ambient temperature	15
2.1.2	Particle bonding at ambient temperature	17
2.1.3	Double layer theory at ambient temperature	19
2.1.4	Double layer theory at elevated temperatures	22
2.1.5	Behaviour of pore water with varying temperature	23
2.2	Microstructure effects on bulk behaviour at ambient temperature . .	24
2.2.1	Consolidation	25
2.2.2	Shear strength	27
2.3	Microstructure effects on bulk behaviour at elevated and cyclic tem- perature variations	29
2.3.1	Impact of elevated temperature on clay microstructure	30
2.3.2	Impact of cyclic temperature on clay microstructure	31

2.3.3	Plastic index	39
2.3.4	Over consolidation ratio (OCR)	40
2.4	Summary	42
2.5	Performance of pile foundation heat exchangers	43
2.6	Influence of elevated temperature on the Bulk Behaviour of Clay . . .	49
2.6.1	Volume change	49
2.6.2	Shear strength	54
2.7	Influence of cyclic temperature variation on the bulk behaviour of clay	56
2.7.1	Volume change	57
2.7.2	Plastic index	65
2.7.3	Overconsolidation ratio	67
3	Apparatus, materials and procedures	68
3.1	Triaxial apparatus	68
3.2	Heating system	69
3.3	Calibration	71
3.4	Clay properties	72
3.5	Sample preparation	72
3.6	Completed tests	73
3.7	Sample consolidation	74
4	Elevated Temperature Tests	82
4.1	Baseline testing	82
4.1.1	Heating stage	83
4.1.2	Stiffness	86
4.1.3	Critical state	88
4.1.4	Summary	89
4.2	Heating Stage	89
4.2.1	Kaolin	89
4.2.2	Durham clay	90

4.2.3	Comparison	91
4.3	Stiffness	92
4.3.1	Kaolin	92
4.3.2	Durham clay	93
4.3.3	Comparison	93
4.4	Critical state	94
4.4.1	Kaolin	94
4.4.2	Durham clay	95
4.4.3	Comparison	96
4.5	Summary of elevated temperature testing	97
5	Cyclic Temperature Variation Tests	98
5.1	Heating stage	98
5.1.1	Kaolin	99
5.1.2	Durham clay	100
5.1.3	Comparison	102
5.2	Stiffness	103
5.3	Critical state	104
5.3.1	Kaolin	104
5.3.2	Durham clay	105
5.3.3	Comparison	106
5.4	Summary	107
6	Understanding the Impact of Cyclic Temperature Variation	110
6.1	Summary of experimental results	110
6.1.1	Volumetric change	111
6.1.2	Critical state friction angle	112
6.1.3	Stiffness	113
6.2	Rationale from literature	113
6.2.1	Heating stage	114

6.2.2	Shearing stage	118
6.3	Proposed conceptual model	120
6.3.1	Heating stage	120
6.3.2	Cooling stage	121
6.3.3	Subsequent cycles	122
6.4	Application of conceptual model to experimental results	125
6.4.1	Volume change	125
6.4.2	Critical state friction angle	127
6.4.3	Stiffness	128
6.5	Application of conceptual model to literature results	129
6.5.1	Campanella & Mitchell (1968) - Volume change	129
6.5.2	Plum & Esrig (1969) - Lower void ratio with an increase in stress	132
6.5.3	Cekerevac et al. (2013) - Effect of overconsolidation ratio . . .	133
6.5.4	Bourne-Webb et al. (2009) - Field study	135
6.6	Summary of conceptual model	137
6.7	Application of conceptual model	142
7	Conclusion	144
7.1	Experimental study	144
7.2	Conceptual model	145
7.3	Application to PFHX design	146
7.4	Recommendations for future research	147
A	Test data	154
A.1	Overview	154
A.2	Triaxial data	154
A.3	Consolidation data	171
A.4	Back volume data during heating stage	174
A.5	Temperature data	180

Abstract

Pile foundation heat exchangers (PFHX) are increasing in popularity as an alternative to conventional air conditioning systems in large, commercial buildings. PFHX provide a sustainable means of building cooling and are compatible with the structure of pile foundations given the constant ground temperatures. However, increased understanding of the behaviour of clay subject to seasonal temperature cycles is required to ensure that PFHX can safely operate for the building's design life.

This study has developed a conceptual model for the microstructural behaviour of clay subjected to heating and cooling cycles. This conceptual model accounts for the effect of temperature on the clay particles, adsorbed double layer and pore water within the clay; identifying how this microstructural behaviour influences the bulk behaviour of the clay and therefore the observed response in the pile foundation.

The conceptual model has been supported through thermal triaxial experiments on kaolin and Durham clays. Testing considered the change in sample volume, critical state friction angle and stiffness of two varying plasticity clays. The model has been further strengthened in its application to existing pieces of similar literature for both experimental and field study findings.

This study concludes by providing an understanding of how this conceptual model applies to the real world response of PFHX installed in low and high plasticity clays, detailing the impact of the initial heating and cooling cycle on the longer term pile head displacement. These results support the use of PFHXs and recommend extending their temperature ranges to increase their efficiency without detrimental impact on the load bearing performance of the clay.

Chapter 1

Introduction

1.1 Pile foundation heat exchangers

Pile foundation heat exchangers (PFHX) are a fast growing technology which has the potential to significantly reduce the carbon emissions associated with space heating and cooling in new build non-domestic buildings, such as large commercial and public buildings. PFHX were first developed in Austria during the 1980's, however they are still a relatively new application for heat exchangers. Their long term effect on the structural integrity of the foundations which they are installed within is yet to be fully understood.

Non-domestic buildings have been found in a recent study conducted for the Department of Energy and Climate Change (now Department for Business, Energy and Industrial Strategy) to attribute 30% of their electricity demand to cooling. This exceeds performance benchmarks. It is now believed that the majority of non-domestic buildings have around 70-80% of their floor space cooled (Buildings Research Establishment 2016). This poses a great potential for PFHX and a need to understand the performance of PFHX with respect to clay's strength during operation.

1.2 Low carbon heating and cooling

By 2020 it is expected that around 40% of commercial floor space will be air-conditioned. This is at a time when the Energy Performance of Buildings Directive (EPBD) is influencing the UK building regulations, providing challenging targets for the conservation of fuel and power (Carbon Trust 2007). A change in refrigerant legislation is also forcing companies to look towards alternative cooling strategies (Evidence Directorate 2009).

PFHX use the ground surrounding the pile foundations as a source and sink for heat from within the building, shown in Figure 1.1. During winter, the PFHX source heat from the ground in order to provide heating whereas in the summer the ground is used as a sink for excess heat, thus providing cooling to the building.

This technology has proved popular in European Countries such as Austria, Sweden and the Netherlands with systems reporting that a single PFHX has the potential to deliver between 25 and 50 W/m depending on size, construction detail, and installed soil type (Amis & Loveridge 2014). Due to the relatively inexpensive price of gas, the take up of ground source heat pumps in the UK has lagged behind other countries, however this is expanding as energy prices increase along with planning incentives for lower carbon options. Figure 1.2 provides an overview of the increased market for PFHX in the UK and the associated carbon savings of these installations.

1.3 Temperature profiles

The temperature profile for PFHX used for predominately heating has been extensively studied within existing literature with a focus on preventing ground freezing (Brandl 2006). However, similar studies are yet to be conducted in determining the maximum sustainable ground temperature which can be applied during ground source cooling, as PFHX used as an alternative to air conditioning is a relative new area of research. Typical fluid temperatures associated with ground source heating

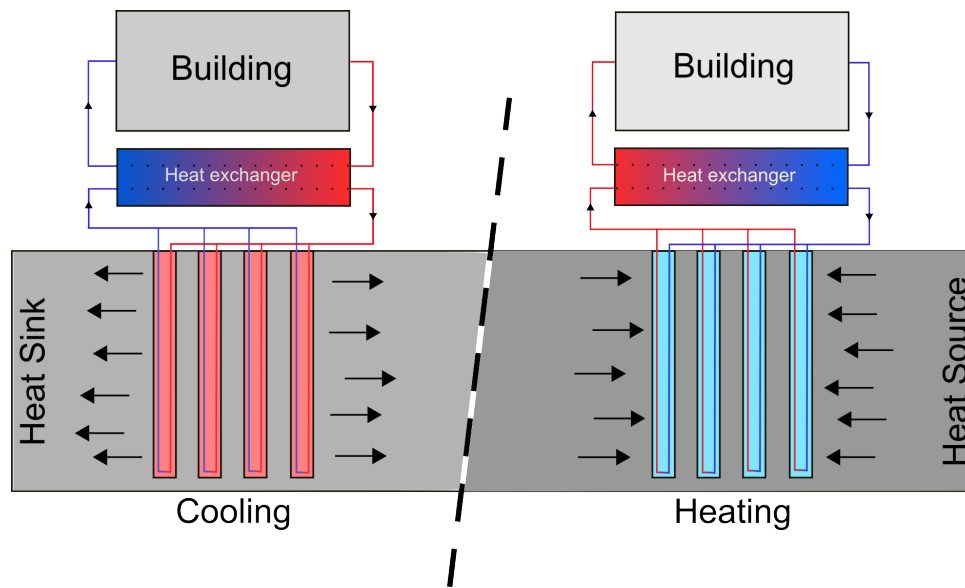


Figure 1.1: Schematic of Pile Foundation Heat Exchanger to provide heating and cooling.

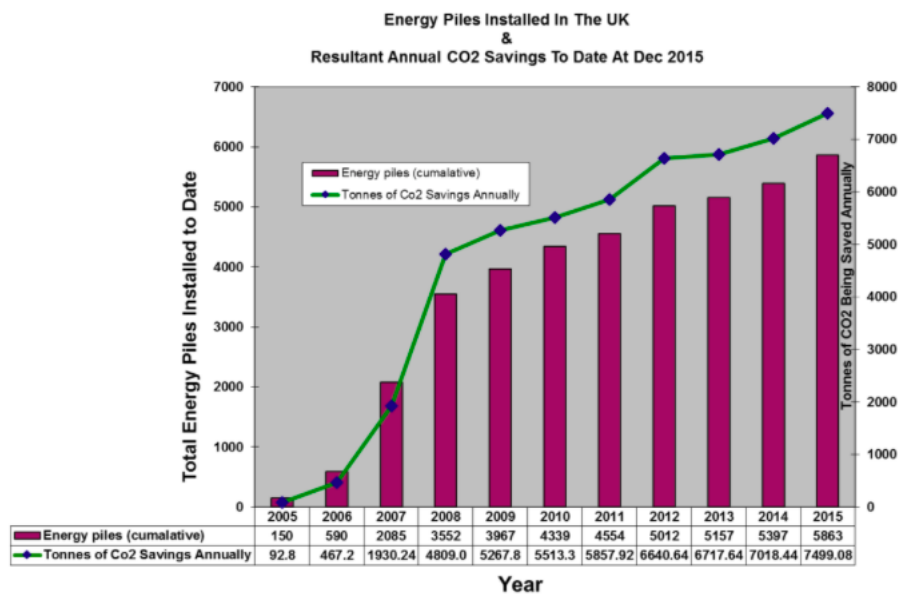


Figure 1.2: UK PFHX market and associated carbon savings (Amis & Loveridge (2014))

range from approximately 3 to 23 °C. The range of ground temperatures used in ground source cooling is typically limited to a maximum of around 30°C due to the lack of studies in this area leading industry to proceed with caution. It is yet to be truly understood how the long term effects of seasonal heating and cooling impact on the clay in which the PFHX are installed and any design considerations required as a result of this response.

1.4 Construction

In the UK, PFHX utilise the near constant ground temperature beyond 15 m in depth. Pile foundations are typically 30-50 m in depth, however they can reach a depth of up to 130 m for very large structures or where the ground is particularly weak. PFHX are most commonly bored, cast insitu foundations with a closed loop heat exchanger system tied to the reinforcement cage.

The requirements for cooling with a PFHX depend on the surface to volume ratio of the heat exchanger. Cooling requires a low surface to volume ratio so is therefore more effective in apartment blocks and offices. Cooling by PFHX may not be as efficient as free/passive cooling, however it may be 20-40 % more efficient than conventional air conditioning. It will become even more efficient if the extracted heat is stored for use in the winter or elsewhere (Banks 2008).

1.5 Research scope

For the PFHX applications cited above, it is increasingly important to develop a full understanding of the thermo-hydro-mechanical behaviour of the ground element of the ground to pile interaction. Extensive research has been conducted in relation to the effects of temperature on the concrete pile. This research will focus on the effect of temperature on the clay in which pile foundations are installed. In previous research in this field there has been limited studies on the bulk behaviour of the clay in which PFHX have been installed. The reason for this behaviour has being

overlooked by many authors, with focus being placed on the change in sample volume, the bulk behaviour of over consolidated clays and how temperature impacts the compression of samples during heating and cooling stages. This research aims to develop an understanding on the relationship between a clay's microstructural response to cyclic heating and cooling and how this is reflected in the bulk behaviour of the clay.

The main objectives of this thesis are:

1. Identify and draw together findings in current literature and produce a consistent theory on their observations with regards to the thermo-mechanics of the ground.
2. Develop and construct a temperature controlled triaxial cell whereby stresses and temperatures can be independently controlled.
3. To conduct an experimental study to identify the thermo-mechanical response of clays.
4. Understand how microstructural changes in clays influence their bulk behaviour.
5. Develop a conceptual model to identify how the microstructural behaviour of clay is reflected in observations of its bulk behaviour.
6. Draw together an understanding of these findings applicable to the PFHX industry

1.6 Thesis organisation

Current literature surrounding the thesis objectives is presented in Chapter 2, with a synthesis of both field studies and experimental work. This Chapter will identify current themes in theories and field observations, providing an overview of where work in this space has developed to date.

To study the effects of temperature on the behaviour of clay, a traditional tri-axial system has been developed in order to accommodate a heating system and an increased level of local strain measurement accuracy. This design, alongside the classification of the clays to be studied within this thesis, are presented in Chapter 3.

Chapter 4 and 5 present the results of the triaxial testing at elevated temperature and following cyclic temperatures variations. Results are presented for the change in pore water volume, critical state friction angle and the small strain stiffnesses of the samples.

In Chapter 6 a discussion is presented based on the experimental results and the results detailed in literature. This section develops a conceptual model to understand a clays response to cyclic temperature variation from a microstructural perspective, considering the relationship between the clay particles, adsorbed double layer water, and pore water. This conceptual model is tested against this study's experimental results in addition to key pieces of existing literature. To relate the findings to those of the 'real world' the conceptual model is tested against a field study presented in literature.

This study is concluded in Chapter 7 where the findings of this study are brought together in relation to how this work be can support industry on the factors which determine the behaviour of clay when subject to heating through the installation of PFHX.

Chapter 2

Impact of pile foundation heat exchangers

Pile foundation heat exchangers are currently used around the world for both heating and cooling of buildings. Current literature presents minimal information on the influence of PFHX on the clay which supports the foundations, with the main focus being their energy performance with regard to sourcing and sinking heat and the structural performance of the pile foundation.

The following review of literature provides an overview of:

- Influence of microstructure on the bulk behaviour of clay;
- Performance of PFHX and field study observations;
- Behaviour of clay with respect to temperature.

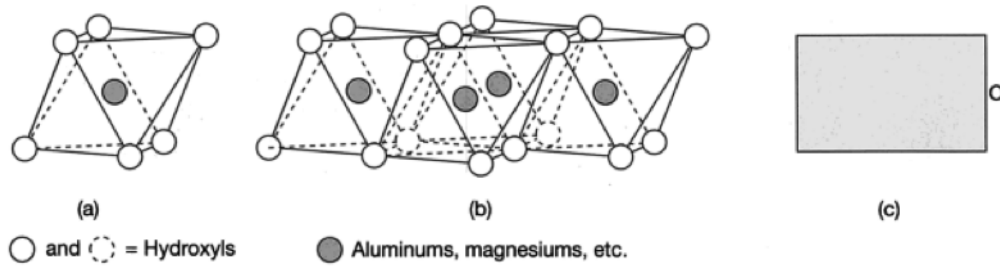
2.1 Understanding clay microstructure

In order to understand the observed bulk behaviour of clay subject to temperature variation discussed later in this Chapter, it is important to first understand the make up of clay and the impact temperature has on the elements of a clay's make up. This section will consider the microstructure of clay, particle bonding and the behaviour of water with temperature.

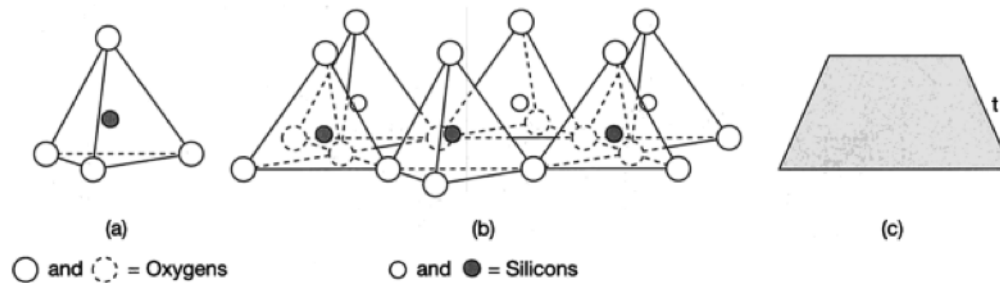
2.1.1 Clay microstructure at ambient temperature

A sample of clay is 3 main elements; clay particles, free water and absorbed water. A great importance should be placed on the nature and magnitude of the forces that act within the clay particles and between the clay particles and water.

Clay particles can be represented by repeating structures with sheet, platelet or sandwich structures being the largest repeating structures (Figure 2.1). A build up of sheets is then considered to be a crystal, with an agglomerate of crystals being defined as a aggregate. A clay particle can be considered as a sheet, crystal or aggregate depending on its smallest apparent unit (Lambe 1953).



(a) Diagrammatic sketches showing a (a) single, (b) sheet and (c) schematic of an octahedral sheet



(b) Diagrammatic sketches showing a (a) single, (b) sheet and (c) schematic of tetrahedral sheet

Figure 2.1: Diagrammatic sketches of clay particles (West (1995))

The most abundant mineral in clay is silicate, with kaolinite, illite and montmorillonite being the most common mineral groups. Kaolinite is formed as a two layer 1:1 structure of silica and gibbsite sheets as represented in Figure 2.2(a). For the case of the montmorillonite group, a substitution of a magnesium atom occurs for every sixth aluminium atom within the gibbsite sheet. This results in a negative charge across every sixth gibbsite cation and is represented in Figure 2.2(b). (Lambe

1953, Reeves et al. 2006).

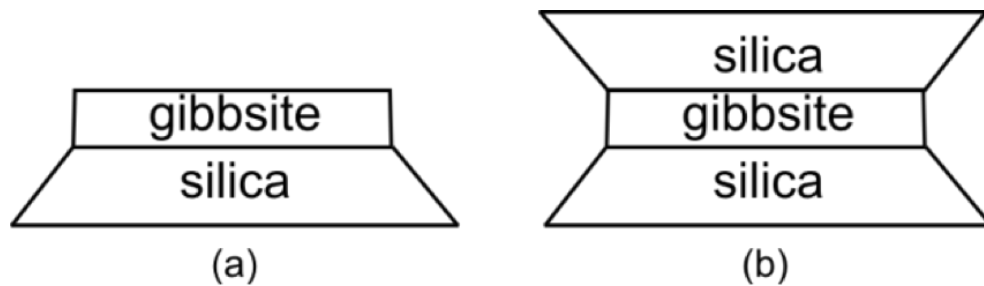


Figure 2.2: Representation of (a) Kaolinite, (b) Montmorillonite (Lambe (1953), Reeves et al. (2006))

For illite minerals 15 % of the silicon atoms are replaced with aluminium atoms. This causes the illite sheet to have a negative net charge, which is partially balanced by non-exchangable potassium ions alongside partially exchangeable cations. All atoms within the mineral sheets and intramineral sheets are connected by primary valence bonds, and can therefore be considered as high strength bonds which are not likely to be broken when subject to forces normally applied in engineering (Lambe 1953, Reeves et al. 2006). The number of sheets within a clay crystal can vary from a single sheet up to hundreds of sheets. The number of sheets in a crystal depends on the environment during growth, attractive forces between sheets and any isomorphous distortions that occur. An isomorphous distortion is caused when cation is exchanged which is different to the original cations' size and shape.

For kaolinite clays, the sheets are stacked with oxygen lying on the hydroxyls of gibbsite with the linkage between adjacent sheets being considered to be hydrogen bonding due to only 0.16 Å between the sheets. In addition to the hydrogen bonding, additional linkages occur. Attraction between polar units (orientation type) and dispersion effects provide secondary valence bonding (Lambe 1953).

For the case of illite, their crystals are primarily linked by the potassium ions which form a integral part of the structure of illite. Between the silica sheets are hexagonal holes large enough for potassium ions to fit between, without distorting the lattice. This allows the potassium sheets to rest partially within the adjacent sheets. Secondary valence forces between the sheets add to the potassium (k-type) bonding as the potassium ions help satisfy the charge deficiency and are held to the

illite sheets by ionic forces. For illite, the orientation forces are less than those for kaolinite due to the lack of symmetry caused by to the isomorphous substitution.

For montmorillonite crystal bonding occurs through exchangeable cations and secondary valence forces. This is why expanding minerals, such as montmorillonite, have a weak intersheet linkage and isomorphous substitution. This promotes crystal to disperse in water enabling them to exist as a single sheet mineral. Kaolinite crystals however have never been found to exist as single-sheet crystals as they have strong hydrogen bonding and minimal amounts of substitution occurring (Lambe 1953). The linkages between kaolinite, illite and montmorillonite crystals are summarised in Table 2.1. For the temperature which a PFHX operates, the relatively small temperature variations are unlikely to contribute to a change in these forces.

Table 2.1: Summary of linkages between clay crystals (Lambe (1953))

Clay Crystal	Type of intersheet linkage	Strength of linkage
Kaolinite	H-bonding + secondary valance	strong
Illite	K-linkage + secondary valence	strong
Montmorillonite	Cation linkage + secondary valance	weak

2.1.2 Particle bonding at ambient temperature

A sample of clay is 3 main elements; clay particles, free water and absorbed water, shown in Figure 2.3.

A great importance should be placed on the nature and magnitude of the forces that act within the clay particles and between the clay particles and water. West (1995) gives details to the microstructure of the clay particles and varying size of clay crystals. Clay crystals such as kaolinites have a small amount of surrounding water, relatively to the size of the clay crystal. Smectites however, have a relatively large amount of surrounding water compared to the size of the clay crystal.

Lambe (1953) proposed a working hypothesis that has been widely accepted and developed upon in more recent years. Lambe (1953) hypothesised that intramolecular bonds form between atoms in order to form molecules, with atoms in one molecule bonding to atoms in another molecule through intermolecular bonding.

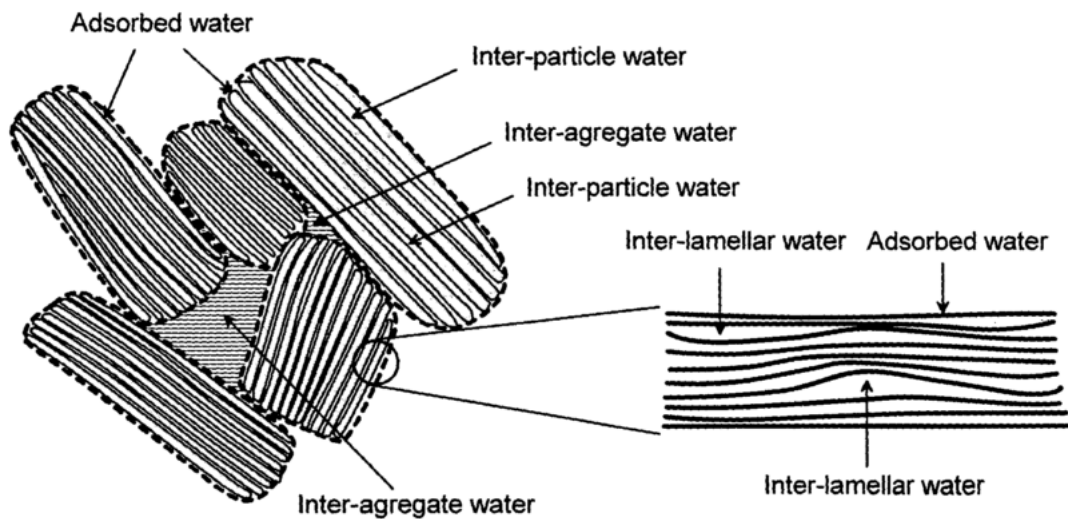


Figure 2.3: Schematic illustration of the two main types of water in saturated soil: Left - free water within inter-aggregate space. Right - adsorbed water located in the inter-particle and inter-lamellar spaces. (Cekerevac (2003))

This intramolecular bonding within clay can be split into primary valence bonding and secondary valence bonding. Types of primary valence bonds include covalent, heteropolar, ionic, coordinate and metallic. Due to the gradual transition from one bonding type to another, the classification of certain forces cannot be obtained. Within cohesive soils such as clay, these bonds are seldom broken (Lambe 1953). Secondary valence bonds relate to the forces acting between the molecules due to the electric moments surrounding the individual molecules. In cases where the centre of action for the positive charges coincides with the centre of action of the negative charge no dipole moment occurs. However, within the atoms in a water molecule, which are held together by heteropolar bonds, the resulting molecule is not symmetrical, therefore a dipole is formed (Lambe 1953). Upon the formation of a dipole there are three effects that contribute to secondary valence forces and have various dependencies on temperature:

The orientation effect: An attraction between the oppositely charged ends of permanent dipoles. The orientation effect is highly dependant on temperature as thermal agitation has been found to upset the alignment of the dipoles, however Lambe (1953) has not indicated the temperature at which this agitation occurs.

The induction effect: When a normally non-polar molecule is placed into an

electric field polarisation is induced. This is due to a slight displacement of the electrons and nuclei of the molecule. This induced effect is only slightly affected by a change in temperature, however Lambe (1953) has not indicated the temperature levels which cause this.

The dispersion effect: The relative displacements between constantly vibrating electrons and nuclei cause temporary dipoles to occur. It is these dipoles that make intermolecular attractive forces possible. The dispersive forces occur in all molecules and are independent of temperature.

A typical relative contribution of each of these 3 effects to secondary valence forces can be deemed as orientation 77%, dispersion 19% and induction 4%. (Lambe 1953) calculated this percentage through a breakdown of energy in the Van der Waals forces effective between water molecules. Another form of bonding which occurs in between atoms is hydrogen bonding. Hydrogen bonding falls between primary and secondary valence bonding as it is typically stronger than a secondary valence bond but weaker than typical primary valence bond. Hydrogen bonding occurs when an atom is strongly attracted by two other atoms, without one atom being more dominant than the other. This causes the hydrogen atom to oscillate between the two atoms. This occurs most commonly between water molecules, with hydrogen oscillating between the two water molecules. Hydrogen bonding can be considered similar to dipolar attraction (Lambe 1953).

Free water occurs within the pores of the clay mineral structure. In high porosity clays, it is thought that the majority of water present within a clay-water system is free water (Baldi et al. 1988).

2.1.3 Double layer theory at ambient temperature

Adsorbed water is known as the water which is present within a clay to water system which does not have the ability to move freely due to the attraction between it and the clay particle, as shown in Figure 2.4. For low porosity clay, it is thought that all water is adsorbed rather than free. Baldi et al. (1988) tested clays with

a water content 12-18 %. In smaller spaces within the clay, water molecules are packed between the walls of voids, held under short-range hydration forces, whereas in large voids a diffused double layer forms within the aqueous electrolyte. Very high forces are in action here, bonding the water molecules to the charged surface of the clay mineral. The thickness of the double layer is dependent on (Baldi et al. 1988):

- The valence of exchangeable cations
- The dielectric constant

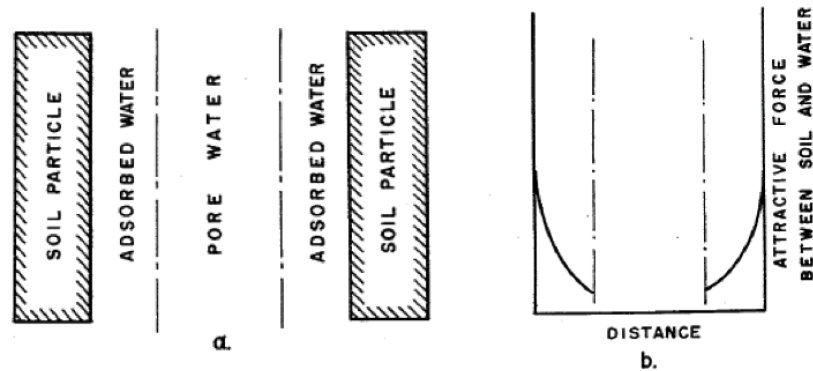


Figure 2.4: Decrease in a particle potential with increase in distance from particle. (Lambe (1953))

As the surface of the clay particle is approached, it is thought that the ionic concentration and holding forces within the sample increase exponentially, with the exception of the last two layers. The density of the absorbed water may vary from 1.0 Mg/m^3 , the density of free water, to 1.4 Mg/m^3 or more, the density of water within the first layers at the surface of the clay particle (Baldi et al. 1988). In low porosity clays, the distance between the clay platelets is smaller, therefore implying the overlapping of double layers between neighbouring particles. For the absorbed water the attractive forces between that and the clay particle are polar bonds. The absorbed water is under the influence attractive forces produced by clay particles therefore its behaviour is different to that of pore water. The absorbed water closest to the clay particle is held by such strong forces that the water is immobile to normal hydrodynamic forces and displays different characteristics such as density

and freezing point to that of pore water. This water can effectively be defined as part of the soil particle (Lambe 1953).

Plum & Esrig (1969) provides a concise summary of the theories considered above. The study considered the microstructural of clay identifying that a cohesive soil may be considered to be composed on clay platelets which vary in shape and size depending on their deposition/preparation and their environment. These platelets then form a complex three-dimensional truss using the point contacts, where Van der Waals forces of attraction and repulsion occur due to the interaction of the electric double layers on the clay surfaces and some portion of the externally applied forces. If, during loading, the electric double layers are expanded and therefore the repulsive forces increased, a readjustment of the soil structure under applied loads can be expected. Kenney (1966) conducted a study into the expansion of the electric double layer during loading. Whilst maintaining constant stress surrounding a sample, salts were leached from samples of non-cemented Norwegian marine clays. During this process the thickness of the electric double layer was increased, whilst observing a decrease in sample volume. This observation was explained by the author as being due to the interparticle forces and Lambe (1959) proposed the mechanistic model detailing soil behaviour, as described earlier in this section. Kenney (1966) suggests that as the electric double layer expands, the effective stress of particle contacts is reduced, therefore permitting shear failures to occur at these contacts. It is thought that this behaviour is experienced in more active clays. Plum & Esrig (1969) used this theory to explain the findings of Lambe (1959), who tested less active clays where interparticle contacts are more important due to the less dispersed nature of the particles. In this case, expansion of the double layer would reduce the effective stress at a point of contact and permit shear deformations and consolidation to occur. This therefore promotes a rearrangement of the clay particle structure until a new stable configuration is formed.

2.1.4 Double layer theory at elevated temperatures

The effect of temperature on the adsorbed double layer water was studied by Yilmaz (2011) and Wang et al. (1990). Yilmaz (2011) found that for temperatures up to 100 °C only the physical sample pore water was removed. The adsorbed double layer water requires temperatures greater than 500 °C before the depletion of its chemically bonded adsorbed water occurs, as seen in Figure 2.5. Wang et al. (1990) found that between 800 and 1000 °C the formation of larger particles occurred.

For the temperature ranges considered in this study, it can be deemed that the adsorbed double layer water will remain intact and no formation of larger particles will occur. The greatest effect due to heating is therefore likely to be attributed to the pore water within the sample.

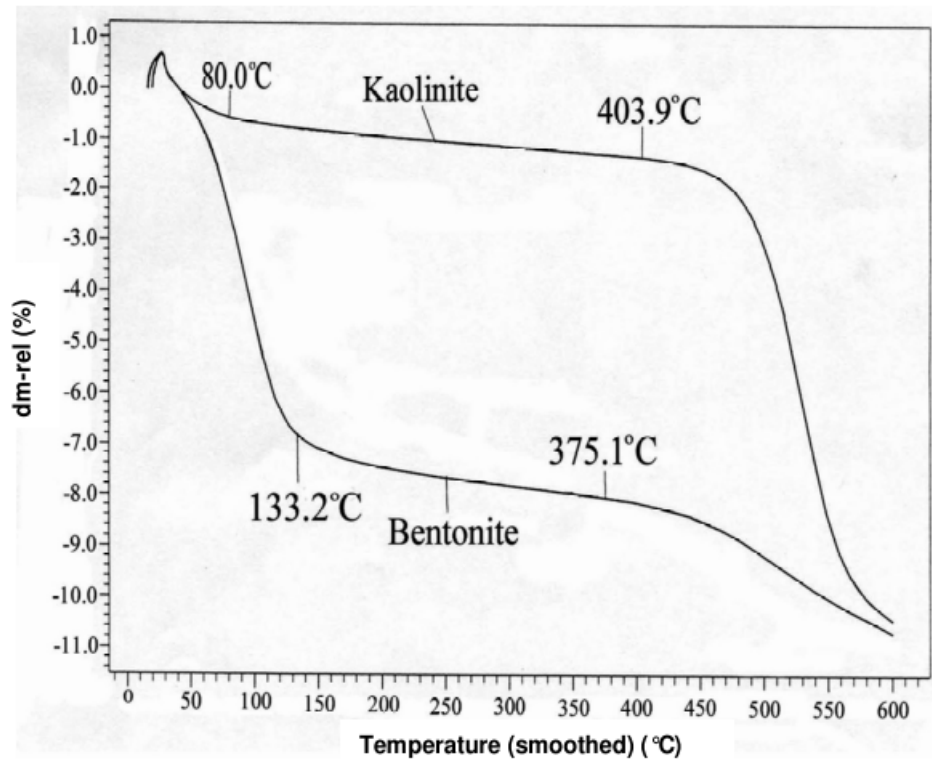


Figure 2.5: Thermal Gravimetric analysis for samples of Kaolinite and Bentonite. dm-rel(%) referring to relative mass loss of the sample. (Yilmaz (2011))

2.1.5 Behaviour of pore water with varying temperature

In understanding the full behaviour of a clay sample during heating and cooling, it is important to understand how the pore water behaves during temperature variation. This section will consider the volume change and viscosity of water with increased temperature.

Volume change

Figure 2.6, shows the specific volume change of water with temperature. The graph provided does not highlight the minimum specific volume of water which occurs at 4 °C. When cooling water below 4 °C, the liquid water molecules begin to rearrange themselves at their lowest energy state, causing them to be tightly packed together. At 4 °C, pure water is at its maximum density of 1 g/cm³. Within the range which PFHX operate, it can be seen that there is a near linear relationship between specific volume and temperature.

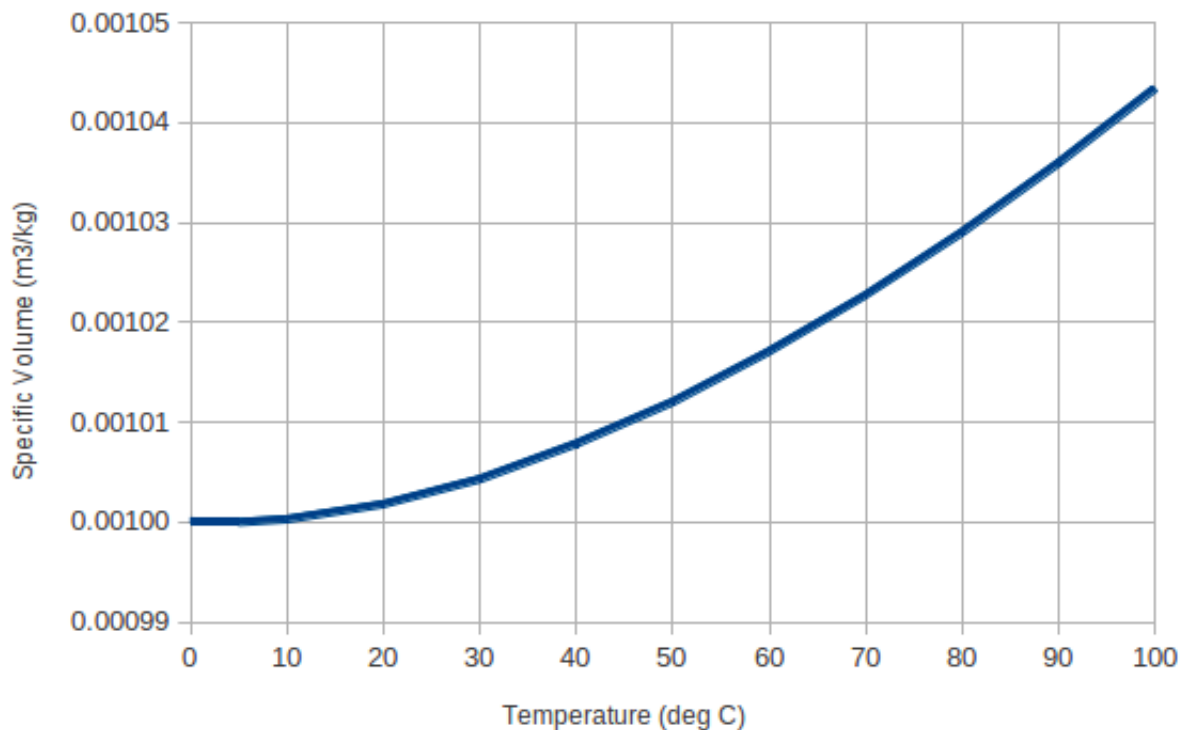


Figure 2.6: Specific volume of water with temperature (The Engineering Toolbox (n.d.))

Viscosity of water

The viscosity of water with temperature is presented in Figure 2.7 as found through laboratory testing by Korson et al. (1969). These results show that as water increases in temperature, the shear resistance between the water particles decreases, in line with the decrease in viscosity experienced.

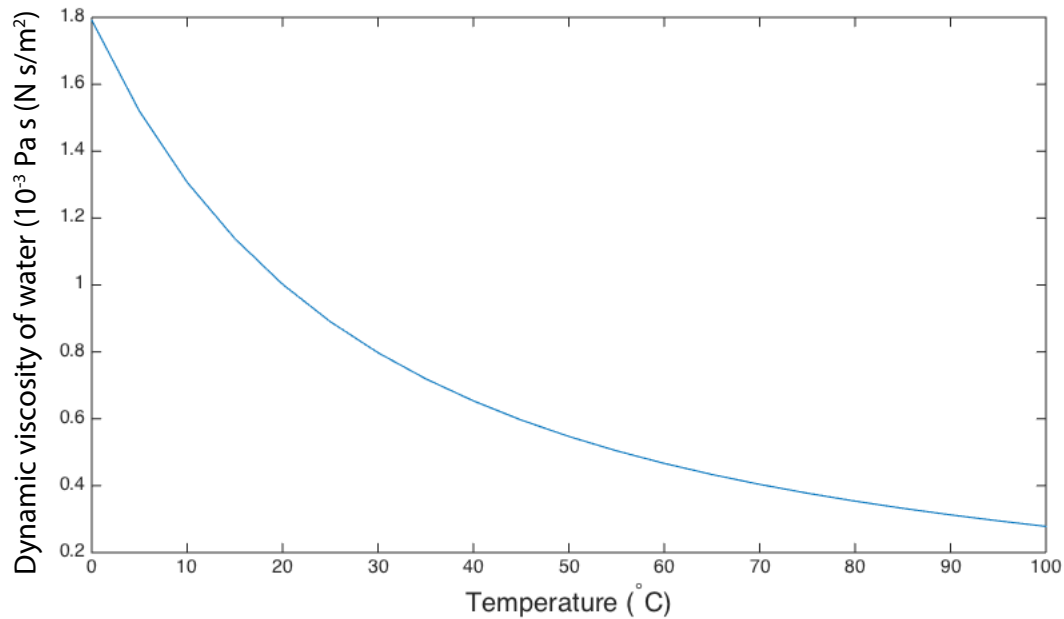


Figure 2.7: The viscosity of water at various temperatures (Korson et al. (1969))

2.2 Microstructure effects on bulk behaviour at ambient temperature

The microstructural changes have been studied during consolidation by McConnachie (1974) who primarily focused on the change in particle aggregation and orientation. Cetin & Gokoglu (2013) identified during triaxial shear testing a change in particle orientation as axial strain occurred. This section will further discuss the findings of these studies.

2.2.1 Consolidation

A key piece of literature which considers the fabric change in kaolin during consolidation is McConnachie (1974). Testing was carried out on purified kaolin which was mixed at a moisture content 1.5 times the liquid limit to form a slurry before consolidation to pressures up to 100 kPa was carried out. It was found that the volume of the sample was reversible from between 1×10^{-4} and 1.5×10^{-3} kPa where a change in gradient of the consolidation curves occurred. From 1.5×10^{-3} to 100 kPa reversible behaviour also occurred, as shown in Figure 2.8.

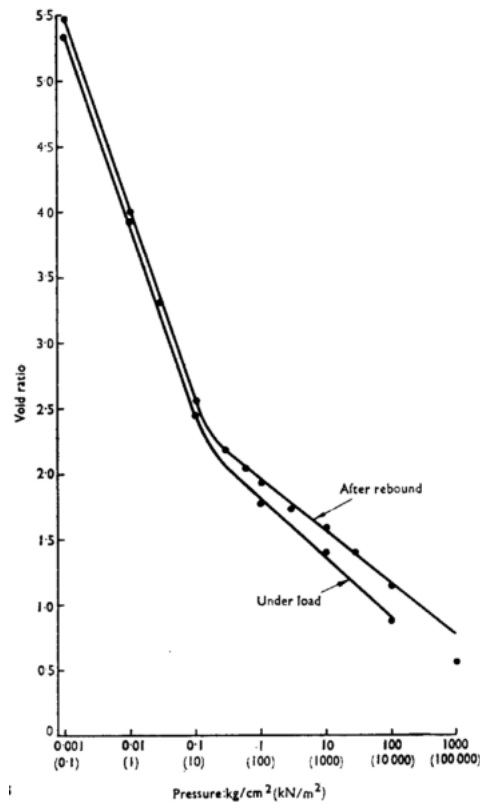


Figure 2.8: Consolidation curves for kaolin tested up to 100 kPa (McConnachie (1974))

Various features of the clay were measured, including length, breadth and orientation of the particle domains, and the voids between the domains, their packing density and the inter-domain contacts, using an electron microscope. A domain has been defined as a group of particles in which contiguous particles have approximately the same orientation and cannot be broken down into smaller groups on the basis of differences in the orientations of its constituent particles.

The study was conducted on purified monomineralic kaolin, mixed to form a slurry at a moisture content of 150% times its liquid limit. Several samples were consolidated to severe pressure in the range of 0.1 to 100,000 kPa. Throughout loading and unloading, the load increment ratio was two, and the final load on the sample was zero allowing them to rebound. Separate samples were used in order to determine the moisture content for each pressure, before and after rebounding.

Following testing, samples were examined using an electron microscope, with the pore water replaced by acetone, which was later replaced by a polyester resin. The impregnated sample was then cut in the vertical direction in terms of the original orientation of the samples. The domains were measured across the pressure ranges, with contacts between domains, and edge-edge or edge-face or face-face contacts also measured.

It was found that the size of domains changed when the pressure reached 10 kPa. The geometric mean size of the domain went from $1.51 \mu\text{m}$ to $1.13 \mu\text{m}$. This change in domain size is thought to have potentially been brought on by several mechanisms:

- Constituent particles in edge-face contact could develop face-face contact by the rotation of one of the particles at the point of contact;
- A lower surface friction at one point of contact causing a rotation could potentially be accompanied by a slip;
- Particles in face-face contact might move parallel to their faces so their interlock increases.

With regard to domain orientation, it was found that domains preferred horizontal orientation increases, suggesting rotation rather than rupture at points of contact. At a pressure of 14.7 kPa it was found that domains are reduced in size significantly, with further pressure increases closing in the gap between domains with the number of edge-face contacts decreasing as face-face contacts increase. At high

pressures of 100,000 kPa the inter domain contacts were found to be primarily edge-edge or face-face. Similarly, as the pressure increases, the void size decreases. The results of the study tentatively show that a different relationship exists between size of voids and low pressures compared to high pressures, although this relationship is not fully explored.

2.2.2 Shear strength

Shear testing changes the structure, composed of microstructural units, by firstly breaking down the particle groups and/or their aggregate assemblages before rearranging them. The final structure of a soil deposit depends on both the initial structure of that soil and the changes that have occurred to the initial structure (Lambe 1958). The final structure of a clay deposit is found to be a combination of the soil composition, stress history and environmental impacts (Mitchell 1993) (Burland 1990).

Cetin & Gokoglu (2013) brought together a theory combining many authors that particles, when in motion, tend towards a significant preferred orientation in space. During shearing, the soil composition, consistency, pore and particles all generally align along their long axes, parallel to the shear stress acting on the plane; the degree at which this occurs is dependant on the magnitude of the shear force. Outside of this shear zone of aligned particles, the particles tend to align with the long axes normal to the major principal stress direction. Within the clay sample, pores of water subjected to stress have a preferred orientation, with the distribution of the pore pattern in the soil depending on both the direction and magnitude of the stresses applied and the distribution of pores within the sample prior to the application of stress.

The study on artificially made clayey soil to investigate how the structure changes during slow, drained and fast undrained triaxial shear tests on a cohesive, sandy silt-clay soil. The orientations, pores and other constituents were measured at a variety of axial strain levels and shear displacements below and above failure point, with

the changes in particle orientation at various points also studied. The natural soil used in testing had a liquid limit of 43.3 % and a plasticity index of 19.7 % whereas the artificial soil tested had a liquid limit of 35.4 % and a plasticity index of 15.4 %. Thin sections of the samples were studied to identify the orientation patterns using vacuum-impregnation with blue epoxy resin. Triaxial testing was carried out under 20 kPa in order to study the variation in orientation due to shear stress. The undrained testing was carried out at a shear rate of 0.04 mm/min, with drained tests conducted at 0.0045 m/min to allow for drainage.

To observe and report on the changes in orientation, 3 locations were defined.

- Centre Zone - 5 mm either side of the shear plane
- Intermediate Zone - 10 mm either side of the center zone
- Outer Zone - the sample beyond either size of the Intermediate Zone.

All samples were taken from the same artificially made block samples, and that the structure examined were identical at the beginning of testing. The orientation of the sample at the beginning of testing, post consolidation, with a confining pressure of 20 kPa is nearly random, with an average angle to failure/shear plane of 59.06° throughout the sample. The voids within the sample are large, generally interconnected and randomly orientated. During the initial phases of undrained shearing at 2 % axial deformation, the angle to the potential/theoretical failure plane decreases sharply to 55.75° across the sample. This orientation remains until 12% axial strain where the average angles to the failure plane reduce further to 43.55° in the centre zone of the sample, 44.74° in the intermediate zone and 45.77° in the outer zone. This preferred orientation increases towards the failure plane, with particles, pores and other constituents tending to become parallel to the shear plane as shearing continues. As shearing continued, in the intermediate and outer zones, there was limited change in the centre zone up to an axial deformation of 15 % however there were slight increases in the other 2 zones. When 20 % axial strain is reached, a sharp decrease occurs across all zones. When assessing the failure of the sample

from an orientation point of view, failure occurred at axial deformation of 12 % as opposed to the 7.65 % given on by the stress-strain curve. To assess the impact of drainage, a second shear test was conducted on an consolidated drained sample. Post consolidation, at 2 % axial strain the particle orientation was random with the average to failure plane $54-56^\circ$ across the 3 zones. This pattern continued up to an axial deformation of 6% with the angles across the zones decreasing to 50.61 to 51.31° . The angle of deformation was found to always be at a minimum within the central zone, indicating that particles, pores and other constituents tend to become parallel to the shear plane as shearing continues. As axial deformation reaches 20 %, the orientation to the failure plan decreases to 46.15° in the centre zone, 49.40° in the intermediate zone and 50.22° in the outer zone. Results for the drained test indicate that failure occurred at approximately 6% as opposed to the stress-strain curve.

Comparing the two tests, towards and at failure, the centre and intermediate angle of orientation in the drained tests were found to be less than those in the undrained tests. This suggested that the drained tests formed a wider zone of preferred orientation. During the drained tests, it is thought that the particles had enough time to respond to the applied shear stress, as opposed to the undrained tests where not enough time was allowed for the particles to respond and change their orientation under the shear stress.

2.3 Microstructure effects on bulk behaviour at elevated and cyclic temperature variations

This section considers the reported microstructure variation which occurs whilst testing at elevated temperatures and following cyclic temperature variation. The effect of microstructural changes are also considered with regards to plasticity index, and consolidation of the clays.

2.3.1 Impact of elevated temperature on clay microstructure

The section aims to understand the microstructural changes occurring to produce the observed bulk behaviour of samples tested at elevated temperature, as reported in Section 2.6.

With regard to the microstructure, Campanella & Mitchell (1968) observed that during initial consolidation at constant temperature, the void ratio decreases until sufficient shear resistance has developed through the inter-particle mineral to mineral bonds. These bonds then have the ability to resist the shear forces resulting from the applied boundary normal stress within the sample. A rapid increase in temperature has the potential to significantly increase the pore water pressure of the sample, even though fully drained, as this depends on permeability. For a low permeability clay, a longer time period is required to dissipate the pore water pressures induced. This drainage trend is comparable to that of primary consolidation behaviour. With regards to secondary consolidation, it is believed that an increase in temperature promotes a decrease in shear strength of individual inter particle contact. The effect can be seen as analogous to secondary compression, under an increase in stress.

Following testing detailed in Section 2.1.1, Towhata et al. (1993) proposed the following hypotheses in relation to the microstructural changes which occur within a clay sample upon heating:

- Every molecule of attracted water, as part of the adsorbed particle double layer water, has a kinetic energy and a chance to get out of the range of the electric attractive force, when the energy is large enough. If this is the case, the water becomes free.
- The double layer thickness reduces as molecules escape. Consequently, clay particles within the sample have the potential to get close together or come into contact with one another. This means on a macroscopic level, clay volume contracts even under the null excess pore water pressure. It has been observed

that this particle movement is irreversible.

- Heating increases the molecular kinetic energy and the rate of volume contraction is accelerated.
- The structure of clay particles that is created by heating is more densely packed or has more particle contact than before, thus becoming stiffer. Heating can be thought to cause a quasi-overconsolidation behaviour of clay, similar to that of prolonged consolidation.
- The amount of cross section occupied by free water increases with temperature increase, as the double layer water decreases, whilst the sample void ratio is held constant. When this effect is combined with a decrease in water viscosity, this expanded channel of water flow leads to an accelerated seepage and volume change within the sample.
- The rate of volume change is substantially accelerated due to heating as heating reduces the viscosity of pore water.

The heating of a sample is analogous to the volume change which occurs over a greater duration for a sample at room temperature. Heating is thought to accelerate the process.

2.3.2 Impact of cyclic temperature on clay microstructure

Cyclic temperature variation causes a reduction in the moisture content of a clay, as found in Section 2.7. This behaviour can be classified similar to that of dehydration and rehydration of a clay which, independent of the mechanism causing the dehydration and rehydration, is caused by the loss or gain of interlamellar water, due to microscopic mechanisms (Hueckel 2002). During the cooling phase of cyclic temperature variation, Campanella & Mitchell (1968) found that water, previously expelled during the heating stage, was reabsorbed. It was observed that not all

expelled water was found to be reabsorbed, leaving a net volume of water volume of water drained from the sample.

Some of the earliest conclusions on the impact of cyclic temperature variation on the microstructure of clay were made by Campanella & Mitchell (1968). From the irreversible volume change detailed in Section 2.6, it can be seen that the heating and cooling of a sample decreases the void ratio, Figure 2.9. During heating, expansion of the pore water occurs, along with the expansion of the mineral solids. These combined expansions lead to a change in soil structure. In a drained condition, subject to effective stresses remaining constant, water will drain from the sample, with the remaining mineral solids reorientating themselves to carry the effective stress, known as physico-chemical adjustments.

During heating, for soil grains in mineral to mineral contact, during temperature increase these particles undergo the same volumetric strain, assuming the coefficient of thermal expansion is constant throughout the sample, leading to a uniform volumetric strain across the sample. Sample volumetric strain is also impacted by the change in inter particle forces as they reorientate themselves to withstand the effective stress.

For the compression index of a clay sample, Campanella & Mitchell (1968) found it independent of temperature; however, higher temperature increases led to lower void ratios for a given temperature. Developing upon the observation of Campanella & Mitchell (1968) in the previous section (Section 2.3.1), with a decrease in temperature, the reverse of the observed behaviour during heating is anticipated. As the clay cools, the relative difference between the volumetric shrinkage of the soil grains and water promote an increase in tension within the pore water. This in turn leads to absorption of water. For cooling, a secondary volume change effect is not observed, as the decrease in temperature causes a strengthening of the sample, no further structural rearrangement is required to carry the effective stresses imposed on the sample. For the subsequent heating and cooling cycles, the secondary effect is observed to be negligible, as the primary heating and cooling cycle has strengthened

the clay, allowing the effective stress to be carried at high temperature. Campanella & Mitchell (1968) discusses the hypothesis that the larger the initial temperature increase, the greater the rate of temperature induced secondary compression.

To further test this hypothesis, Campanella & Mitchell (1968) carried out identical testing on remoulded samples of illite, results shown in Figure 2.9 & 2.10. The temperature of the sample was increased from 4 °C to 60 °C at 25 °C increments for the first two temperature cycles. For the third cycle, the temperature was increased from 18 °C to 59 °C, at a rate twice that of the 4 °C to 60 °C cycles. During the larger temperature increase (cycle 1) the rate of secondary compression was much greater than cycles 2 and 3, with decreasing amount of secondary compression occurring in the latter temperature cycles. With exception of the initial temperature increases, the curves in 2.9 are essentially identical to those in 2.10. Campanella & Mitchell (1968) compared these curves to those of Leonards & Girault (1961). Curves 1, 2 and 3 of Figure 2.10 were found to match the curve of Type 2 secondary consolidation curves, with curve 1 in Figure 2.9 found to be characteristic of Type 1 primary consolidation curves. Leonards & Girault (1961) described Type 1 curves are those occurring under relatively high load-increment ratios, of the order of 1.0, with Type 2 curves being those observed under small load-increments, or those which straddle the preconsolidation pressure. Campanella & Mitchell (1968) thus highlighted the similarity between temperature induced consolidation and pressure induced consolidation and the comparable change in microstructural behaviour. Campanella & Mitchell (1968) suggests the analogy of a sample's temperature history being thought to be similar to a sample's stress history effect on volume change, implying that subjecting a clay to temperature cycles may be equivalent to over-consolidation. A permanent volume change of 1 % was found to correspond to a void ratio decrease of approximately 0.02, which would equate to a effective stress increase of approximately 25 kPa.

Campanella & Mitchell (1968) inferred reversible changes in the clay structure volume with temperature variations, which indicated a swelling of the clay structure

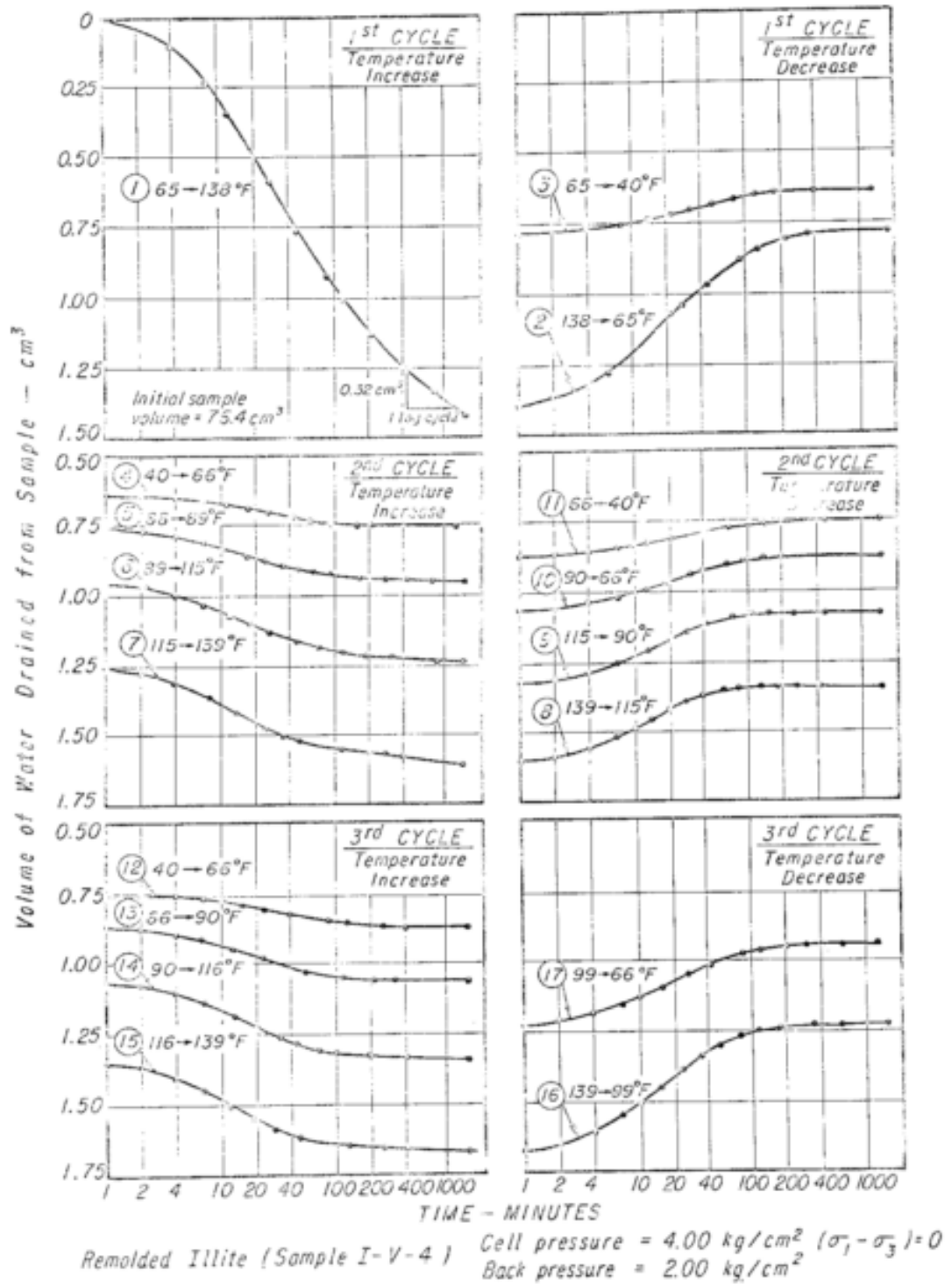


Figure 2.9: Relationship between volume of water drained from a sample and time during temperature changes at constant stress. Test with large initial temperature change followed by incremental temperatures changes (Campanella & Mitchell (1968))

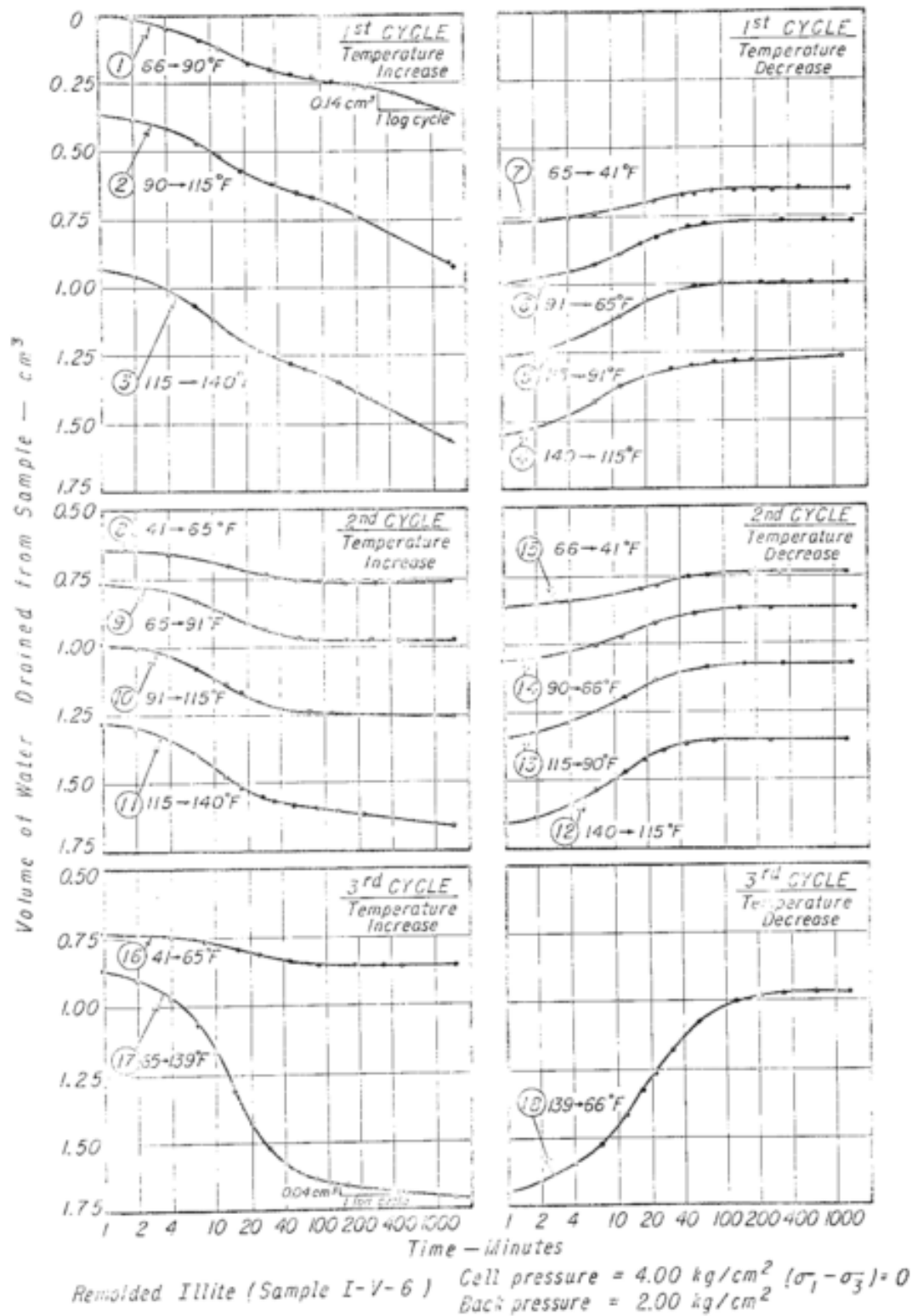


Figure 2.10: Relationship between volume of water drained from a sample and time during temperature changes at constant stress. Test with two incremental temperature cycles followed by a large temperature increase (Campanella & Mitchell (1968))

during temperature decreases and a compression during temperature increase. This was found to be the reverse of what would be anticipated if the soil structure simply expanded and contracted in response to the volumetric strain of the clay particles alone. It was therefore presented that a temperature dependent physico-chemical phenomena was occurring during the normal thermal expansion and contractions, dominating the effects. The possible effects identified were greater water adsorption force fields and higher osmotic pressures at lower temperatures. These could both account for swelling on cooling. The data available from Campanella & Mitchell (1968) was not able to provide a specific interpretation of these effects.

The influence of temperature was further investigated by Campanella & Mitchell (1968) through the testing of 3 remoulded illite specimens in a triaxial consolidation test. Each sample was heated to a different temperature for the duration of the test, following consolidation to an effective stress of 196 kPa. The samples were tested at temperatures of 25, 38 and 51 °C and remained under stress for 5800 minutes in order to ensure negligible additional secondary compression effects due to the initial stress. Following the secondary compression, the effective stress of the sample was then increased over 24 hours using a load increment ratio of 0.20 to 0.27. Results showed that the higher temperature samples produced lower void ratios after the initial stress application of 196 kPa. As all void ratios were identical prior to the initial stress, the successively lower void ratios were determined to be due to the initial higher temperature. This order of void ratio was expected due to the weak soil structures at higher temperature. The soil structure was predicted to densify at higher temperatures in order to carry the effective stress. The consolidation curves for the samples were essentially parallel; this was found to match the results of Finn (1952) whose results showed that compressibility was not affected by temperature within the range of 4 to 26 °C for one-dimensional consolidation of remoulded clay.

Plum & Esrig (1969), through the use of Kenney (1966)'s theory, suggested that during the cooling stage, a temperature decrease produces an overconsolidation effect as the decreasing temperature promotes a decrease in the double layer. As the

double layer is compressed, the shear resistance at the point of contact is increased, thus enabling the sample to carry a greater external load.

For the testing of bentonite and MC clay by Towhata et al. (1993), it was inferred that the behaviour of bentonite could be characterised by the instantaneous volumetric expansion upon heating. This was deemed to be due to the permeability of bentonite being much lower than MC clay, which prevented the drainage of water upon the expansion of pore water. This meant the pore water cause a swelling of the soil skeleton, which was measured during testing. Towhata et al. (1993), in addition to Agar et al. (1986) and Houston & Lin (1987), found evidence supporting the hypothesis that heating clays without sufficient drainage would lead to a reduced shear strength.

Burghignoli et al. (2000) considered the microstructural changes during temperature cycles, following testing featured in Section 2.7. The hypothesis proposed agreed with previous authors, that the temperature increase of a drained sample produced a rearrangement of particles which led to the volume deformation. It was believed that due to the small thermal expansion of the clay particles, they would not impact greatly on the bulk volume reduction. Through the temperature decrease and low temperature stages it was found that the volume reduction occurs at virtually constant porosity. It is therefore thought that no further particle rearrangement occurs during these stages, and hence the irreversible volume change is produced. This idea conflicts that of Campanella & Mitchell (1968) and Towhata et al. (1993), as both authors observed a degree of recoverable volume change during the cooling stage of their testing. When heating a normally consolidated sample, an irreversible volume change was found by Abuel-Naga et al. (2007), however when compared to mechanical unloading prior to heating, the material is found to expand, with greater amounts of expansion occurring with higher OCR. This provides evidence that the behaviour of clay subject to a temperature cycle is not analogous to the behaviour of clay observed during mechanical loading cycles, and therefore a differing microstructural change must occur, according to Burghignoli et al. (2000).

For undrained samples the observations showed the microstructural behaviour to be consistent with that of drained samples. During heating, water within the sample expands. In drained samples, heating was believed to be responsible for a thermal contraction behaviour of the soil skeleton (similar to that experience when mechanically loading a sample) with positive excess porewater pressures generated during heating in any initial condition. During cooling, the volume of water reduces. For drained samples, this reduces the porewater pressure proportionally to that of the coefficient of thermal expansion of soil grains. Since the coefficient of thermal expansion for water is greater than that of soil grains, negative excess pore pressure is induced during the cooling phases. A theory originally proposed by Campanella & Mitchell (1968) is followed by Burghignoli et al. (2000) in that under constant total confining stress, the amount of excess pore-water pressure induced by temperature variation is not only related to the differing dilation and contraction behaviour of the soil skeleton and pore water pressure, but also to the volumetric stiffness of the solid skeleton. This idea was tested using qualitative analysis. For a sample with normally consolidated initial conditions, a positive excess porewater pressure was induced during heating which approximately followed a swell curve. This observation was in agreement with the void ratio reduction observed in drained heating.

This reduction in void ratio, and therefore consolidation of a sample, has been termed ‘thermal consolidation’ by Burghignoli et al. (2000) to indicate the deformation process which occurs when excess porewater pressure generated through the temperature variation is dissipated from a sample. For normally consolidated Todi clay and Fiumicino clay, when samples were subject to undrained heating, the change in void ratio observed due to the dissipation of porewater pressure was very similar to that observed in mechanical consolidation. The study found that the thermal consolidation process which followed the heating of a normally consolidated sample was strongly influenced by creep behaviour within the soil skeleton. During heating, compression occurs which produces a void ratio reduction much greater than the increase resulting from the previous unloading due to undrained heating. Further

significant volume deformations were observed during secondary thermal compression. It was determined that this behaviour was justified by considering that the dissipated excess pore-water pressure which is generated during heating, induces conditions of normal consolidation and therefore as the mean effective stress increases, creep deformations become increasingly significant. It was found that the deformations which occurred during secondary consolidation following a heating phase were most significant due to the relatively small magnitude of deformations occurring during primary consolidation. Following a cooling phase, a sample is subject to ‘thermal swell’. Following thermal swell, the absence of secondary swelling indicated that no significant creep deformations occurred. This is when the negative excess porewater pressure is induced and a swelling process takes place when the drainage lines are opened. The behaviour of undrained samples was consistent with that of both normally consolidated and overconsolidated drained samples, which confirmed the role of the time-dependant behaviour of the soil skeleton. Burghignoli et al. (2000) state that during the consolidation processes, the viscous component of the mechanical behaviour of the soil skeleton plays an important role.

In summary, the following observations and hypothesis have been made, in relation to the the microstructural behaviour of clay during cyclic temperature variations:

- During drained conditions, an increase in temperature produces a change of volume of the soil grains and promotes a particle rearrangement.
- The rearrangement of soil particles during the heating process can be thought as an amplification of the rearrangement responsible for the creep deformations of the soil skeleton

2.3.3 Plastic index

Testing carried out by Towhata et al. (1993) as discussed in Section 2.7 found that heating reactivated the development of volume contraction, which suggests that the structure of clay particles is deteriorated by heating, however it was observed that

the bentonite sample experienced greater volume contraction under 2230 kPa than MC clay tested at the same pressure. Abuel-Naga et al. (2007) considered the plasticity index of samples during the study described in Section 2.7. The temperature induced volumetric strain with PI of different types of normally consolidated clays, with a temperature change of 65 to 70 °C. For Bangkok clay with a plastic index of 60, a measured volumetric strain of approximately 6% was observed. This gives rise to the role of plasticity index in a clay's volumetric response to temperature, with higher plasticity clays experiencing a greater volumetric response than lower plasticity clays.

2.3.4 Over consolidation ratio (OCR)

The OCR of a clay sample has been found by many authors, including Towhata et al. (1993) and Abuel-Naga et al. (2007) to influence the behaviour change of a clay upon heating.

Towhata et al. (1993) considered overconsolidated specimens under a variety of stresses. As previously discussed, specimens were consolidated under a pressure of 2230 kPa followed by unloading to a specific pressure between 40 kPa and 1280 kPa, producing samples with OCR's between 1.7 and 56. All samples swelled upon unloading. Once volume equalised, the sample temperature was then increased, with the effects of heating observed. It was found that a lightly overconsolidated sample (OCR = 1.7) swelled under the room temperature, however upon heating to 40 °C swelling was reactivated, this also occurred when heating to 60 °C, as shown in Figure 2.11. It is thought that the instantaneous swelling occurring at 60 and 90 °C was due to the thermal expansion of pore water, with the magnitude of this increase being much less than that of bentonite, due to the higher permeability of MC clay allowing the pore water to drain at a faster rate. Upon reaching 90 °C, the sample begins to contract. This observation was believed to occur due to the thermal deterioration of clay skeleton as observed in normally consolidated samples, which exceeded the thermal reactivation of swelling caused by unloading. For highly overconsolidated

samples, volume expansion occurred upon heating, with samples of higher OCR tending to swell upon unloading. This volume change appeared to be activated upon further heating with higher OCR being associated with a greater extent of swelling. It was deemed that thermal swelling is dependent on stress level, which contrasts that of normally consolidated samples. Upon reload testing, the samples tended to be compressed, even after the primary stage of compression. Sample heating triggered or further accelerated additional volume contraction. Two different thermal effects are proposed, firstly, the thermal deterioration or contraction of the clay skeleton and secondly, the thermally-increased permeability of the clay, which promoted an accelerated volume change.

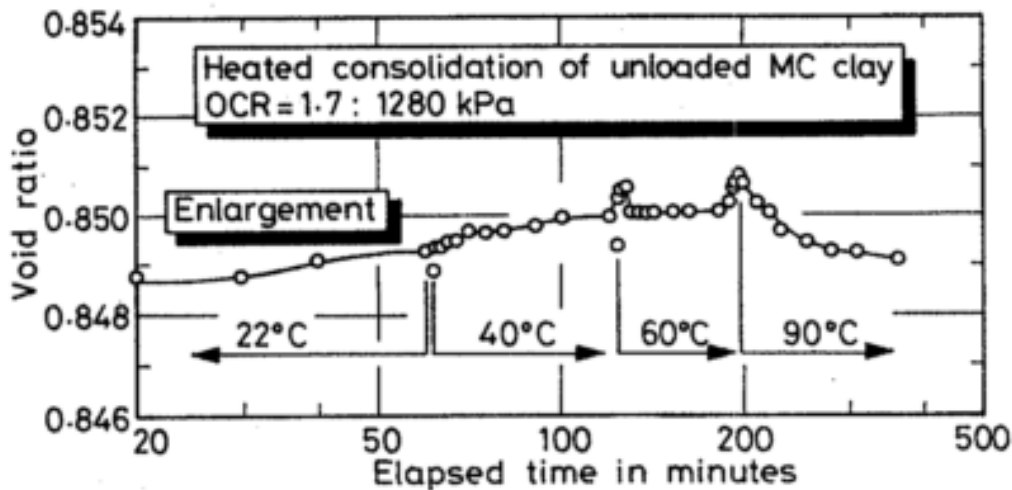


Figure 2.11: Effects of heating on swelling of unloaded MC clay with an OCR = 1.7 (Towhata et al. (1993))

Variations in OCR ratios were studied in oedometer testing by Abuel-Naga et al. (2007) as detailed in 2.7. The results given in Figure 2.12 show the effect thermally induced volume change with stress history for samples with a preconsolidation pressure of 100 kPa. For increasing OCR, the magnitude of the thermally induced volumetric strain contraction shows a relatively rapid decrease until the point of approximately OCR = 3, then gradually showing dilative behaviour with further OCR increases. These results have also been found by Olmo et al. (1996) in a study of 3 deep clays; Boom clay, Pasquasia clay and Spanish clay.

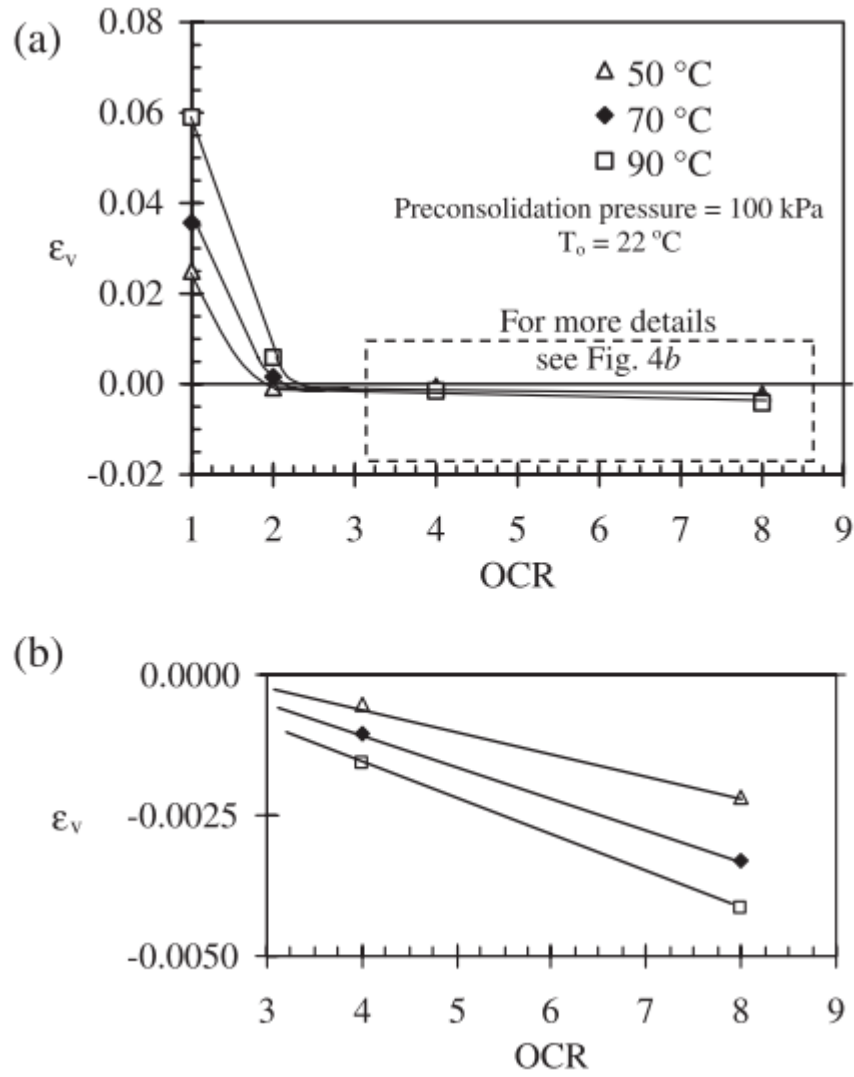


Figure 2.12: (a) Effect of OCR on thermally induced volumetric strain for soft Bangkok Clay; (b) Detailed results at high OCR values (Abuel-Naga et al. (2007))

2.4 Summary

In summary, literature has provided evidence that a clay's microstructure is highly responsive to temperature, with key observations being made in the volume change and stiffness being found. The responsiveness of a clay to temperature variation has been found to be associated to the plastic index and over consolidation ratio of the clay. These factors have been taken forward for further consideration in literature and this study.

2.5 Performance of pile foundation heat exchangers

Pile foundation heat exchangers (PFHX) operate as part of a complex system which combines both the pile foundation, and the ground which surrounds it. This section builds upon the understanding of how a clay responds to temperature variations with the application of a PFHX system.

PFHX provide ground source cooling through the utilisation of the near constant UK ground temperature beyond a depth of 15 m, as shown in Figure 2.13. As PFHX typically extend to depths below 15 m, the seasonal temperature variation does not influence the ground temperature surrounding the piles. The constant temperature allows for ground heating, thus building cooling, throughout the year. For commercial buildings with a year round cooling demand, a ground-temperature unaffected by seasonal air temperatures is particularly favourable.

Sinking heat into the ground poses potential for a long-term build up of heat surrounding a PFHX, especially if many are used across several congested city sites. Given the UK climate, stakeholders predict a 60% demand for cooling, averaged over a year, which would cause thermal cycling of the ground around a PFHX and an increased ambient ground temperature (Evidence Directorate 2009).

The thermal interactions of the pile foundation have been studied by Loveridge & Powrie (2012) and Bourne-Webb et al. (2011) with respect to the thermal integrity of the piles, the imposed thermal loading and the subsequent considerations required for the design of the pile from a structural performance perspective.

With regard to the installation of PFHX, they are installed using the same method as conventional pile foundations. The difference between conventional piles and PFHX is the inclusion of heat exchanger loops. Heat exchanger loops can be installed in both driven and cast in-situ piles. The heat exchanger loop works in combination with a heat pump to allow for heat energy in the building to be transferred into a refrigerant that circulates within the heat exchanger loops and

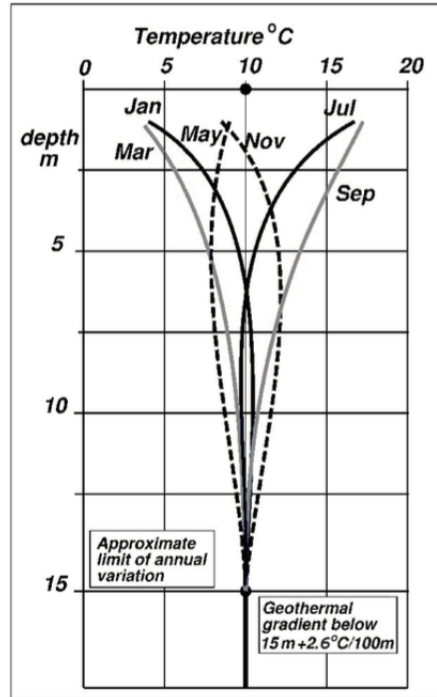


Figure 2.13: Ground temperature profile (Busby et al. (2009))

into the ground surrounding the foundation (Loveridge & Powrie 2012).

A wide variety of field studies has been produced relating to installed PFHX systems, each providing details on their individual application. These are summarised in Table 2.2 to provide a broad overview of the areas studied in PFHX field studies. The quality and comprehensiveness of the information and conclusions for the case studies vary considerably.

Table 2.2: Summary of PFHX case studies

Author	Location of study	Building	Aim of test	Size of piles	Load	Ground Profile	Temperatures	Summary of results	Conclusion
Laloui et al. (2006)	Swiss Federal Institute of Technology	4 storey building	Study the increased loads on the pile due to thermal effects	Diameter: 8.8 m Length: 25.8 m	Maximum: 1300kN	Alluvial moraine soil	Initial test: 21 °C, Subsequent: 15 °C	Heating of pile lead to global swelling of the top soil surface. Induced vertical strains in the soil were mainly dilative, with compressive strains generated at the bottom of the pile.	Friction resistance is not affected by temperature and relief of side friction mobilization is seen during heating. Strains in the soil do not affect pore water pressure
Pahud & Hubbuch (2007)	Zurich Airport	Airport terminal	To confirm the necessity and suitability of a detailed and careful design process is required for PFHX	206 piles Diameter: 0.9-1.5 mm Length: 26.8 m	not given	moraine	Heating: 8.3 °C out of piles. Cooling: 17 °C into the piles	No results provided	Energy pile systems can operate as designed, emphasising the importance of the design phase. Measured COP of 5.1, geocooling effect a COP 6.1. System deemed economical.
Hamada et al. (2007)	Hokkaido, Japan	Designed as a house combined with an office, 2 storied with semi-basement. Building area: 92.70 m ²	Field performance of air conditioning with an energy pile system. Main focus: air conditioning design	Diameter: 3.02 m Length 9 m	not given	not given	Brine: 2.4 °C Pile surface: 6.7 °C	Pile surface temperature remains constant between 6 and 8 degrees.	The seasonal amount of heat supplied accounted for 90% of the predicted value. A COP of 3.2 was measured, with a 23.2% reduction in primary energy required by the building
Bourne-webb et al. (2009)	Lambeth College, UK	5 storey building	Address the engineering issues associated with energy piles: impact on performance through cyclic heating and cooling, and the thermodynamic response	Diameter: 600 m Length: 23 m	Working load: 1200kN Maximum load: 3600kN	River Terrace Deposits, London Clay	Range: -6 °C, to +56 °C	Daily expansion and contraction during temperature cycles. Cooling phase: Movement of the pile head generally coincides with the changes in temperature imposed by the loops	Under normal operational temperatures, with relatively short cycles of cooling, freezing at the pile/soil interface is unlikely to develop. Mobilisation of skin friction during heating and cooling cycles needs further examination, to gain further insight into any detrimental impacts.
Wood et al. (2009)	unknown	Detached 2 storey residential building 72 m ²	Analyse the effect of the use of energy piles on the stored thermal energy within the ground local to the pile location.	21 piles Diameter: 0.3 m Length: 10 m	heat load only	Made ground above very soft red-brown clay	35 °C flow temperature	Top 2.5 m, the temperature is due to solar radiation and higher daily mean air temperatures. Top 10 m are naturally effected by the seasons, the effect is dependent on the heat flux and temperature change	Natural heat movement occurred in the ground, through either potential ground water movement or season ground temperature change. Greater amount of heat are available for extraction in soils with a high thermal conductivity and greater amount of ground water movements

The main focus of field studies has been the pile displacement as a response to temperature cycles in order to validate numerical modelling carried out by the author. The two key field studies which have been carried out are Lambeth College (Bourne-Webb et al. 2011) and École Polytechnique Fédérale de Lausanne (EPFL) (Laloui et al. 2006). These studies have been considered in further detail.

The foundations of a four storey building at EPFL were studied by Laloui et al. (2006). The building's footprint was 30 m by 100 m founded on 97 pile foundations, which included a single test PFHX with a diameter of 0.88 m and length of 25.8 m. The foundations were installed in moraine clay, with the pile's temperature being increased by 15 °C after an initial temperature increase of 21 °C. A maximum structural load of 1300 kN was applied to the pile. Thermal loading and structural loading of the pile, as the building's construction progressed, were not carried out simultaneously. An alternating sequence, of thermal loading and building construction was carried out until completion of a structural section. The testing at EPFL aimed to provide validation for finite element modelling, developed by Cekerevac (2003) as part of the same EPFL research group, to simulate the behaviour of PFHX during operation.

During the test period of 28 days, a net displacement of 1 mm at the pile head was witnessed, however a maximum displacement of 4 mm was observed 12 days into the test period. 12 days into the test was the point where maximum heading was reached before cooling began. Conclusions of the testing reported thermo-elastic strains within the pile, with their intensity dependant on the type of surrounding soil. Due to the difference in directional movement, uplift for thermal loading and settlement for static loading, the friction resistance of the pile was deemed not to be impacted, however relief of side friction mobilisation was observed during heating. As the induced thermal strains were limited, it is thought by Laloui et al. (2006) that there was no effect on the pore water pressure or the effective stress. The EPFL study provides evidence that temperature load cycles contribute to vertical movement of a pile foundation, however Laloui et al. overlook the response of the

clay, using the results to verify a numerical model; the results of the field study could be attributed to the expansion and contraction of the pile itself or the surrounding ground, or a combination of both. Further information from this study evidencing that an increase in temperatures does not affect pore water or effective stress would further the understanding of other authors.

The study at Lambeth College, by Bourne-Webb et al. (2009) aimed to address the thermo-dynamic behaviour of an energy pile during heating and cooling cycles. Testing was carried out during the construction of a five storey building founded on 143 pile foundations, installed in London Clay, with a diameter of 0.6 m and lengths ranging between 19 m and 24 m. An average structural load of 1025 kN was applied to the piles, with a heating load imposed on the piles between -6 °C and 56 °C. Following a period of pile cooling and heating, daily heating and cooling cycles were carried out. The net pile head displacement over the duration of testing was 3 mm, with a maximum displacement of 10 mm. Similarly to the EPFL field study, it is not possible to determine the nature of this displacement. The displacement could be due to either the expansion and contraction of the pile structure, the movement of the ground in which it is founded, or a combination of both elements.

Across these two studies, conflicting views were detailed with regard to the change in skin friction of a pile foundation through heating and cooling cycles. Bourne-Webb et al. (2011) discussed the hypothesis that a thermal load on an in situ pile foundation creates expansion and contraction within the foundation as axial forces develop. This movement of the pile is thought to lead to an impact on the shaft resistance of the pile foundation. This theory was applied to the field studies at Lambeth College (Bourne-Webb et al. 2011) and EPFL (Laloui et al. 2006). It was found that the hypothesis proposed by Bourne-Webb et al. (2011) is supported by case study field results from both Lambeth College and EPFL. This provides evidence that cyclic temperature variation does impact on the skin friction of a pile foundation. The magnitude of this impact however has not been detailed by either group of authors.

In contrast to Bourne-Webb et al. (2011) and Laloui et al. (2006), Brandl (2006) proposed that a PFHX pile operating properly would not be affected by a change in shaft resistance. This is thought to be true, by the authors, due to the point load at the base of the pile remaining constant, independent of the total load to the pile and temperature variation in and around the pile. Proper PFHX operation is defined by Brandl (2006) as reducing a local ground temperature of 10-15 °C, in a controlled manner, to approximately 5-10 °C, thus preventing the ground reaching freezing point and the formation of ice lenses occurring. The formation of ice lenses leads to heave and unsettled ground conditions. It is also deemed by Brandl (2006) that excessive heat input to the ground is less critical than heat extraction, although no maximum temperature is provided.

Both Bourne-Webb et al. (2011) and Laloui et al. (2006) provide valid arguments for their understanding of the thermo-mechanical behaviour of PFHX. It is clear from the contrasting arguments that temperature and PFHX set up, including clay type and pile loading, affect the resultant behaviour of PFHX's.

Table 2.3: PFHX Field Trials

Study	Lambeth College	Lausanne, Switzerland
Author	Bourne-Webb et al. (2011)	Laloui et al. (2006)
Ground profile	London Clay	Moraine: Clayey-sandy silt
Foundation type	Single pile	Piled raft
Pile length (m)	19 - 24	25.8
Pile diameter (m)	0.6	0.88
Total number of piles	143	97
Number of PFHX	1	1
Mechanical load on PFHX (kN)	1025	500-900
Temperature range of PFHX (°C)	-6 to 56	20.9, 13.4
Maximum pile head displacement (mm)	10 upwards	4.2 upwards
Range of pile head displacement (mm)	not given	1 upwards

2.6 Influence of elevated temperature on the Bulk Behaviour of Clay

This section will consider the behaviour of clay at elevated temperature and following cyclic temperature variation. Current literature has been reviewed in order to gain an understanding of the impact temperature on the consolidation of clay, volume change and strength and stiffness properties. The section reports on the observed volume change and shear strength of clays. Figure 2.14 has been provided as a reference to the plasticities of various clays studied in literature and this thesis. In addition, Table 2.4 summarises the clays and testing methods used in the literature discussed.

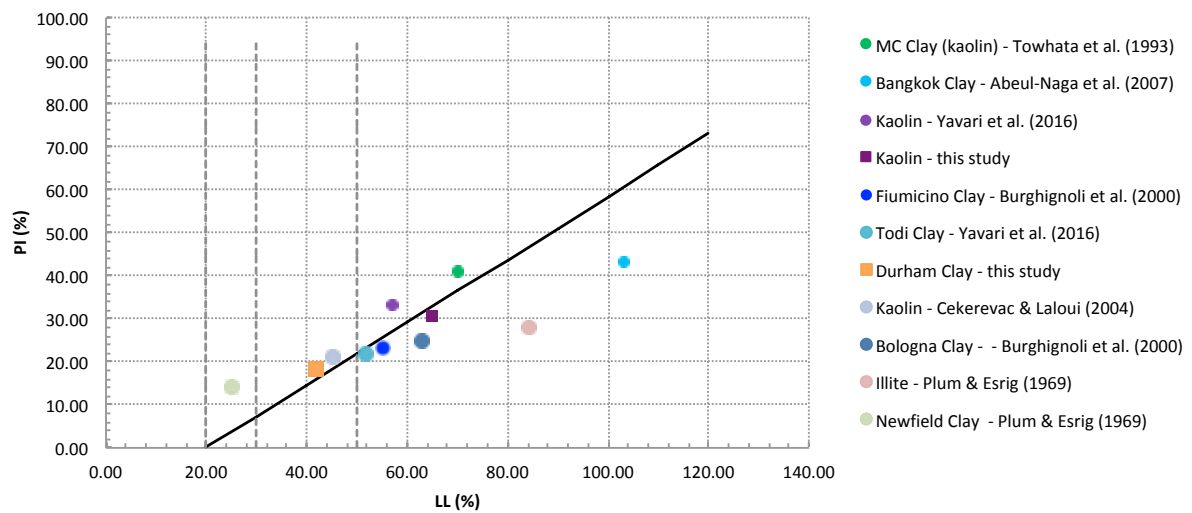


Figure 2.14: Plasticity chart for clays studied in literature, in addition to kaolin and Durham Clay tested within this study

2.6.1 Volume change

A series of authors conducted a series of laboratory tests to identify the effect of increased temperature on the behaviour of clay. These include Campanella & Mitchell (1968), Towhata et al. (1993), Yavari et al. (2016), Abuel-Naga et al. (2007), Burghignoli et al. (2000), Cekerevac & Laloui (2004), Plum & Esrig (1969)

Table 2.4: Clays tested in laboratory thermal studies

Author	Clay studied	LL	PI	Test
This study	kaolin	65	34	Triaxial
	Durham clay	42	23	
Campanella & Mitchell (1968)	kaolin	-	-	Triaxial
	Illite	-	-	
Plum & Esrig (1969)	Newfield clay	22	44	Consolidometer
	Illite	112	84	
Towhata et al. (1993)	MC clay (kaolin)	70	29	Consolidometer
	Bentonite	450	421	
Hueckel & Pellegrini (1992)	Boom clay	High plasticity		Triaxial
	Pasquasia clay	Low plasticity		
Burghihnoli et al. (2000)	Fiumicino clay	55	32	Odometer
	Bologna clay	63	38	
Cekerevac & Laloui (2004)	kaolin	45	24	Triaxial
Abuel-Naga et al. (2007)	Bangkok clay	103	60	Odometer
	Todi clay	52	30	
Yavari et al. (2016)	kaolin	57	24	Direct shear

and Hueckel & Pellegrini (1992), as described in Table 2.4.

Campanella & Mitchell (1968) studied the thermal effects of clay using modified triaxial equipment, permitting simultaneous control of both the temperature and stress conditions applied. The cell temperature was controlled to an accuracy of ± 0.5 °C with temperature varying between 4 °C and 60 °C. Testing was carried out on cylindrical samples with a diameter of 35 mm and length of 89 mm. Campanella & Mitchell (1968) studied remoulded illite specimens consolidated under an isotropic stress of 196 kPa at 18 °C. Primary consolidation was complete after 700 minutes, with secondary consolidation reported to be complete after 10,000 minutes. The sample was heated from 18 °C to 58 °C. During the heating phase water was drained from the sample. The amount of water drained was 1.8% of the sample volume.

Further work on elevated temperature effects on clay samples was conducted by Plum & Esrig (1969). Testing was carried out on Illite and Newfield clay. The remoulded samples were tested in a fixed ring consolidometer around which water circulated at a constant temperature. Testing was carried out at 50 °C and 24 °C, with three hours required to increase the temperature from 24 °C to 50 °C. For one test, the clay slurry was consolidated at a constant temperature of 24 °C with the

other test sample consolidated at 50 °C, both with a relatively low consolidation pressure applied. For a third test, a sample was loaded to 206 kPa for Newfield clay or 275 kPa for illite at 24 °C before heating to 50 °C where loading was continued. The testing showed that for lower pressures, samples were more compressible when tested at 50 °C as opposed to 24 °C. During the transitional tests, which were subject to 206 kPa of loading prior to temperature increase, Newfield clay experienced no volume change, whereas illite experience 1 % volumetric strain.

Towhata et al. (1993) conducted testing on a clay similar to kaolin, MC Clay, in addition to bentonite, using a conventional consolidometer which was equipped with a heater and a thermostat. The aim of this testing was to further understand the effect of temperature on consolidation effects of clay. The clay slurry was consolidated within an oedometer, which was within a water bath with a heater connected alongside an electric motor propeller to continuously stir the water creating a homogenous temperature. The clay slurries were first consolidated under a low pressure, with stress increments doubling the current pressure. Sample temperature was increased once the volume change had become negligible and primary consolidation was complete. For MC clay, the total stress was increased from 80 kPa to 160 kPa followed by temperature increases from 22 to 40, 60 and 90 °C. It was found that the temperature increase reactivated the volume change, as shown in Figure 2.15.

In normally consolidated clays, it was found that following primary consolidation, heating of the sample caused the volume contraction of the sample to be reactivated, providing further consolidation of the sample. Through normal consolidation of MC clay, the void ratio of a sample under 160 kPa was found to be around 0.2, with 2230 kPa producing a void ratio around approximately 0.1, both after 300 minutes without heating. With a temperature increase from 22 °C to 90 °C the void ratio of a sample was found to reduce by around 0.015, irrespective of the stress level applied. The only case in which stress level impacted upon the volume contraction was at 40 kPa. This was deemed due to the sample being similar to that of a slurry

and therefore more susceptible to contraction. Similar trends were found in the testing of bentonite.

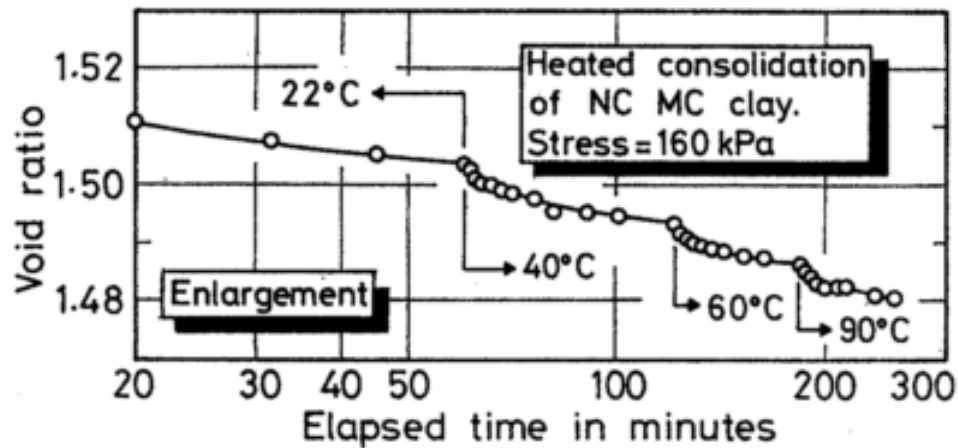


Figure 2.15: Development of consolidation with time for MC clay heated from 22 to 90 °C . (Towhata et al. (1993))

Identical testing was carried out on a sample of bentonite, which was consolidated under 20 kPa and 2230 kPa. For both pressures, heating reactivated the development of volume contraction which is similar to the behaviour observed for MC clay. Results show that the volume contraction of bentonite under 2230 kPa is greater than that of MC clay under the identical pressure. This gives an indication that the magnitude of temperature induced volume change is related to the plastic index of both clay.

More recently, Cekerevac & Laloui (2004) conducted a study on kaolin clay, using a temperature controlled triaxial cell which allowed for independent control of stresses, strains, pore water pressure and temperature. In this set up, heating of the sample occurred by indirectly heating a metal tube placed within the triaxial cell to spiral around the sample. The temperature within the cell was monitored by two thermocouples diametrically placed approximately 0.5cm from the sample. Normally consolidated samples were tested at an effective stress of 600 kPa, and overconsolidated samples were tested with an OCR = 1, 1.5, 2, 6 and 12. Results, given in Figure 2.17, showed normally consolidated samples producing a light contraction, lightly consolidated samples showed small thermal contractions following

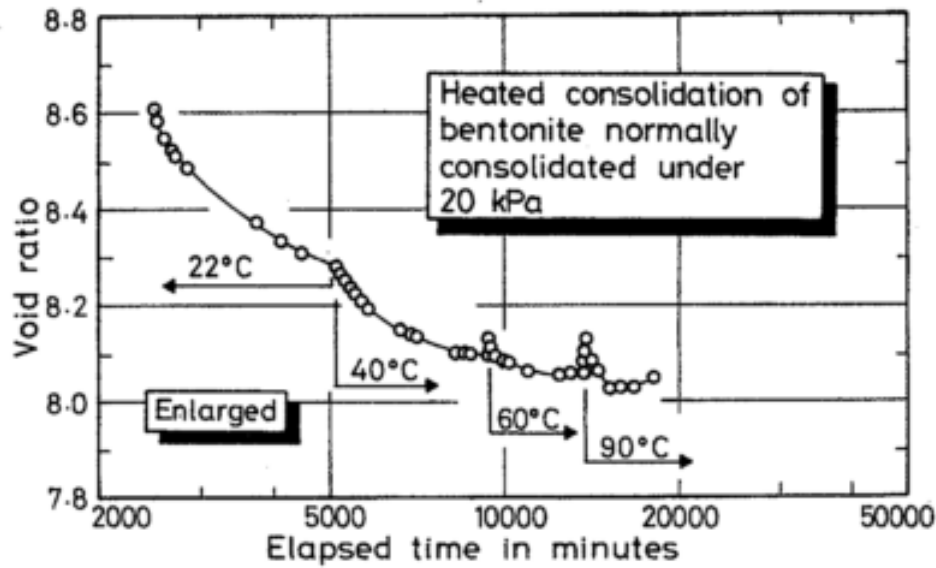


Figure 2.16: Development of consolidation with time for Bentonite heated from 22 to 90 °C . (Towhata et al. (1993))

initial dilation and overconsolidated samples displayed thermal expansion. It was noted that thermal expansion increased with increasing OCR values. Cekerevac & Laloui (2004) concluded that thermal volumetric strain depends on the stress history (OCR) of samples, with heating of normally consolidated samples producing contraction of the sample, whilst overconsolidated samples dilate.

When considering the effect of the maximum temperature which a sample is heated to, Burghignoli et al. (2000), through oedometer testing, found that for samples which had not previously been subject to temperature increase, the absolute maximum temperature the sample is exposed to does not appreciably impact on the mechanical behaviour of the soil skeleton. However, samples that have previously experienced higher temperatures show an increase in initial stiffness.

In summary, all authors observed a volume change in the clay samples subjected to temperatures below 100 °C. The degree of volume change has been found varying depending on the plasticity and stress history of the samples. Across the studies, it can be seen that there is a variety of approaches to testing and material considered. This has produced a range of discrete tests and evidence, however difficulty comes in presenting a unified understanding of a clay's bulk behaviour response to

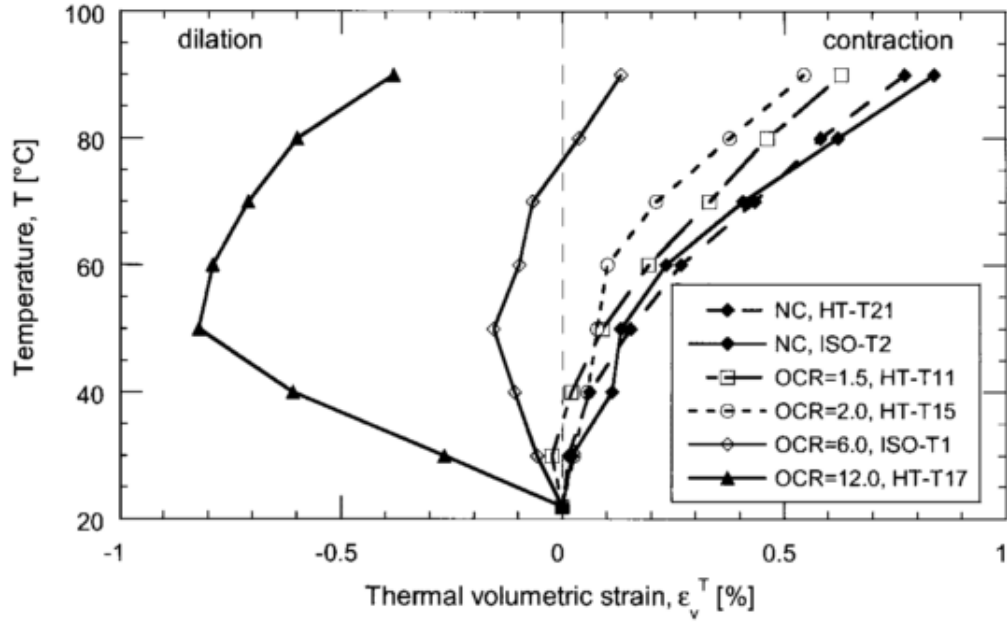


Figure 2.17: Thermal volumetric strain of kaolin during heating from 22 to 90 °C with an initial consolidation pressure of 600 kPa. (Cekerevac & Laloui (2004))

temperature.

2.6.2 Shear strength

This section discusses the work of Hueckel (2002), Yavari et al. (2016) and Cekerevac & Laloui (2004) in developing an understanding of shear strength variation with temperature, through triaxial and direct shear testing.

Hueckel (2002) identified that peak strength of Spanish clay, with $OCR = 6$, decreased during constant heating at a confining pressure of 0.75 MPa. A study was conducted by Yavari et al. (2016), using direct shear testing, to investigate the shear strength of clay and the clay concrete interface. Both clay specimens, and the clay concrete interface were tested at temperatures of 5 °C, 20 °C and 40 °C, with normal stress values ranging from 5 kPa to 80 kPa. Testing was carried out using direct shear apparatus, equipped with a temperature controlled system. The kaolin clay samples tested had a liquid limit $w_L = 57\%$ and plastic limit $w_P = 33\%$. The samples were consolidated with a vertical stress of 100 kPa in a 100 mm diameter oedometer cylinder.

To test the clay concrete interface, the thickness of the test specimen was reduced to 10 mm to accommodate a 10 mm piece of concrete, with a maximum roughness of 0.7 mm. This roughness was assumed to remain constant throughout the duration of testing. During each test, 100 kPa normal stress was applied to the sample to match that of the preconsolidation pressures. This range of stress is comparable to that of shallow geotechnical structures such as retaining walls and shallow foundations. Once vertical displacement was stabilised the temperature was increased from the sample's initial temperatures of 20 °C to 40 °C, in 5 °C increments every 15 minutes. This time duration enabled the vertical displacement to stabilise. Once 40 °C was reached, the sample temperature was held constant for 2 hours to dissipate the excess pore water pressure induced during heating. The aim of the study was to test samples within their thermoelastic domain, with similar void ratios for all tests, therefore the normal stress applied to the sample was decreased in accordance to the sample temperature. This, the authors stated, allowed for better detection of the shear behaviour, without the coupled effects induced by thermal consolidation. The shear stage of the test were carried out under drained conditions, with a shear rate of 14 $\mu\text{m}/\text{min}$, sufficiently slow to ensure no excess pore pressure accumulated within the sample during shear. Results showed shear hardening behaviour, whilst that of clay concrete interface shows a softening behaviour. For tests at the same normal stress, the peak shear strength of clay concrete interface was smaller than the shear strength of the clay specimen. This reduction from clay specimen shear strength to clay concrete interface is estimated to be 5.5 % at 5 °C, 12.5 % at 20 °C and 7.5 % at 40 °C. Overall, the author found the effect of temperature to be negligible on the shear strength of samples.

Cekerevac & Laloui (2004) studied the shear strength of clays with several OCR values with a effective stress of 600 kPa. The results of drained triaxial compression testing with identical initial states, for different temperature 22 °C and 90 °C, were compared for various OCR values. The results provided in Figure 2.18 indicate that samples with higher temperatures show high shear strength, however at large strains

the shear stresses obtained for high temperatures tend to the same critical state as samples tested at ambient temperature. It was concluded that high temperatures induce a more ductile mechanical behaviour, with heated samples displaying a higher shear strength. This effect was deemed to be more important for samples initially normally consolidated as opposed to over consolidated. No clear trend was apparent between the volume variation for samples sheared at different temperatures.

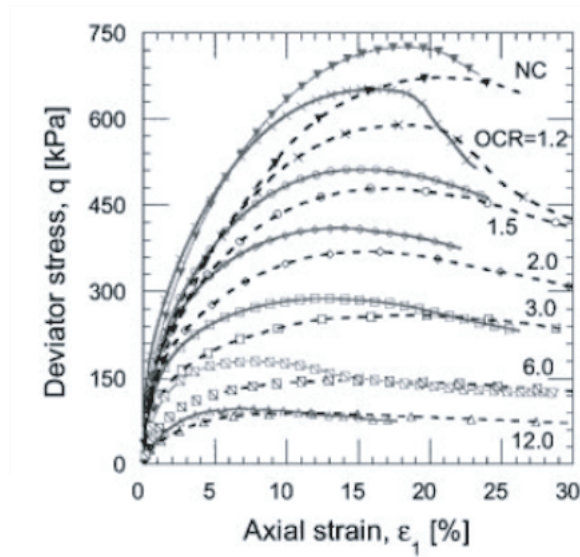


Figure 2.18: Drained triaxial tests at ambient (22 °C) and high (90 °C) temperatures: Consolidation pressure 600 kPa. Deviator stress vs axial strain, (Cekerevac & Laloui (2004))

2.7 Influence of cyclic temperature variation on the bulk behaviour of clay

This section builds upon the previous section to develop an understanding of the effects of cyclic temperature variation on the behaviour of clay samples. The following areas are again considered within this section:

- Volume change
- Plastic index

- Over-consolidation ratio

2.7.1 Volume change

Campanella & Mitchell (1968) studied the cyclic effect of temperature variation of clay samples, following on from the elevated temperature increase in Section 2.6.1, which saw a 1.79% decrease in an illite sample volume following the primary temperature increase from 18 °C to 58 °C. During the primary temperature decrease to 18 °C, 0.74% of the 1.79% relative sample volume was reabsorbed. The sample was then further cooled to 4 °C, which saw an addition 0.50% of sample increase. This equates to a decrease in sample volume at an average rate of 0.04%/°C and a average increase in sample volume of 0.02%/°C. During the second heating phase, from 4 °C to 59 °C, 1.36 % of the sample's relative volume was drained, with 1.20% being reabsorbed over the same temperature range during the second cooling phase. The volume change relative to the initial sample volume is illustrated in Figure 2.19. It can be seen that there is a significantly larger initial volume loss during the initial temperature cycle only. Subsequent cycles drain relatively less volume to that of the initial cycle. The drainage curves for this test, followed similar trends to normal consolidation curves, with volume change being a result of effective stress changes. The variation in drainage amounts from first to third cycle has been described to be similar to that observed during recompression cycles.

Campanella & Mitchell (1968) evaluated the experimental results, producing Figure 2.20, which shows the change in height of the sample, alongside the calculated water drained from the sample due to the change in temperature. These results showed that a permanent volume decrease of approximately 1% occurred following the initial temperature cycle, with subsequent permanent volume changes being relatively small at around 0.1%, occurring only at high temperatures.

Following from the testing described in Section 2.6 by Towhata et al. (1993), the testing continued with further temperature cycle variations with results shown in Figure 2.21. It was found that similar, irreversible volume change occurred in

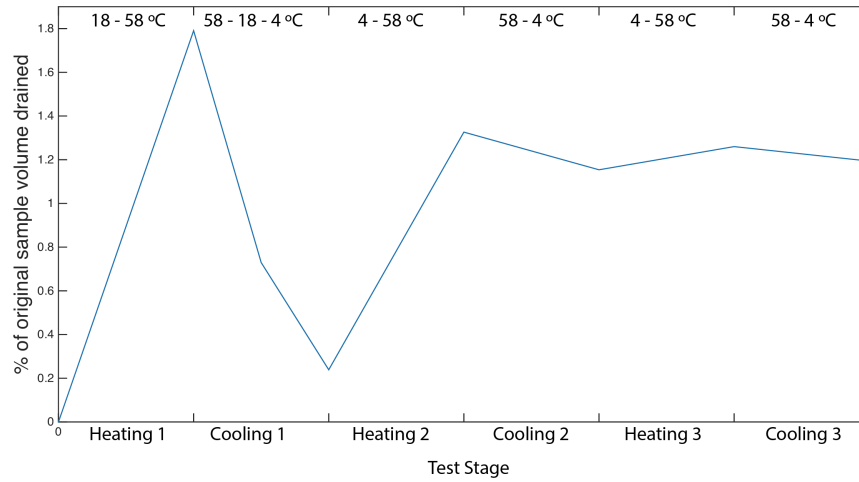


Figure 2.19: Relative volume change over 3 heating cycles for illite sample tested in Campanella & Mitchell (1968)

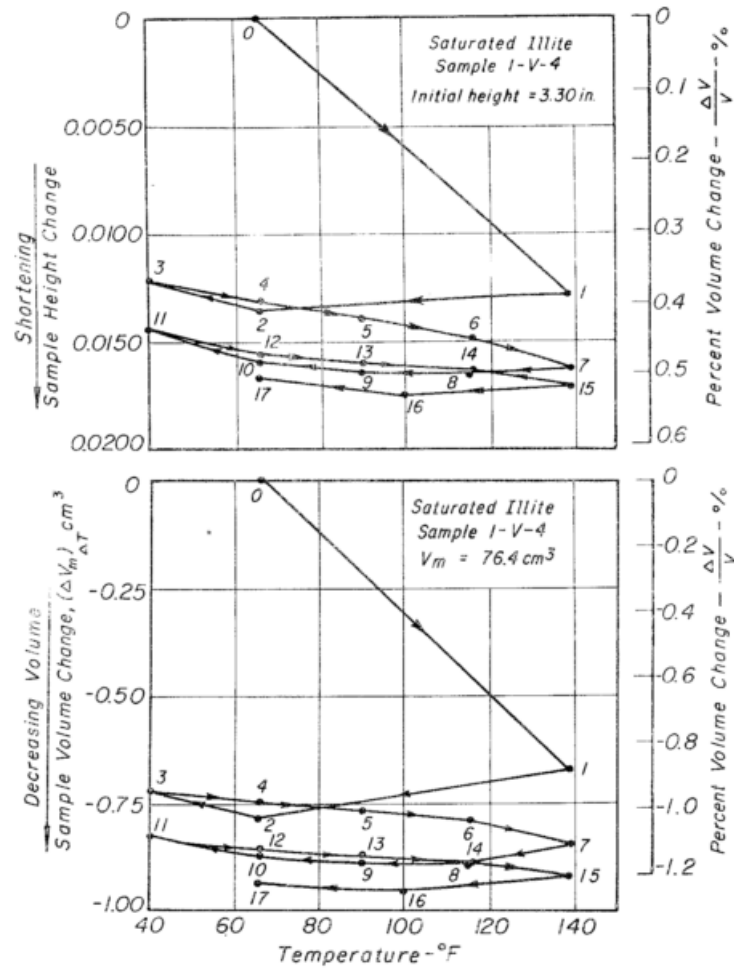


Figure 2.20: Effect of cyclic temperature variation on height and volume change for Illite sample (Campanella & Mitchell (1968))

MC clay, as reported by Campanella & Mitchell (1968). This irreversible volume change was also observed under a higher stress level of 2230 kPa. In summarising the observations it was found that the amount of volume contraction was found to be independent of stress level, with the exception once more of 40 kPa stress, which remained as a slurry, as previously described in Section 2.1.1.

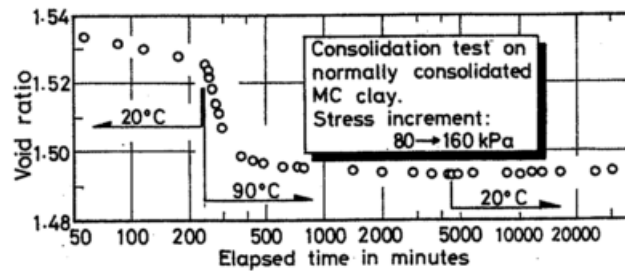


Figure 2.21: Effect of temperature cycle on volume change of MC clay (Towhata et al. (1993))

Hueckel & Pellegrini (1992) conducted an experimental study using a high pressure, high temperature triaxial apparatus. A lateral heater was placed around the cell to heat the cell water and sample. Samples tested were Boom clay which is of high plasticity and Pasquasia clay which is of medium plasticity. Both samples were tested under un-drained conditions at a constant total non-isotropic stress state. Samples were heated un-drained in small temperature increments to allow pore pressure to stabilise within the sample. The results presented derived some basic conclusions on the thermomechanical failures of clay. The first test was carried out on a sample normally consolidated to 2000 kPa at a temperature of 21 °C. Heating was then conducted in an undrained condition to 74 °C then onto failure at 92 °C, with constant total stress. It was found that pore water pressure development during heating was substantial. Testing was subsequently conducted on an overconsolidated Boom clay sample ($OCR = 0.94$) subject to a temperature cycle 22.5 - 60 - 22.5 - 100 °C. During the 22.5 to 60 °C temperature increase a pore water pressure of 860 kPa was reached, however during the cool phase a pore water pressure drop of 1250 kPa was observed. An increase in water pressure of 1250 kPa was observed during the second heating phase from 2.5 to 60 °C. From 64 °C increased

axial strain, up to 5.4% was observed prior to stabilisation, before a slight drop in pore pressure occurred.

To further understand the reduction in pore water pressure induced by the drop in temperature, a second test was carried out at a lower temperature to provide a smaller change in temperature within the cooling phase. Cooling was initiated at 54 °C with the sample temperature decreasing to 29 °C. A significantly lower drop in pore water pressure was observed. A comparison of the strain was produced during isotropic unloading and reloading along the same stress path as that used in the thermal experiments. During this test, water was forced mechanically through variation of back pressure to equal that of the pore water pressure in the overconsolidated testing. Upon reaching 1200 kPa through mechanical methods, a much smaller axial strain was observed when compared to the thermally induced axial strain. Once the sample reached 2000 kPa, a smaller again axial strain was observed, 1.76 %. It was concluded through these series of tests that upon completion of undrained heating and cooling of saturated clays, a residual negative pore water pressure is induced. This was believed to be caused by a large plastic dilatancy occurring at an effective stress state close to the critical state.

To understand the compressibility of samples, Plum & Esrig (1969) used the same methodology as in Section 2.7. During transitional testing from 24 °C to 50 °C post heating, both materials continued to behave as normally consolidated clays. The effects of the material behaviour during heating and cooling were investigated, with results shown in Figure 2.22. It can be seen from the results that although cooling caused a slight expansion of the material, the volume change is too small to be shown within the figure. What is evident from Figure 2.22 is that the heating and cooling cycle has caused the soil to behave as if it were overconsolidated. It can be seen that as the pressure on the sample is increased post cooling, the new line of the consolidation curve has been displaced to the right, behaving more overconsolidated than the volumetric strain associated with heating would suggest. Plum & Esrig (1969) highlights that this response to temperature variation could pose issues with

the testing of natural soils that have been heated and re-cooled during the handling period. This temperature variation could lead to an incorrect evaluation of the maximum previous pressure the sample had been subject to. It was found that when a sample is unloaded and then reloaded, it arrives at the void ratio associated with the maximum previous pressure at a somewhat lower stress level and does not rejoin and continue its original stress-strain curve until the maximum previous pressure is exceeded.

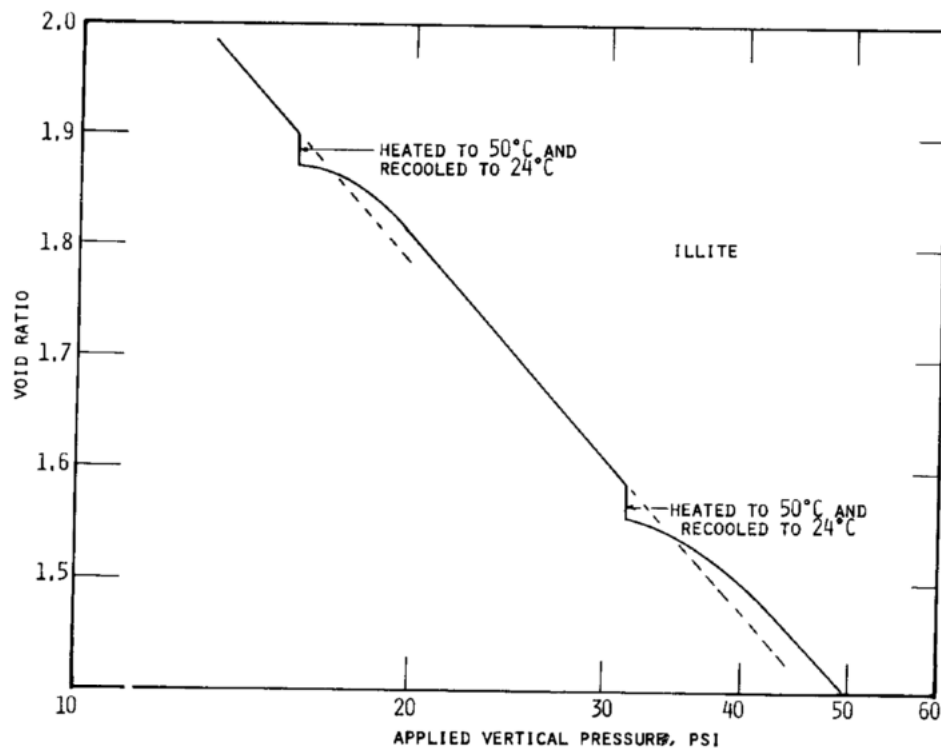


Figure 2.22: Effect on stress-strain behaviour in consolidometer of heating and cooling illite. (Plum & Esrig (1969))

With regard to how temperature affects pore water pressure, following on from Campanella & Mitchell (1968), a thorough investigation found that for undrained conditions, pore water pressures variation during heating and cooling should form a hysteresis loop, with porewater pressures increasing and decreasing with temperature, similar to that of repeated loading, suggesting that clays such as Newfield clay should experience no significant decrease in volume during temperature variation and that pore water pressure should be predictable from results of a triaxial tests with all principal stresses equal.

Plum & Esrig (1969) tested this hypothesis on a undrained sample where it showed that there was a gradual increase in pore water pressure for four temperature cycles after which no increase in excess pore pressure was observed with additional cycling. Therefore four temperature cycles were required before the hysteresis loop was developed, unlike testing carried out by Campanella & Mitchell (1968) on San Francisco Bay mud which immediately produced a hysteresis loop. Plum & Esrig (1969) believes the differences in the two sets of results is due to drained tests which were carried out on the sample tested by Campanella & Mitchell (1968) prior to the undrained testing. This subsequently allowed for a hysteresis loop to be formed from the onset for illitic soil and the use of kaolitic material which was overconsolidated. Plum & Esrig (1969) concluded that the volume change associated with overconsolidated clays was less important than normally consolidated clays.

Burghignoli et al. (2000) conducted an experimental study using modified tri-axial testing on three different types of clay. Clays tested were of medium to high plasticity; Todi clay, Fiumicino clay, and Bologna clay. Testing was carried out at effective stresses ranging from 20 kPa to 980 kPa. During the drained heating phase for normally consolidated samples, a volume reduction was observed, which was far greater than that experienced with a sample which remained at constant temperature. Once the samples reached their maximum temperature, they were held at constant temperature where additional large volume changes were observed, although at a decreased rate to that during the heating phase. Upon cooling, the sample continued to reduce in volume until the initial temperature was once again reached. Once the sample reached its initial temperature, no further volume change occurred. This trend was observed across different values of effective stress. For overconsolidated samples, ranging from $OCR = 1$ to 20, it was found that during heating the sample experienced an increase in both volume and void ratio, which continued to develop, but at a decreasing rate once the temperature was held constant. This trend was observed across the range of OCR. Once cooling occurred, a very small volume reduction developed at almost constant void ratio. At the point

which the initial temperature was once more reached, no further appreciable volume or void ratio variation were observed. Test observations showed that the thermal behaviour depends upon; the duration of time elapsed between the end of the consolidation period and the beginning of the temperature increase, the duration of the heating phase, and the thermal history of the sample. Different overconsolidation ratios and recent stress histories were shown to produce significantly different behaviours.

To further understand the behaviour of clay under cyclic temperature variations, Burghignoli et al. (2000) conducted undrained testing in addition to drained testing. Undrained testing was conducted on large-size specimens whose results produced more quantitatively significant data due to the relatively smaller influence of volume change within the measuring equipment. During the initial heating phase on normally consolidated sample, the increase in temperature promoted an increase in pore water pressure. The increasing levels of pore water pressure continued during the period of constant pressure, albeit at a lower rate. During the following stage, drainage was allowed with excess pore water pressure dissipating. A second heating phase was then carried out under undrained conditions, again an increase in pore-water pressure was observed alongside the temperature increase. After drainage was allowed, the temperature of the sample was then decreased with undrained cooling occurring. During the two cooling phases, the porewater pressure decreased as the temperature decreased thus a build up of negative pore water pressure was observed. During the drained periods of cooling, almost all excess negative pore water pressure was dissipated. Similar observations were found across the range of drained, normally consolidated samples tested. When testing a sample with $OCR = 4$, during the initial heating phase pore water pressure increased with temperature, until the temperature was held constant when the pore water pressure tended to progressively decrease. This behaviour was repeated during the second temperature increase. After being held at a constant high temperature, the sample was subjected to a drained cooling phase, followed by an undrained cooling phase. Burghignoli et al. (2000) do

not provide the observations for the overconsolidated sample during cooling.

The amount of volumetric strain generated at a constant effective stress due to heating has been found by Hueckel (2002) to be dependant on the effective stress which is applied to the sample. During heating, volumetric strain results are expansive and reversible at low stress, however during high stress compression is observed which is irreversible. This observed behaviour is shown in Figure 2.23. What is not apparent from this study is the duration over which heating and cooling was carried out and the subsequent pore water pressures.

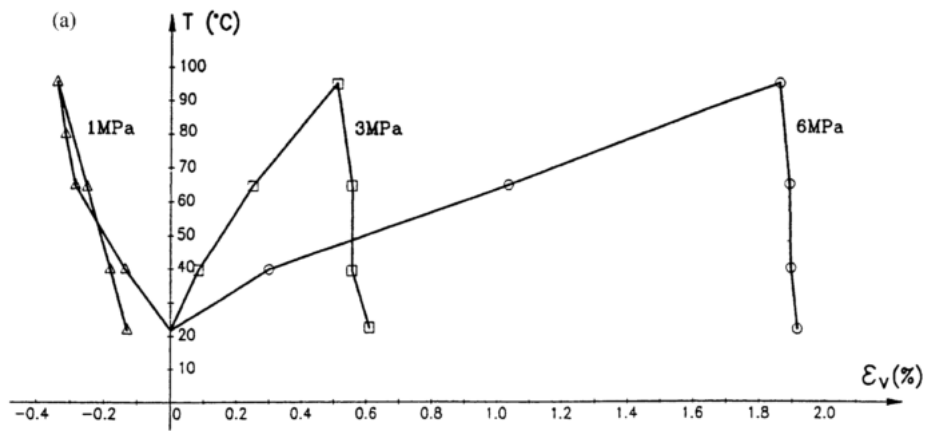


Figure 2.23: Thermal strain of Boom clay during heating stage during oedometer testing, at different constant stress values (Hueckel (2002))

Abuel-Naga et al. (2007) conducted cyclic oedometer testing on soft Bangkok clay within the temperature range of 22 - 95 °C. The testing equipment featured conventional oedometer equipment, with the inclusion of a ring heater attached to the outer ring of the oedometer. The heating system was regulated using a thermocouples and a water bath. Ambient temperature of 22 °C was increased to 90 °C over a 20 minute duration, ensuring no excess pore pressure was induced. Sample temperature was held until the sample volume change stabilised. Samples were tested with different pre-consolidation pressures of 100, 200 and 300 kPa and with varying OCR of 1, 2, 4 and 8. Testing showed that normally consolidated clays contracted irreversibly and nonlinearly upon heating, with highly overconsolidated clays found to exhibit reversible expansion. Further study of the normally consolidated samples

showed that under an 100 kPa vertical effective stress followed by a drained heating and cooling cycle, an apparently overconsolidated state was induced, with further loading required before the sample reached the yield mode again.

In summary, there is consensus across authors that:

- increasing sample temperature without adequate time for drainage will increase a sample's pore water pressure
- thermally induced change in void ratio and therefore volumetric strain of samples is independent of the magnitude of the applied stress
- normally consolidated samples, when heated, produce a volume and void ratio reduction
- cyclic temperature variation on normally consolidated samples has been found to produce an apparent overconsolidated state, found to be independent of stress level
- there is a strong dependency between OCR and a sample's response to cyclic temperature variation
- heavily overconsolidated samples display a thermal volumetric dilation
- lightly overconsolidated samples display an initial thermal volumetric dilation before contraction, providing a net contractive behaviour
- post heating phase cooling does not produce an appreciable change in void ratio

2.7.2 Plastic index

Towhata et al. (1993) developed a temperature controlled oedometer in which samples of MC clay (kaolin) and bentonite were tested to understand the differing response to temperature for clays of different plasticities. The results of testing by Towhata et al. (1993) are provided in Figure 2.24 and 2.25.

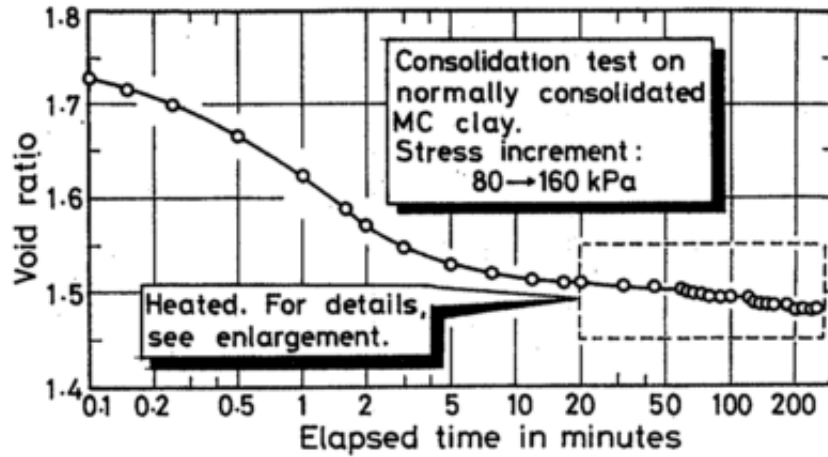


Figure 2.24: Development of consolidation with time of MC clay undergoing 160 kPa stress (Towhata et al. (1993))

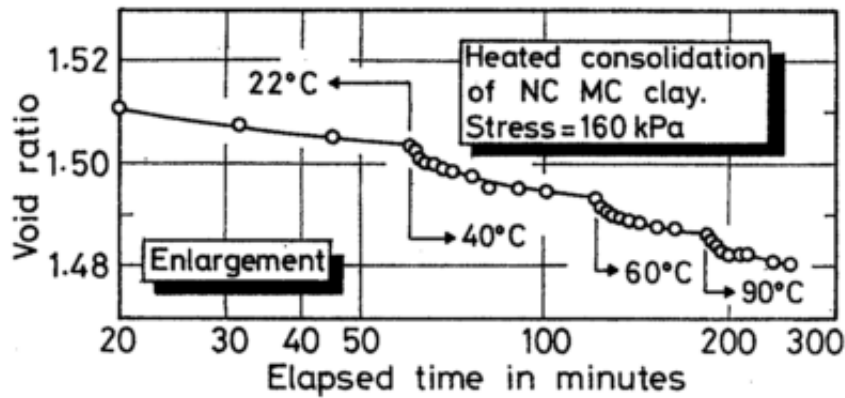


Figure 2.25: Details of test results illustrated in Figure 2.24 (Towhata et al. (1993))

Following consolidation at 2230 kPa, MC clay of low plasticity had a resulting void ratio of 0.845. For the same consolidation pressure, the high plasticity bentonite sample had a resulting void ratio of 0.615. Following the staged temperature increase, it can be seen that the MC Clay has a reduction of 0.025 in void ratio, whereas bentonite has a reduction of 0.075. This is a void ratio change of 3% for MC clay and 12% for bentonite.

Within the literature by Towhata et al. (1993) no consideration has been given to the impact of surrounding water and clay particle size on the clay's response to temperature cycling. In summary, it has been observed that clays of higher plasticity drain greater amounts of pore water over identical temperature increases.

2.7.3 Overconsolidation ratio

By studying Boom Clay, Hueckel (2002) found that changes in the overconsolidation ratio (OCR) occurred. Following a cycle of drained heating and cooling, at a constant pressure, a normally consolidated clay, upon further loading behaved elastically, requiring a significant amount of further stress increments in order to reach its yield mode again, shown in Figure 2.26. This implies that heating and cooling cycles significantly increase the yield domain.

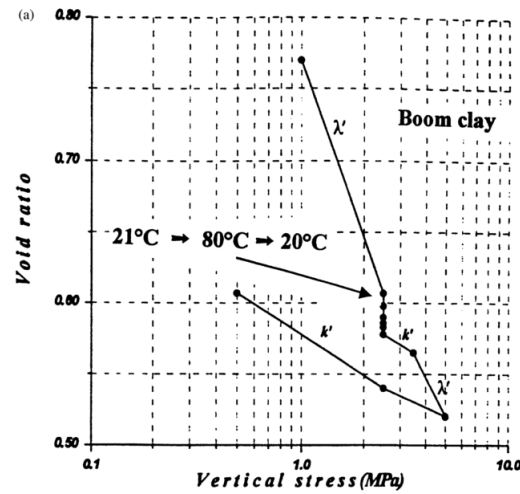


Figure 2.26: Change in apparent overconsolidation ratio occurring in Boom Clay due to heating (Hueckel (2002))

Chapter 3

Apparatus, materials and procedures

This section discusses the chosen test methodology which includes a series of element testing within the laboratory using a developed thermal triaxial set-up. Clays of two different plasticities have been tested at elevated temperatures including cyclic temperature variation.

3.1 Triaxial apparatus

The triaxial system used for testing is a Bishop and Wesley stress path triaxial cell which has been modified to accommodate thermal testing as detailed in Section 3.2. The cell accommodates samples of 100 mm length and 50 mm diameter. The system combines three Global Distribution System (GDS), as shown in 3.1, pressure control transducers to apply cell, back and lower chamber pressure (axial load) to the sample.

Throughout testing the following variables were recorded:

- Pore water pressure at the top and bottom of the sample – from pore pressure transducers
- Axial strain in the sample – from local Linear Variable Differential Transducers

(LVDT)

- Radial strain in the sample – from local LDVT
- Temperature of the sample – from thermocouples embedded in base and top cap
- Cell volume – from GDS pressure controller
- Cell pressure (σ_3 – from GDS pressure controller)
- Back volume (sample volume) – from GDS pressure controller
- Back pressure (u) – from GDS pressure controller
- Lower chamber pressure – from GDS pressure controller
- Axial load - from load cell

The local LVDT's used have an accuracy of 0.1% and resolution for $\pm 5.0\text{mm}$ of $0.2\mu\text{m}$. It was confirmed through correspondence with GDS Instruments that the LVDT's were unaffected by the temperatures used within this study. The membrane used was also confirmed by the manufacturers to be unaffected by the temperatures used in this study.

3.2 Heating system

In literature, many authors have applied different approaches to include temperature variability in their testing. A thermally controlled triaxial apparatus has been developed to allow elevated and cyclic temperature to be monitored and applied to samples. This has been developed following the guidance provided by Cekerevac (2003). The thermally controlled triaxial equipment used for testing is shown in Figure 3.1. A copper coil has been constructed using 4 mm copper piping with a height 170 mm and diameter of 140 mm. This coil surrounds the clay sample to provide constant heating ($\pm 0.5^\circ\text{C}$) across the length of the sample. This allows for

the temperature of the water within the triaxial cell to be increased and decreased by changing the temperature of the circulating water. Water is circulated through the coil from the water bath using a peristaltic pump. Water returns from the cell to the base of the water bath. The combination of the pump outlet and the return inlet provides a self stirring water bath to ensure a consistent temperature within the water bath.

The temperature within the cell is monitored using 7 k-type thermocouples. In order for these to be accommodated the additional entries to the cell were located within an expansion ring which was developed during this study. Thermocouples were mounted within drilled blanking plates and sealed with epoxy resin. A National Instruments CompactRIO data acquisition controller was used to control the temperature cycling of the sample, allowing for the temperature within the triaxial cell to control by the temperature of the water bath circulating the cell coil.

A bespoke NI programme controlled the temperature of the water bath allowing the temperature profiles, given in Figure 3.2, to be applied. The 24 °C test was conducted with water circulating the copper coil at laboratory temperature. During testing, water was circulated constantly at the profile temperature to ensure the sample remained at the desired temperature. Photographs of the set up are provided in Figures 3.3, 3.4 and 3.5 to give further understanding of the test set-up.

In previous literature by Cekerevac & Laloui (2004) it has been stated that a temperature increase at a rate of 10 °C per 3 hours in kaolin with drainage allowed, was sufficiently slow enough for the temperature to increase without a generation of excess pore pressures. The same rate of heating was applied during this series of tests, with the pore water pressure monitored to ensure no build up of excess pore water pressure occurred.

During the heating stage of the test, drainage from the sample was permitted, followed by undrained shearing on the sample. This approach has been adopted following the literature review findings that the clay's microstructural response which identified a complex range of effects, potentially occurring within a sample during

the heating and shear stages. Through consolidated undrained testing, the ability to isolate the effects of the combined microstructural effects was achieved, with pore pressures being recorded during testing. Undrained testing is also representative of a ‘real world’ impermeable clay where the level of drainage is reduced. Shearing of the sample was carried out at a slow rate of 0.005 mm/min, comparable to the drained testing carried out by Cekerevac (2003). The slow rate of shearing is representative for testing carried out to understand the influence of static building imposing a load onto the clay, and therefore providing an understanding of the clay’s ultimate strength.

3.3 Calibration

In order to calibrate the volume change of system water and to isolate the temperature effects on the system without the influence of a clay sample, a brass sample was installed within the cell. Unfortunately, when processing the results it was realised that a leak occurred within an internal fitting during testing, whereby water continually drained from the cell volume to sample volume, which is not possible for a brass sample.

An alternative approach was used to determine the system water volume change by measuring the temperature of the outlets, using a laser thermometer, and the volume of water within the piping. The thermal volumetric expansion of the water within the outlets was then calculated for application of the 40 and 60 °C temperature profiles.

The total volume of the external outlets within the system was found to be $7 \times 10^3 \text{ mm}^3$ which was found to expand by $6 \times 10^{-5}\%$ for a 40 °C temperature profile and $3 \times 10^{-5}\%$ for a 60 °C temperature profile. For the internal outlets, a total volume of $6 \times 10^3 \text{ mm}^3$ was found to increase by $3 \times 10^{-4}\%$ for both a 40 °C and 60 °C temperature profile

As the percentage volume change falls within the accuracy of the equipment and is constant in all sample tests with the same applied temperature profile, no

correction was applied for the system volume change.

3.4 Clay properties

This study focuses on two clays; kaolin and Durham Lower Boulder Clay, known as Durham Clay throughout this thesis. The plasticity indices of the clays are provided in Table 3.1.

Table 3.1: Plasticity indexes of clays studied

	W_l	P_i	Source
Durham Clay	41.7	18.50	Glendinning & Hughes (2014)
Kaolin	64.75	30.45	Experimental testing

The mineralogy of kaolin with the same plasticity as used in this study has been detailed in Cekerevac et al. (2013). It was found by x-ray diffraction that the mineralogy of kaolin was kaolinite (67%), illite/mica (2%) and quartz (31%). This compares to Durham Clay, reported by Hughes et al. (2009), which found clay mineralogy to be composed of variable amounts of illite/smectite (mean of 49%), chlorite/smectite (mean 5%), illite (mean 19%), and kaolinite (mean 26%), with 2 μm fractions also containing small quantities of quartz and lepidocrocite. Durham Clay was found to be comparable to London Clay (Glendinning & Hughes (2014)) and therefore presented the type of clay found over 60% of the British Isles, representative of UK infrastructure.

3.5 Sample preparation

Testing was carried out on a high plasticity clay, kaolin and a low plasticity clay, Durham Clay. The Durham Clay was prepared by oven drying clay particles which passed through a 425 μmm sieve. Both kaolin and Durham Clay were mixed with water to form a slurry at a water content of 1.5 times their liquid limits. The slurries were then isotropically consolidated up to 500 kPa. Due to the sample height needed

for triaxial testing and the limitation of the consolidometer, upon reaching 200 kPa the samples were unloaded, with additional material added, before loading was reset and the consolidation continued. The confining and consolidation pressures are the same as those used by Cekerevac & Laloui (2004).

In order to verify the calibration and set up of the thermally controlled triaxial system, an initial unheated test was carried out using a kaolin sample. This initial test (further detailed in Section 4.1) allowed for any issues and problems, which had a potential to arise with setting up a new system, to be rectified.

To verify the sample temperature during testing, a sample of kaolin was installed within the triaxial cell with three thermocouples embedded into the sample through the membrane, sealed with silicon sealant. These were embedded into the sample at the top, bottom, and one in the middle of the sample. The sample volume was monitored during testing to ensure no cell volume leakage occurred, which would have potential to impact the sample temperature. Following testing, Figure 3.6 was produced showing the internal sample temperature during one temperature cycle, across the 100 mm height of the sample (Embedded top, middle and bottom). In order to determine the temperature of the sample from subsequent tests without embedded thermocouples, the top cap temperature has been used as a reference.

3.6 Completed tests

Testing has been carried out on both kaolin and Durham Clay, with the tests complete detailed in Table 3.2. Following calibration and control testing, the next stage of testing was addressed: elevated and cyclic temperature loading. As the temperature of the lab is at a constant of $24\text{ }^{\circ}\text{C} \pm 1^{\circ}\text{C}$, this formed the lowest temperature used in testing. Testing was carried out at either an elevated temperature or post cyclic temperature variation. Elevated temperature testing was carried out using a $40\text{ }^{\circ}\text{C}$ and $60\text{ }^{\circ}\text{C}$ temperature profile, with shearing taking place at laboratory temperature. For post cyclic temperature variation, testing was carried out following 5 and 10 temperature cycles, once the sample returned to room temperature.

For simplicity, the temperature applied will be reported rather than actual sample temperature through the chapters in this thesis.

Due to system failures and limited research time, the number of tests conducted with samples of Durham Clay and availability of repeated tests were significantly reduced from the original test plan. Table 3.2 details all tests which were terminated prior to completion. Testing was terminated for a variety of reasons, including the perspex triaxial cell wall fracturing, and leaks occurring through the thermocouple port. With regard to Durham Clay, one of the most common failures which occurred in testing was the LVDT's falling off the sample. This occurred due to the shrinkage of the sample and therefore the sample membrane contracting. This lead to the cell membrane peeling itself from the adhesive, midway through testing. This meant that many tests were terminated prior to their completion after up to 2 weeks of testing.

At various stages, testing was delayed due to thermocouple damage requiring replacement fittings to be made up, lower chamber leakages at pressure requiring replacement parts, damage to the heating coil fittings and a second fractured perspex cell wall.

Photos have been provided in Figure 3.7 of both kaolin and Durham clay samples following triaxial testing. It should be noted that a section of the sample has been removed for moisture testing, however the failure plane of the sample is still very visible. This failure is representative of all samples tested as part of this work.

3.7 Sample consolidation

In order to ensure a reliable laboratory set-up, graphs showing the consolidations stage for both clays across all tests have been provided in Figure 3.8 and 3.9. Table 3.3 provides an overview of the volumetric creep constant ($C\alpha_c$) for the test samples. Testing as part of this study did not consider secondary consolidation, therefore sufficient time was not allowed to assess the volumetric creep constant of the samples.

Table 3.2: Sample properties and laboratory testing overview

Test Name	Material	Moisture Content before test (%)	Void Ratio, e	Consolidated?	Test Type	Temperature profile (°C)	Comments
1_K_5C	Kaolin	30.59	1.15	Yes	5 Cycles	23 - 60 - 29 - 60 - X	Test failed after 2nd heating cycle
2_K_10C	Kaolin	-	-	-	-	-	Leak occurred during saturation stage
3_K_10C	Kaolin	29.14	1.04	Yes	10 Cycles	21 - 59 - 23 - 59 - 24 - 59 - 23 - 60 - 24 - 60 - 24 - 60 - 24 - 60 - 24	Complete test
4_Brass	Brass	-	-	Yes	-	-	Leak during heating stage
5_K_60	Kaolin	30.23	1.11	Yes	Elevated to 60C	24 - 60	Complete test
6_K_20	Kaolin	30.73	1.16	Yes	Bench mark	23.5 (average)	Complete test
7_K_40	Kaolin	30.83	1.28	Yes	Elevated to 40C	23 - 46	Complete test
8_K_5C	Kaolin	30.02	1.10	Yes	5 Cycles	24 - 52 - 33 - 54 - 33 - 53 - 33 - 54 - 24	Local LVDT failure
9_DC_20	Durham Clay	-	-	-	-	-	Leak during saturation
10_DC_5C	Durham Clay	20.90	0.66	Yes	5 Cycles	24 - 50 - 35 - 50 - 33 - 50 - 33 - 49 - 33 - 49 - 24	Complete test
11_DC_10C	Durham Clay	-	-	-	-	-	Leak during saturation
12_K_5C	Kaolin	27.68	1.00	Yes	5 Cycles	22 - 54 - 24 - 52 - 25 - 53 - 25 - 54 - 24 - 54 - 22	Radial LVDT fell off
13_DC_40	Durham Clay	-	-	-	-	-	Leak occurred during saturation stage, peak state data included
14_DC_60	Durham Clay	20.54	0.62	Yes	Elevated to 60C	22 - 57 (average)	Complete test
15_DC_10C	Durham Clay	20.21	0.63	Yes	-	-	Leak occurred during first heating cycle - consolidation stepped to prevent LVDT's dislodging
16_DC_10C	Durham Clay	20.00	0.61	Yes	10 Cycles	24 - 60 - 26 - 59 - 26 - 58 - 25 - 59 - 25	Leak occurred after 4 heating cycles. Consolidation stepped to prevent LVDT's dislodging
17_K_40	Kaolin	-	-	-	-	-	Leak occurred during saturation stage
18_DC_40	Durham Clay	-	-	-	-	-	Leak occurred during saturation stage
19_K_40	Kaolin	-	-	Yes	Elevated	22 - 41 (average)	Local LVDT's failed & missing moisture test results
20_DC_40	Durham Clay	-	-	-	-	-	Cracked cell
21_DC_40	Durham Clay	-	-	-	-	-	Fault occurred in GDS unit midway through consolidation, making multiple file test. Consolidation and heating unrepresentative.
22_DC_40	Durham Clay	20.41	0.64	Yes	Yes	23 - 42 - 45 (20 hours) - 42	
23_DC_40	Durham Clay	-	-	-	-	-	Leak from cell to atmosphere
24_DC_40	Durham Clay	-	-	-	-	-	Sample heated only
25_K_Verify	Kaolin	25.85	0.89	-	Elevated	22 - 53 - 24	

Table 3.3: Volumetric creep constants for kaolin and Durham clay samples tested

Clay	Test	$C\alpha_c$	Average
Durham clay	10_DC_5C	2850	3256
	16_DC_10C	1327	
	21_DC_40	5592	
kaolin	3_K_10C	4160	6046
	5_K_60	7038	
	8_K_5C	6940	

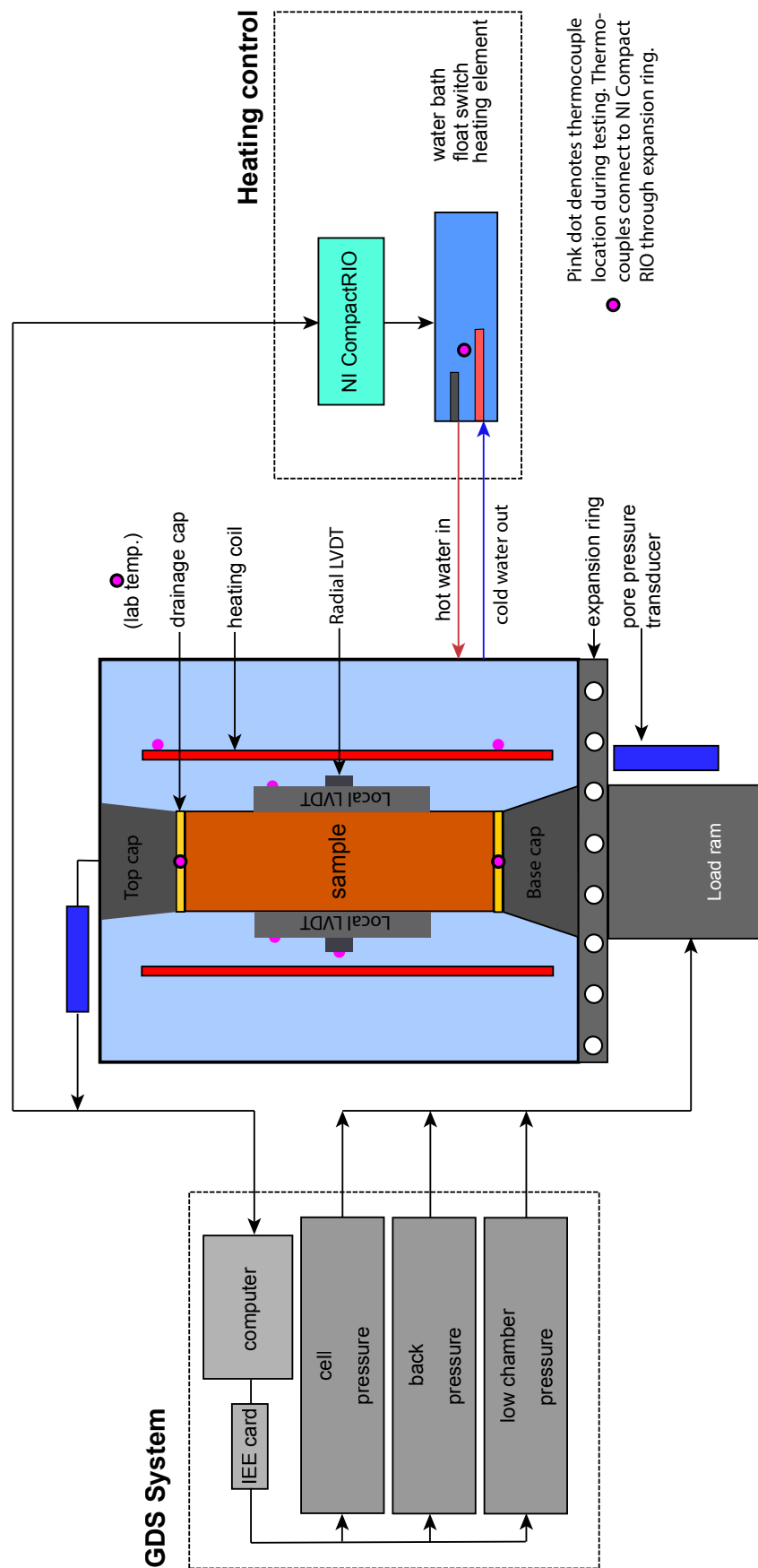


Figure 3.1: Schematic of modified triaxial apparatus

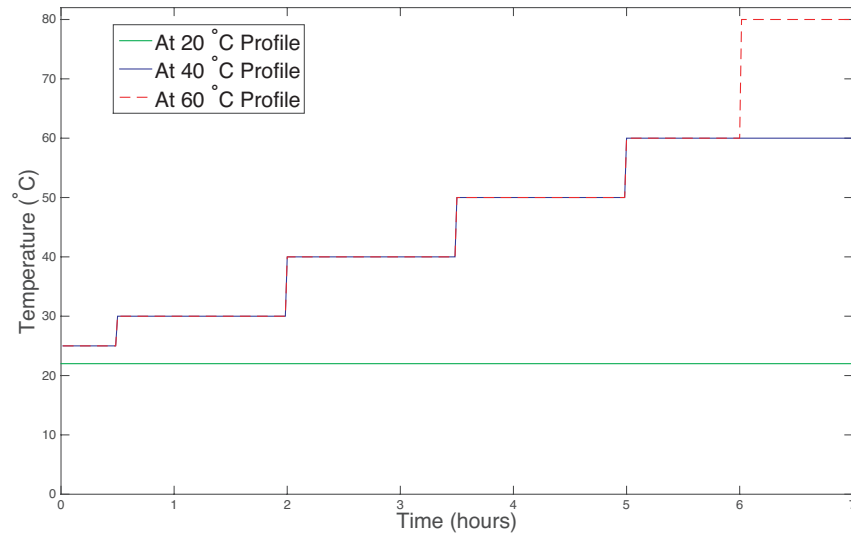


Figure 3.2: Water bath temperature profile for elevated temperature profiles

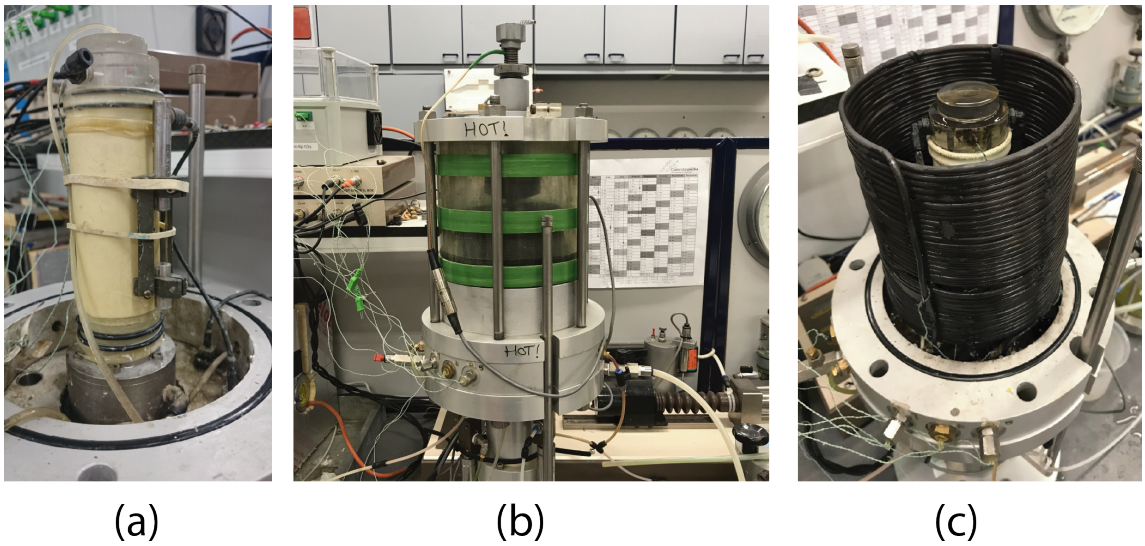
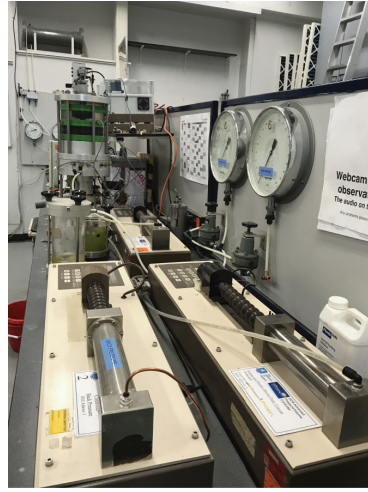


Figure 3.3: (a) Sample set up with local axial LVDT's being glued to sample (b) Triaxial Cell (c) Heating coil

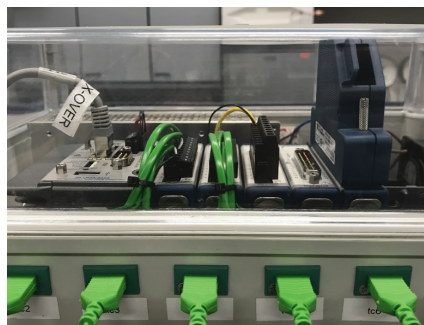


(a)



(b)

Figure 3.4: (a) GDS pressure transducers (b) Water bath and circulating pump



(a)



(b)

Figure 3.5: (a) National Instruments Compact RIO (b) Housed National Instruments Compact RIO on top of GDS LDVT data acquisition units

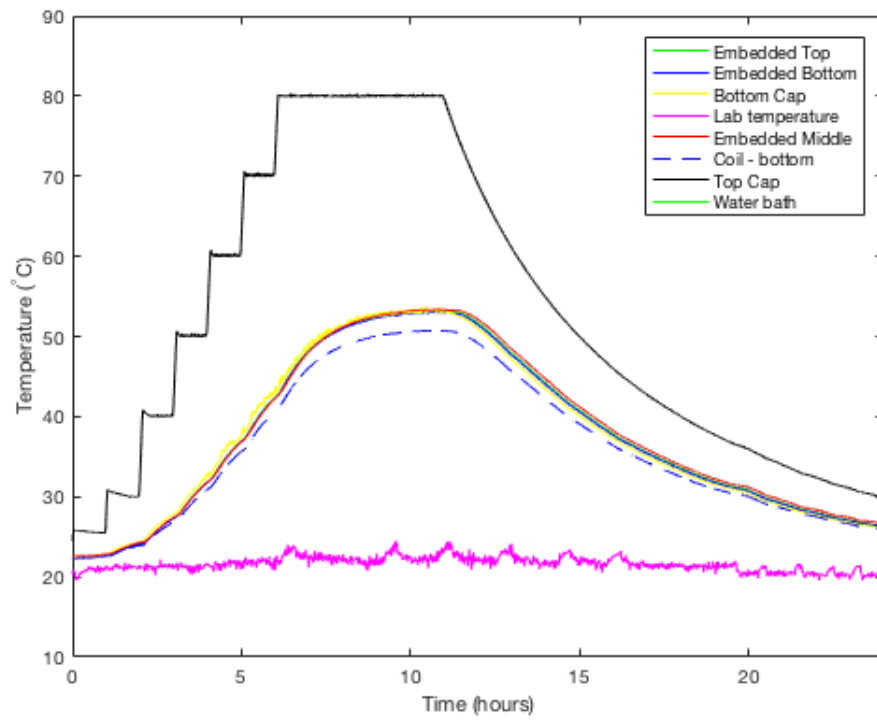


Figure 3.6: Temperature measured during thermal verification - 1 temperature cycle



Figure 3.7: Photographs showing samples post triaxial testing. Left -kaolin, Right - Durham clay.

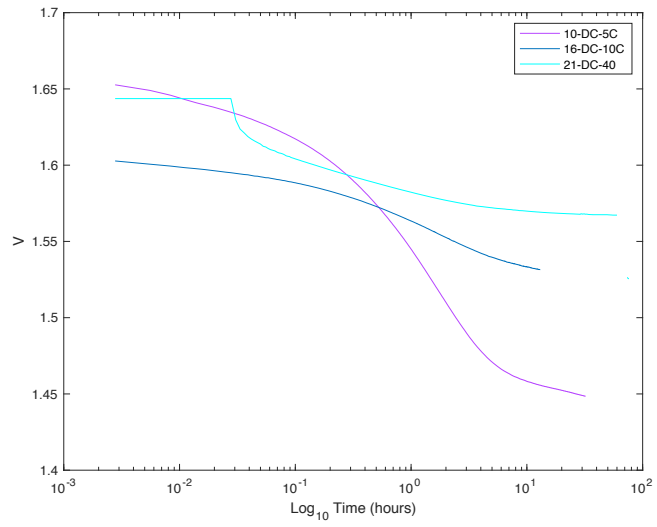


Figure 3.8: Consolidation stage - Specific volume vs. time for Durham clay samples

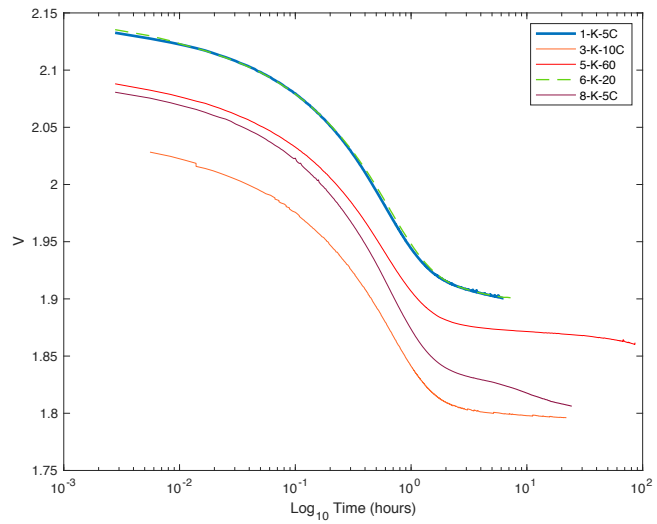


Figure 3.9: Consolidation stage - Specific volume vs. time for kaolin samples

Chapter 4

Elevated Temperature Tests

This section begins by reporting tests of kaolin tested at 24°C, lab temperature, as a baseline for thermal testing. Once the baseline for testing is established, presented are the experimental test results for kaolin and Durham clay subject to 40 °C and 60 °C temperature profiles. Full details of tests and actual test temperatures are provided in Figure ???. Samples were prepared following the methodology provided in Section 3.5, with all temperature profiles provided in Appendix A.

First the sample was tested by applying the associated temperature profile, 20 °C, 40 °C or 60 °C; the temperature was then held until the back volume of water remained relatively constant before the axial stress was applied to the sample. Testing was conducted following the stress path shown in Figure 4.1.

The stages of the stress path are as follows:

- 0 - 1 mean effective stress increase
- 1 - 2 temperature of sample increased
- 2 - 3 shear stress applied

4.1 Baseline testing

This section describes in detail the stages of a test carried out at 24°C (lab temperature), determining the volume of the sample water drained during heating, the

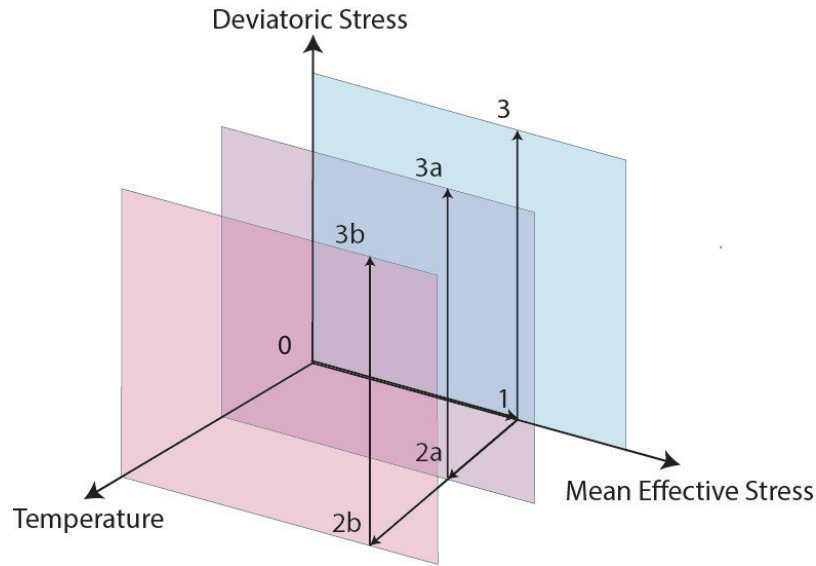


Figure 4.1: Stress path for samples tested at elevated temperatures

shear stage and the derivation of the angle of friction and finally the stiffness of the clay during undrained shear. The processes detailed in this section for the baseline test were subsequently applied to the additional samples within this study.

4.1.1 Heating stage

Testing was first conducted at laboratory temperature, which was maintained at 24°C. This ensured that the system was set up correctly, operated as expected and provided a benchmark for testing carried out at temperature. The data record during this test is given in Figure 4.2. The period between 0 and the dashed cyan vertical line represents the saturation period, cyan to dashed magenta vertical line the consolidation period, with the final stage magenta to end of testing being the shear stage.

For Test 6-K-20, as there was no heating period unlike subsequent tests, the final 18 hours of the consolidation period was taken to be the ‘heating period’ in order to provide comparison data.

Figure 4.3 has also been included, detailing Test 7K-40, to illustrate a test which was subject to heating, with the heating period shown between the dashed magenta and red vertical lines. The shear stage continuing after the dashed red vertical line.

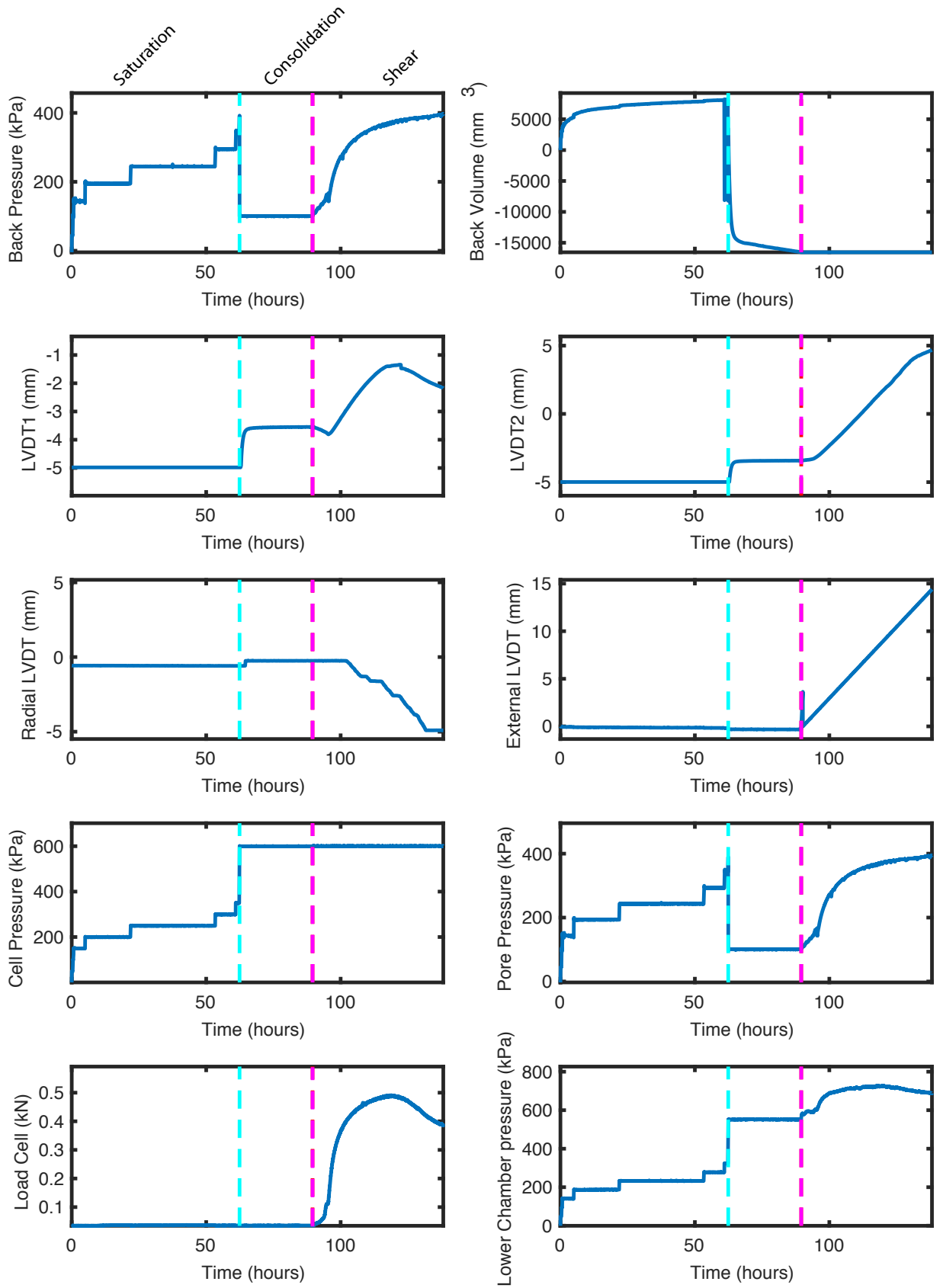


Figure 4.2: Plot of triaxial data for kaolin for Test 6-K-20

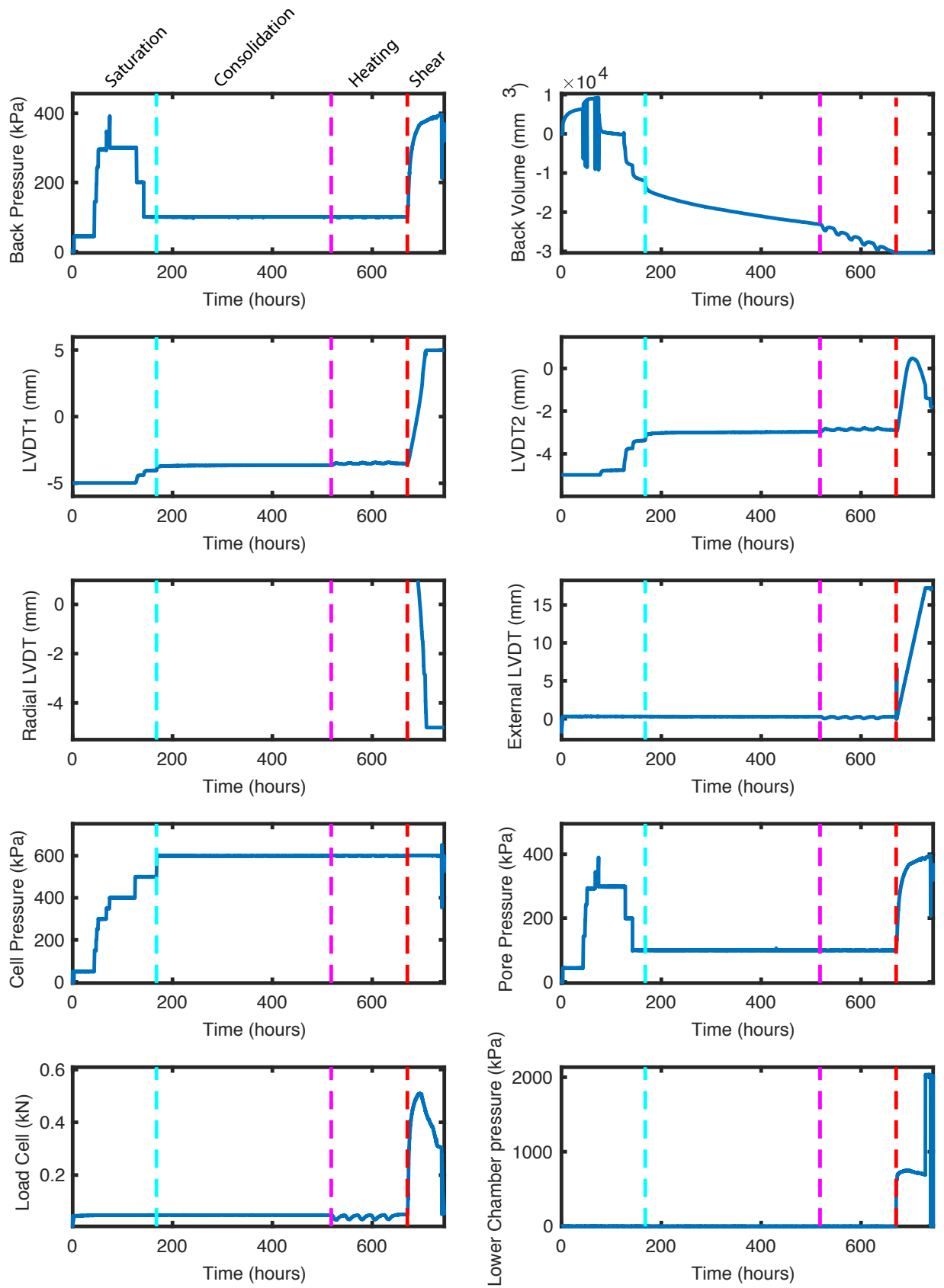


Figure 4.3: Plot of triaxial data for kaolin for Test 7-K-40

4.1.2 Stiffness

The undrained secant stiffness of the sample (G_u), has been determined through the stress-strain curve, as shown in Figure 4.5. Conventionally, when assessing the small strain stiffness of the material (G_u) the secant modulus is taken for a strain of 0 to 0.1 % as shown in Figure 4.4 for local LVDT's, a small strain stiffness. The following equations were used to determine G_u :

$$\delta\epsilon_q = \frac{\delta q}{3G_u} \quad (4.1)$$

$$G_u = \frac{\delta q}{3\delta\epsilon_q} \quad (4.2)$$

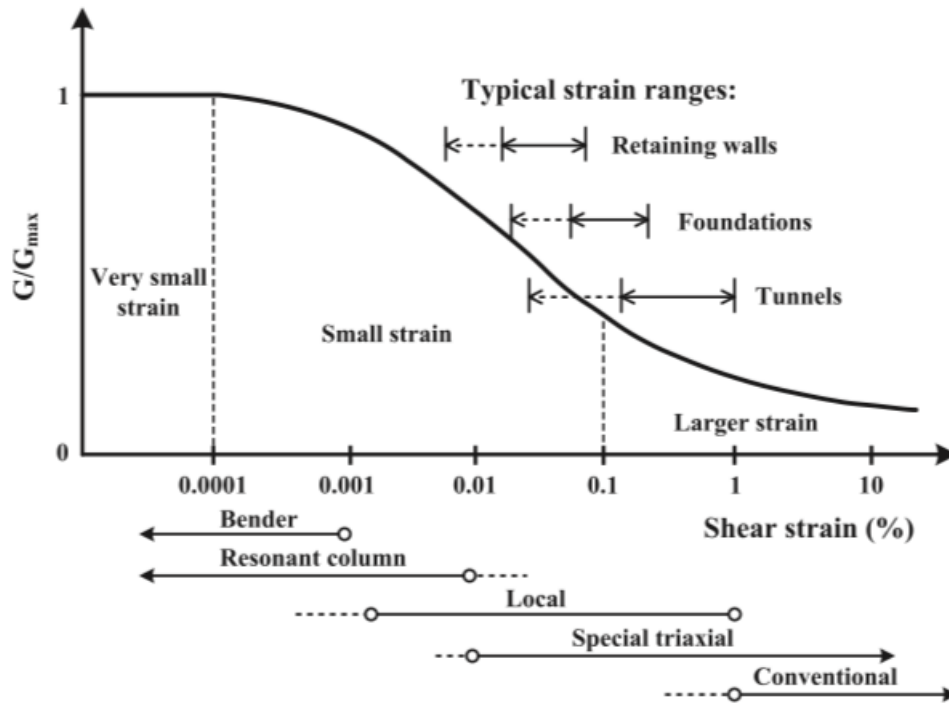


Figure 4.4: Normalised stiffness degradation curve. Taken from Likitlersuang et al. (2013)

Following this approach, a secant stiffness of 82 kPa was determined for the Test 6-K-20, however when considering the results in Figure 4.6 it can be seen that the small strain stiffness between 0 and 0.1 % is unrepresentative of the sample's actual stiffness, considered to be due to experimental errors as detailed by Likitlersuang

et al. (2013). Therefore the small strain stiffness of these samples has been considered between 0.21 and 0.24 % axial strain, with a reduction in range of axial strain due to portion of the small strain stiffness effect occurring during the initial stage which have been masked by the experimental errors. A secant stiffness of 159 kPa has subsequently been determined.

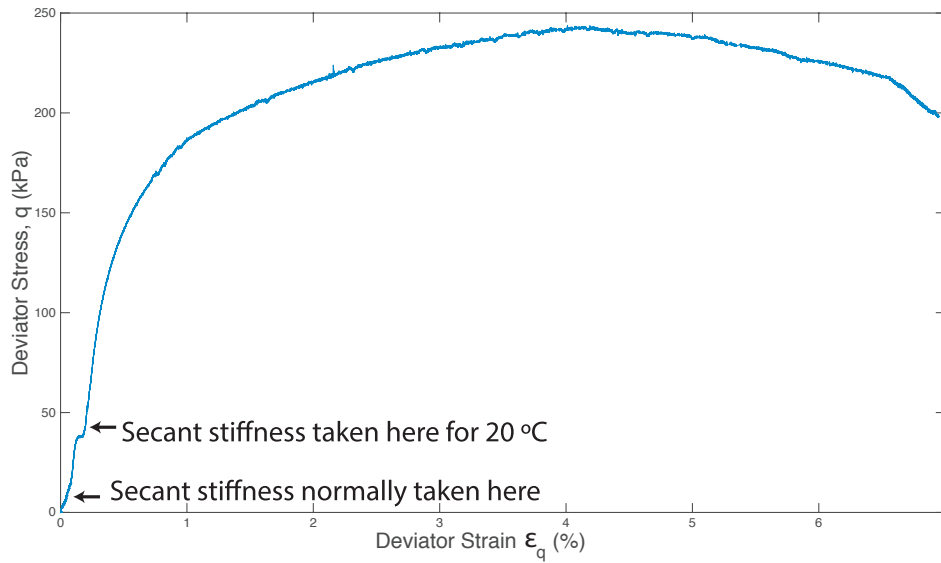


Figure 4.5: Deviator stress vs. deviator strain for Test 6-K-20

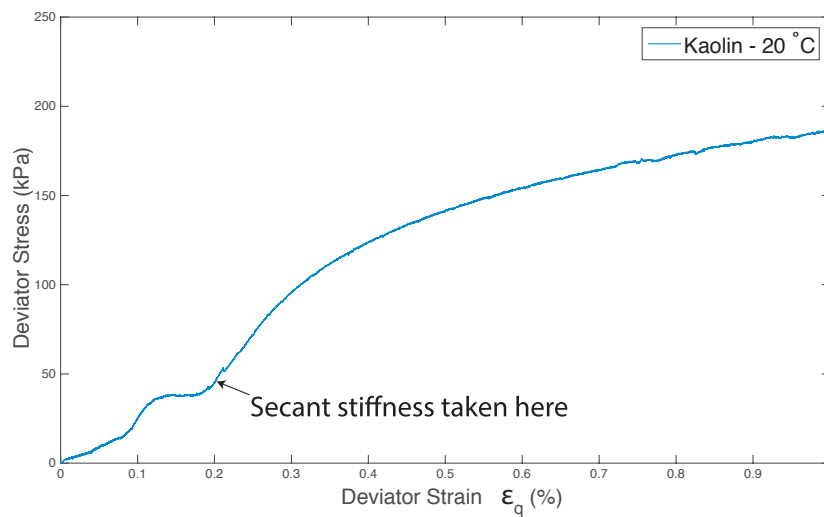


Figure 4.6: Deviator stress vs. deviator strain for sample tested for Test 6-K-20 up to 1 % Axial Strain

4.1.3 Critical state

Following the heating period, the drainage pathways were closed and shearing of the sample began. Data was plotted showing mean effective stress (p') vs. deviatoric stress (q) plots, as shown in Figure 4.7 where:

$$p' = \frac{\sigma'_1 + 2\sigma'_3}{3} \quad (4.3)$$

$$q = \sigma'_1 - \sigma'_3 \quad (4.4)$$

Where σ'_1 is the effective axial stress on the sample, calculated using the force from load cell and the cross sectional area, and σ'_3 being the effective cell pressure.

A frictional constant value (M) of 0.83 was found from the gradient of the Critical State Line (CSL), shown in Figure 4.7. Using the following equation:

$$M = \frac{6\sin\phi'}{3 - \sin\phi'} \quad (4.5)$$

A critical state friction angle (ϕ') was determined as 21° . This value is consistent to the 21° critical state angle of friction determined by Cekerevac (2003) discussed in Section 2, thus providing evidence of the accuracy of the experimental set up.

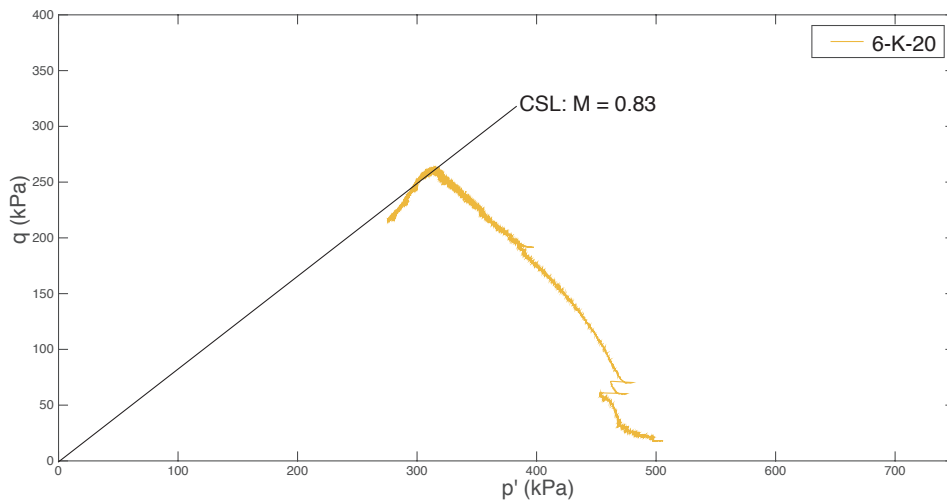


Figure 4.7: p' vs. q plot for kaolin Test 6-K-20

4.1.4 Summary

This section has described the methodology used to interpret the experimental results for Test 6-K-20, including the normalisation of the sample back volume, determination of the critical state friction angle and the small strain stiffness of the samples. It has been evidenced that the experimental system is set up to provide reliable results with regard to the critical state friction angle of the samples. The approach detailed in this section has been replicated for the elevated temperature samples within this section and the cyclic temperature variation samples included in Section 5.

4.2 Heating Stage

The results in this section show the variation in back volume during the heating stage when the 20 °C, 40 °C or 60 °C temperature profile was applied, for both kaolin and Durham Clay (tests 6-K-20, 7-K-40 and 5-K-60). It can be seen that the duration of heating varies between the tests in Appendix A. This is due to the varied durations required to increase the temperature of the sample whilst mitigating excess pore pressures. Details of the heating profile applied can be found in Section 3.2.

4.2.1 Kaolin

Building on the results for Test 6-K-20, samples were subject to the 40 °C (Test 7-K-40) and 60 °C (5-K-60) temperature profiles. The results of these are given alongside Test 6-K-20 in Figure 4.8. The variation in test duration between Test 6-K-20, Test 7-K-40 and Test 5-K-60, is due to the time required to heat the sample. The heating was carried out over a period of 6 hours for Test 7-K-40, and 7 hours for Test 5-K-60. Following the heating period, for the elevated temperature samples the temperature remained constant during the shearing of the sample. Figure 4.8 shows an increasing amount of water draining from the sample with an increase in temperature; Test 7-K-40 drained 12.5% of its relative volume whereas Test 5-K-60

drained 13.8% over the same heating duration. This is an approximate increase of 1.3% increase in water drained with a 23 °C temperature increase and 13.8% increase over a 36 °C temperature increase.

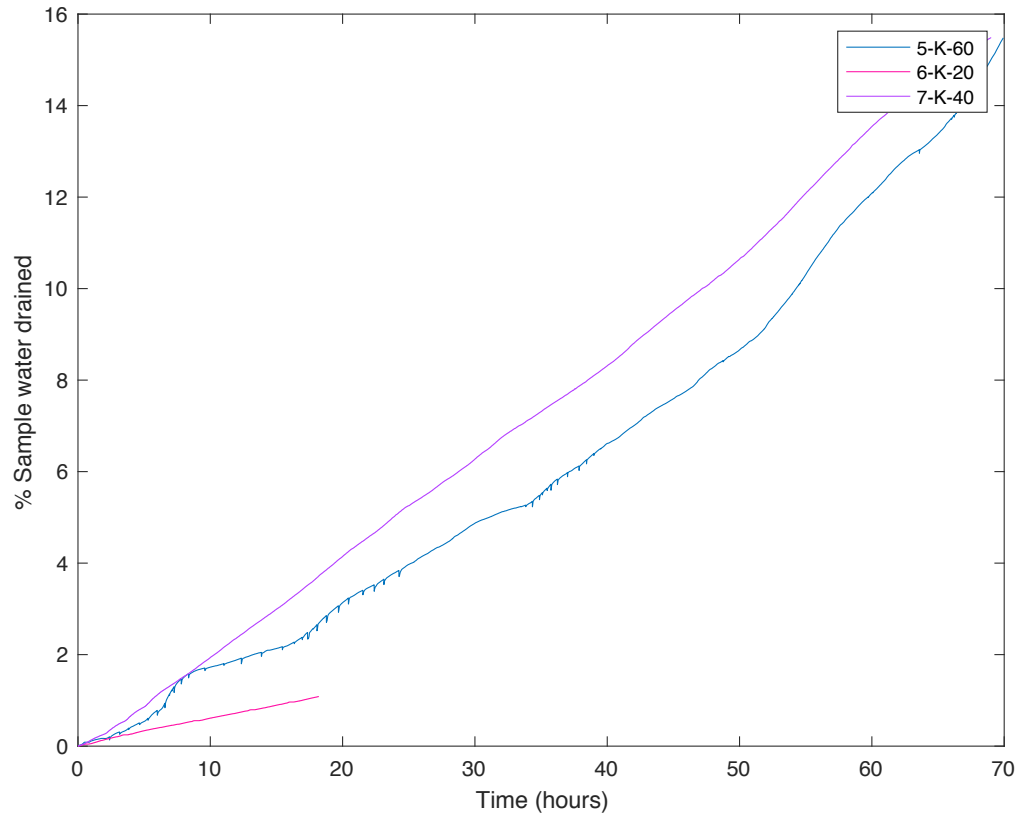


Figure 4.8: Volume of water drained from kaolin during heating stage

4.2.2 Durham clay

Following the testing on kaolin, samples of Durham Clay were tested at 20 °C, 40 °C and 60 °C. Due to equipment failures, only the Test 14-DC-60 provided representative data to be reported. Figure 4.9 shows the raw and corrected normalised sample volume drained for these samples. Upon completion of the heating stage Test 14-DC-60 had drained 7% of its original sample volume.

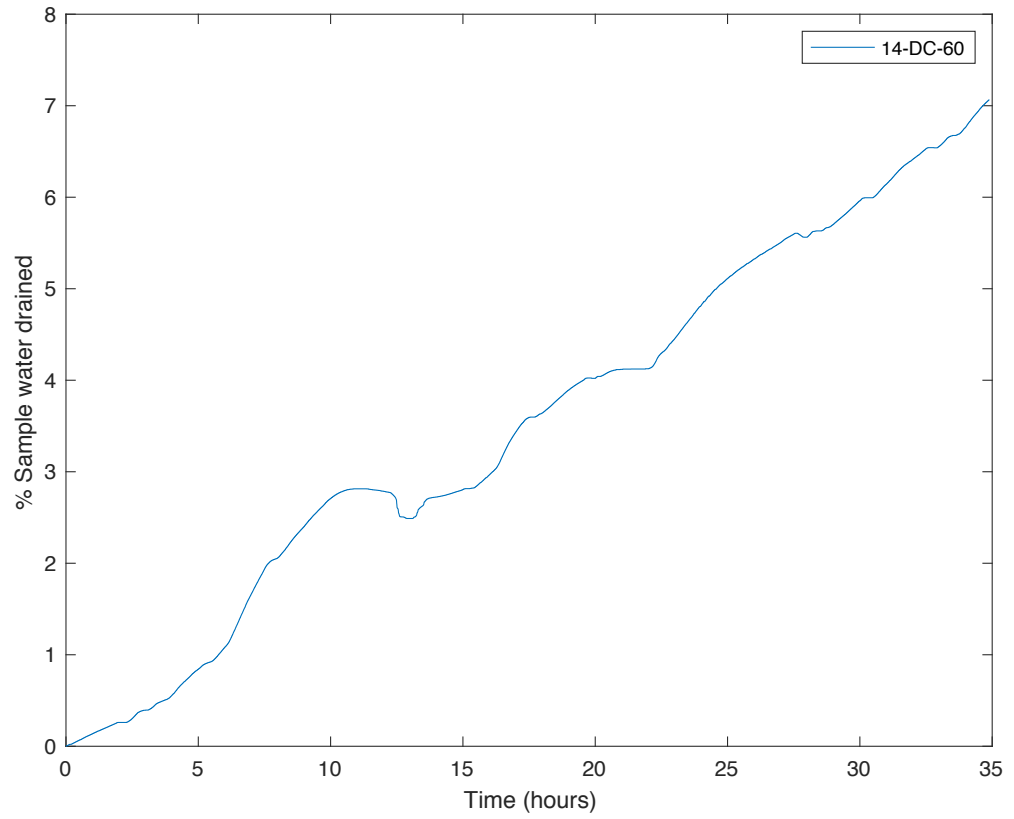


Figure 4.9: Volume of water drained from Durham Clay during heating stage

4.2.3 Comparison

To compare the results of kaolin and Durham Clay, both results have been plotted in Figure 4.10. It can be seen that for Test 14-DC-60 the relative percentage of water drained from the sample is larger when compared to the amount drained from kaolin tested under the same temperature profile. Considering the same time period of 36 hours, kaolin tested at 60 °C drained 5.4% of its relative volume, whereas Durham clay drained 7.0%. To further understand the relationship between elevated temperature and water drained, new experimental methodologies have been developed, further testing is required, beyond the time available for this study.

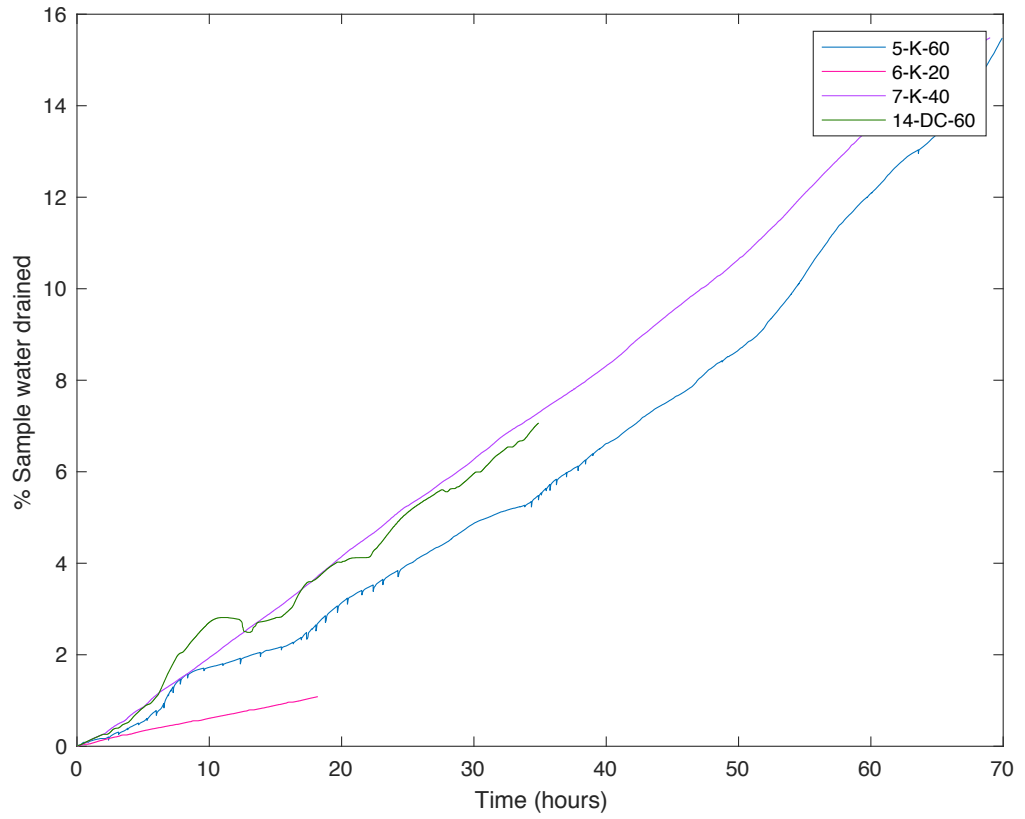


Figure 4.10: Volume of water drained during heating stage from kaolin and Durham clay

4.3 Stiffness

The stiffness of the samples tested at elevated temperature has been determined using small scale stiffness up to a strain of 0.1%.

4.3.1 Kaolin

The deviator stress vs. axial strain for the undrained shearing of kaolin has been produced in Figure 4.11.

The small strain secant stiffness (G_u) was calculated for each of the temperatures using the secant modulus, shown in Figure 4.12 by the dashed line. The results of small strain stiffness are shown in Figure 4.13. It can be observed that with increased temperature, there is an increase in stiffness of the sample.

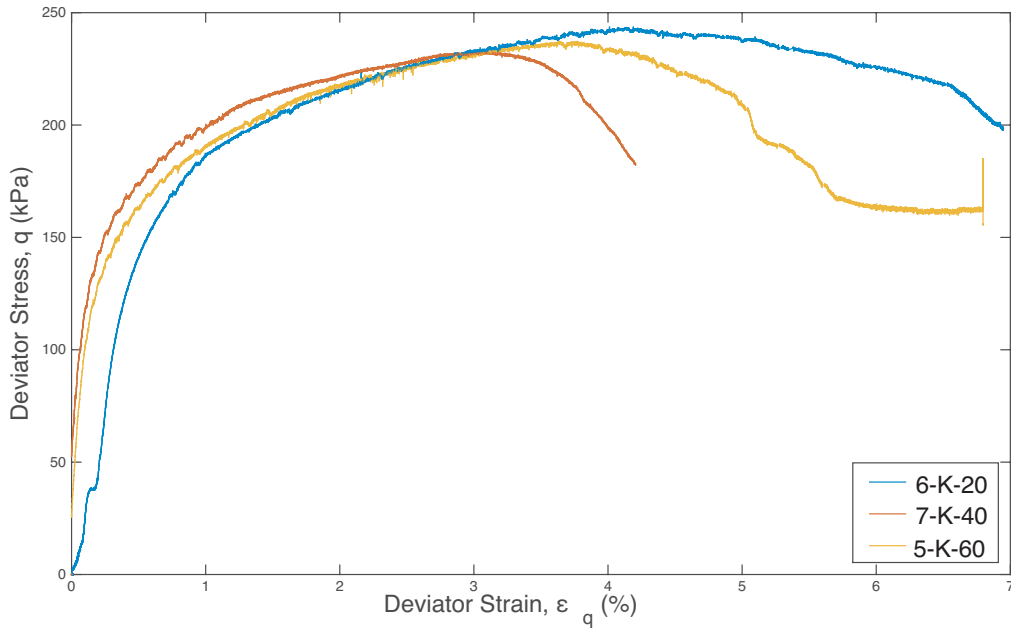


Figure 4.11: Deviator stress vs. deviator strain for kaolin samples tested at elevated temperatures

4.3.2 Durham clay

The stiffness results for Durham clay could not be produced due to experimental difficulties. As detailed in Section 3.6, this is a result of the tendency for the local LVDT's becoming detached from the sample during the heating periods. It was found that the relative shrinkage of the Durham Clay during consolidation within the triaxial set up peeled the membrane from the LVDT's which were fixed with silicone sealant paste. This meant that local strains could not be determined.

4.3.3 Comparison

Comparing the results for elevated temperatures results for kaolin, the same trend was found as identified by Cekerevac & Laloui (2004), with samples tested at higher temperatures producing a higher friction angle. Cekerevac & Laloui (2004) tested consolidated drained samples, whereas in this test consolidated undrained samples were tested therefore a comparison to absolute values cited in literature is not possible.

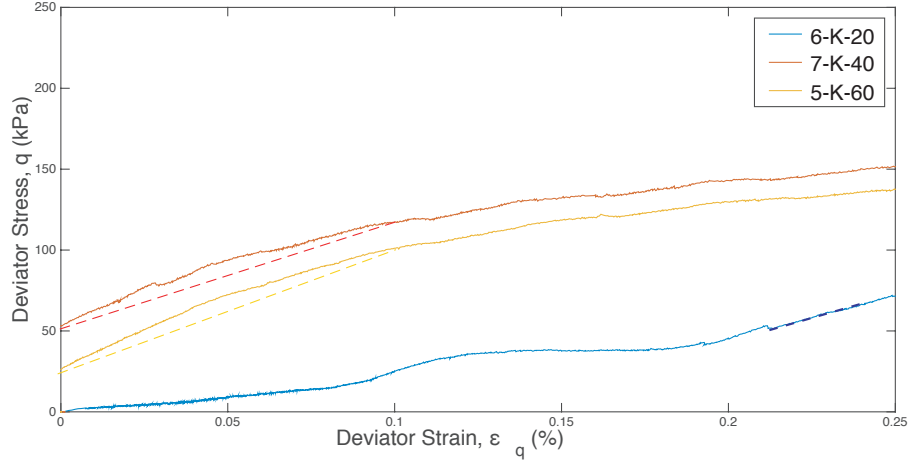


Figure 4.12: Small strain stiffness deviator stress vs. deviator strain for kaolin samples tested at elevated temperatures. Dashed lines representing the secant modulus

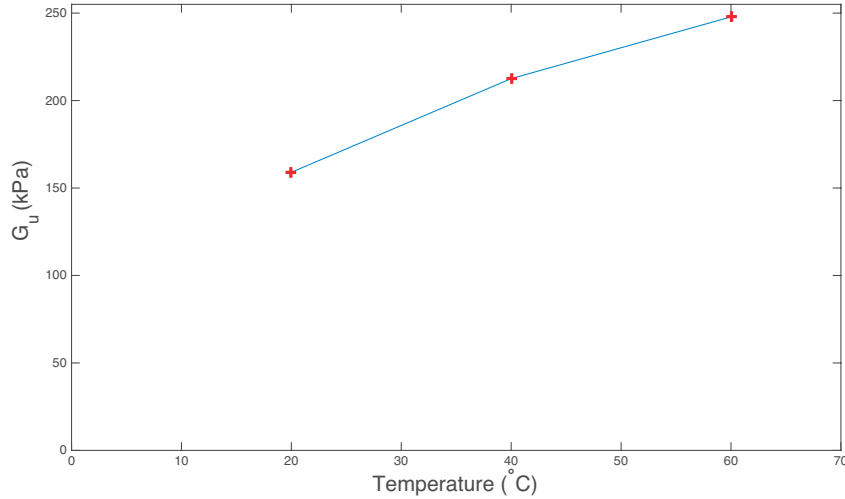


Figure 4.13: Small strain stiffness for kaolin at elevated temperatures

4.4 Critical state

The results in this section show the CSL for the kaolin and Durham clay samples tested at elevated temperatures. Tests 6-K-20, 7-K-40 and 5-K-60 for kaolin and 13-DC-40 and 14-DC-60 for Durham clay.

4.4.1 Kaolin

For the kaolin samples, Figure 4.14 shows p' vs q for Tests 6-K-20, 7-K-40 and 5-K-60. It can be seen that all 3 of the profiles fall on the same CSL, with $\phi' = 21^\circ$.

This shows that the critical state slopes are independent of temperature. This was also observed by Cekerevac & Laloui (2004) when studying drained tests of kaolin.

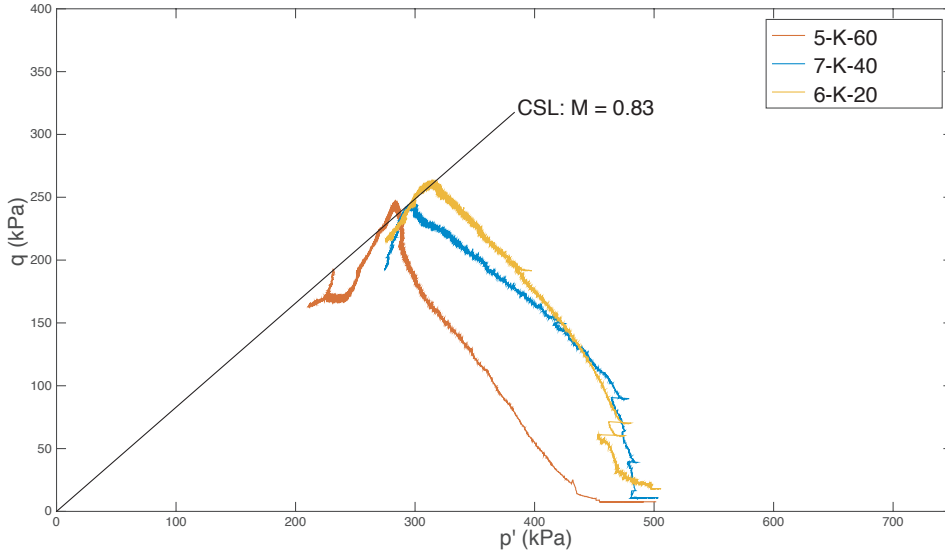


Figure 4.14: p' vs. q plot for elevated kaolin testing

4.4.2 Durham clay

For the Durham Clay samples, Figure 4.15 shows p' vs q for the application of Tests 13-DC-40 and 14-DC-60. It can be seen that both profiles fall on the same CSL with $\phi' = 28^\circ$. Prior to reaching the critical state line, both sample appear to undergo a phase transition, as discussed by Yin et al. (2013) and Yu et al. (2014). With both profiles falling on the same CSL, this shows that for Durham Clay, the critical state slopes are independent of temperature, with both results falling on the same CSL. This result compares with $\phi'_{peak} = 27^\circ$ found for normally consolidated samples by Hughes et al. (2009).

The variability in the test results, in comparison to the clearly defined CSL found in the kaolin testing, meant that determining the CSL line was challenging. The CSL in this instance has been taken to be at the point where inflection occurs for Test 14-DC-60. This point corresponds to the end of the phase transition in the 13-DC-40 results, although not as clearly defined.

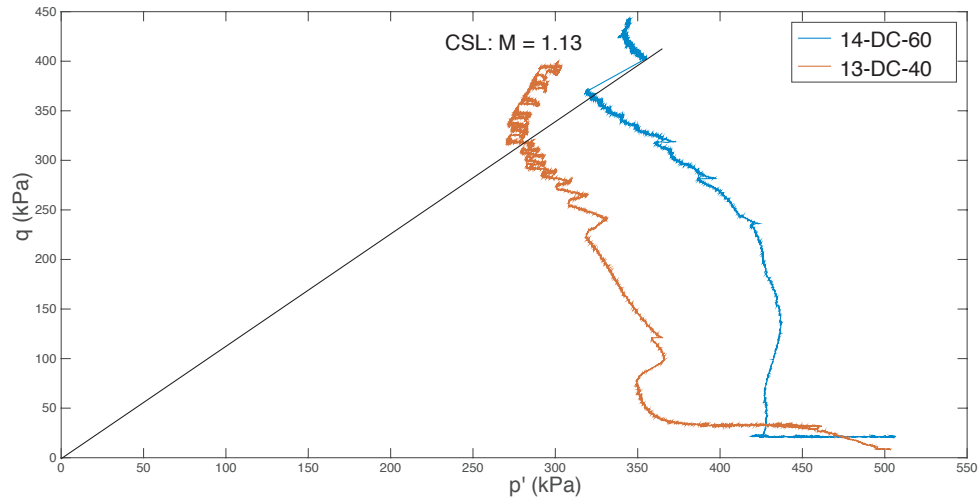


Figure 4.15: p' vs. q plot for elevated Durham Clay testing

4.4.3 Comparison

A comparison between Kaolin and Durham Clay is shown in Figure 4.16. It can be seen that for both samples, the CSL line is independent of the temperature at which the sample shear stress is applied. Durham Clay has been found to have a higher critical state friction angle than that of kaolin. This trend is consistent with those reported in literature, as discussed.

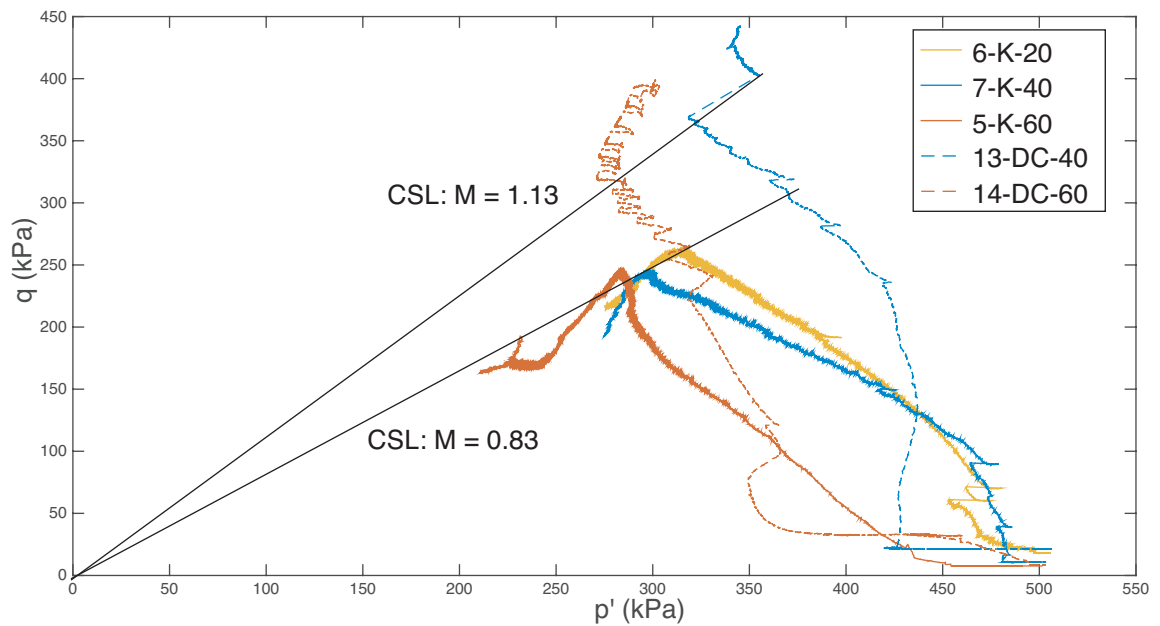


Figure 4.16: p' vs. q plot for elevated kaolin and Durham clay testing

4.5 Summary of elevated temperature testing

The results of consolidated undrained triaxial testing at elevated temperatures have shown:

- During drained heating of a sample, water is expelled from the sample, with the normalised volume of water drained being proportional to the increase in sample temperature
- Higher plasticity kaolin drained relatively more water during heating than lower plasticity Durham Clay
- For the same increase in temperature, it was found that kaolin drained a relatively higher proportion of its original sample volume when compared to Durham Clay
- The CSL of both kaolin and Durham Clay remains constant even when testing is carried out at elevated temperatures
- The small strain stiffness of kaolin increases for samples tested at elevated temperature.

Chapter 5

Cyclic Temperature Variation Tests

This section details the results of the triaxial testing of kaolin and Durham Clay samples which have been subject to cyclic temperature variation (as detailed in Section 3.6). Once loaded into the triaxial cell, the samples were first saturated, prior to consolidating to $\sigma' = 500kPa$, with a cell pressure of 600 kPa and pore water pressure of 100 kPa. The stress path for testing is provided in Figure 5.1.

The stages of the stress path are as follows:

- 0 - 1 mean effective stress increase
- 1 - 2 temperature of sample increased
- 2 - 1 temperature of the sample is decreased
- 1 - 2 and 2 - 1 are repeated for 5 or 10 temperature cycles
- 2 - 3 shear stress applied

5.1 Heating stage

The results in this section show the variation in back volume drained during the heating stage when a 5 or 10 cycles temperature profile was applied, for both kaolin

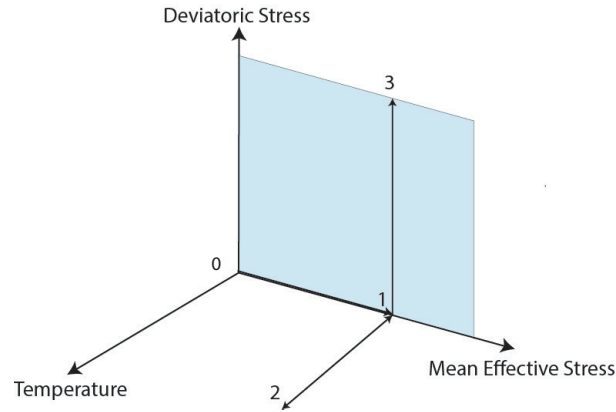


Figure 5.1: Stress path for samples tested following cyclic temperature variation

and Durham Clay. Results are presented for kaolin sheared following 5 and 10 cycles and Durham Clay sheared following 5 cycles. Where samples did not complete the heating stage due to errors described in Section 3.6, part results are included in the analysis to provide further evidence.

5.1.1 Kaolin

The sample volume results for kaolin subjected to 5 and 10 temperature cycles can be seen in Figure 5.2. For the 5 cycle tests (1-K-5C, 8-K-5C and 12-K-5C), it can be approximated that regular volumes of water are drained and reabsorbed to the sample following each cycle. Similar trends are also seen in Test 3-K-10C post experimental error. It should be noted that due to early stage experimental errors with the heating system, Test 8-K-5C was carried out over a reduced duration.

For the 10 cycle test, it appears that errors led to an incorrect assessment of the drained back volume from the sample. During this test, a GDS pressure transducer reached its limit, which occurred due to an internal fitting within the triaxial cell becoming dislodged during heating, with cell pressure bridging across into the back pressure. The test paused when the GDS unit reached its limit and this occurred whilst the sample was held at temperature, preventing drainage. It appears that the increase in pressure whilst the test was paused in combination with the leak of cell pressure to back pressure produced an overall net gain of water to the sample. What can be observed however, is the approximately regular volume of water which

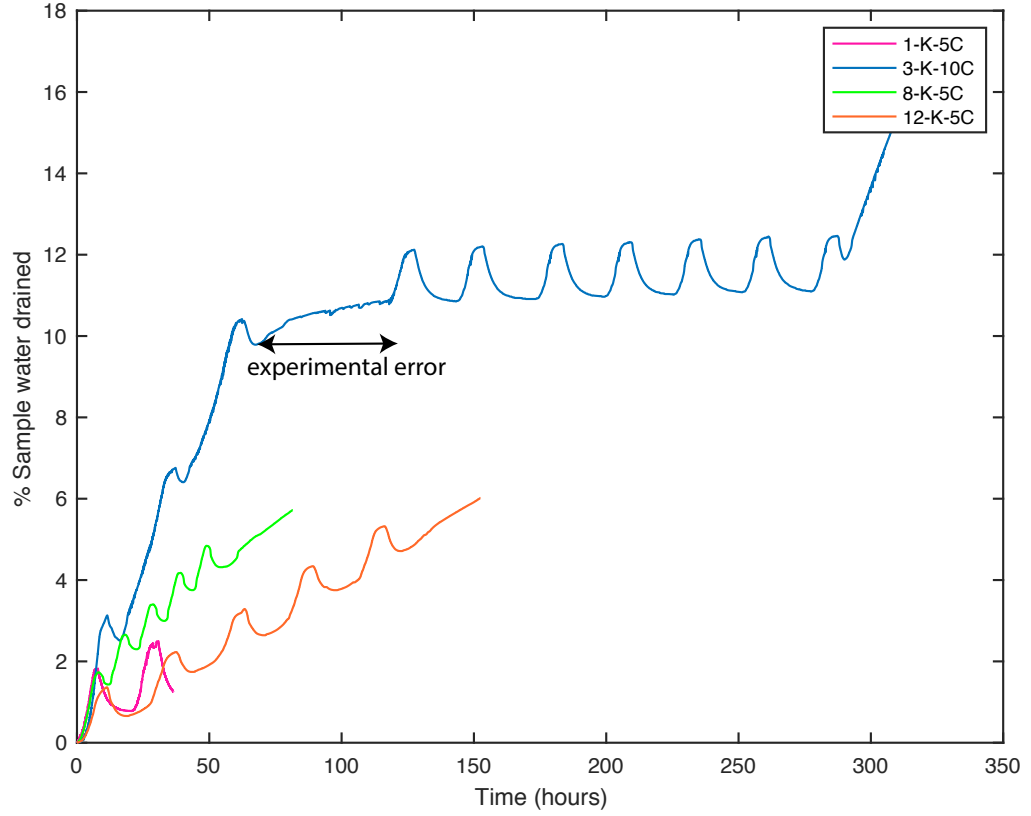


Figure 5.2: Raw and normalised volume of water drained from kaolin during cyclic temperature variation - 5 cycles

had been drained from the sample, considering the 3 cycles prior to the error and the 7 cycles following.

5.1.2 Durham clay

Testing of Durham Clay was carried out by applying the 5 cycle and 10 cycle temperature profiles (Test 10-DC-5C and 16-DC-10C), however due to experimental errors (as described in Section 3.6) only 4 cycles of Test 16-DC-10C were recorded. The results of both tests, with respect to the volume of water drained from the sample during heating, is provided in Figure 5.3.

It can be seen for both tests that following the initial temperature increase complete at 12.5 hours, the sample fails to re-absorb water upon cooling, which is not consistent with kaolin results. This also does not fit with results from this study and those of literature (Campanella & Mitchell 1968) as samples have been

found to re-absorb water upon cooling. When considering the pore water pressure result from the test, Figure 5.4, it can be seen that this sample was subject to a experimental error during the consolidation stage (to the left of the magenta line) whereby the GDS pressure transducer reached its limit and therefore paused the mechanical aspects of the testing. This resulted in an increase in pore water pressure within the sample, which was not equalised prior to commencement of the heating stage. This residual pore water pressure had in turn led to accelerated drainage of water, to dissipate the excess pore water pressure, which can be observed by the relative large initial volume of water drained from the sample and the absence of water re-absorption following the initial temperature increase. For Test 16-DC-10C the initial failure to re-absorb water is thought to be due to early leaking occurring within the system, however to fully understand the reason for this, further testing beyond this study is required.

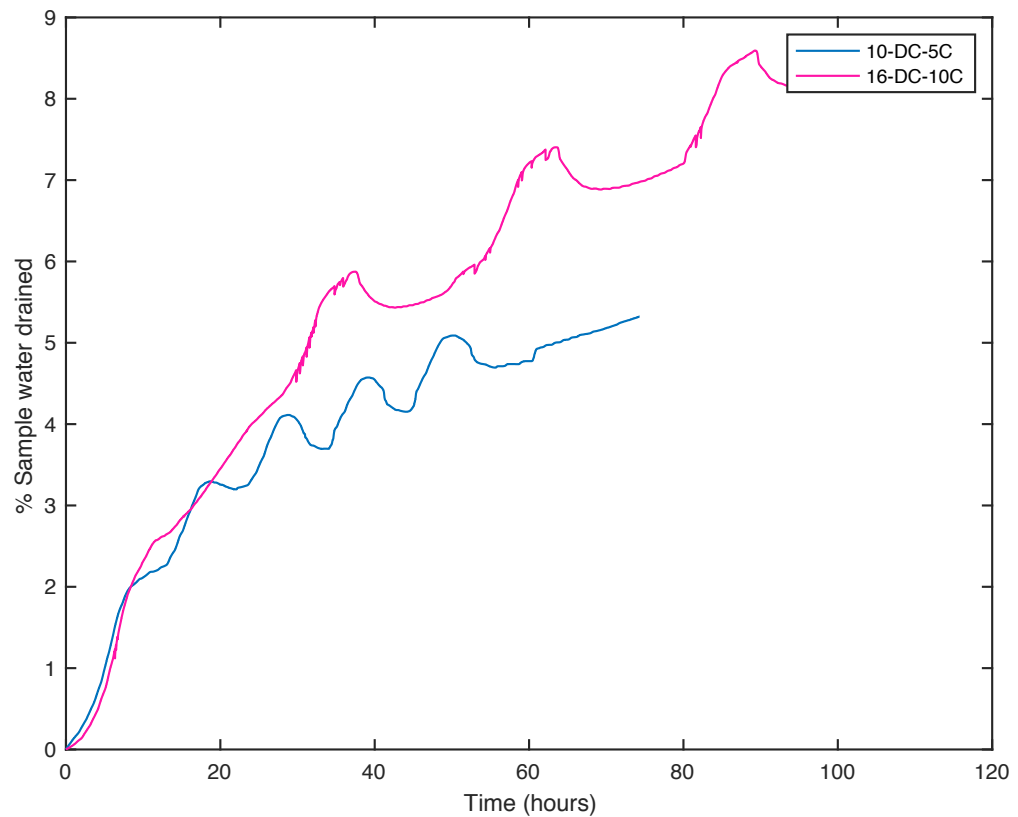


Figure 5.3: Volume of water drained from Durham Clay during cyclic temperature variation

With regard to the trend identified across Test 10-DC-5C, it can be observed that

there is a relatively greater volume of water drained within the initial temperature increase, however following the initial temperature increase, the relative volume of water drained and re-absorbed appears to be near regular.

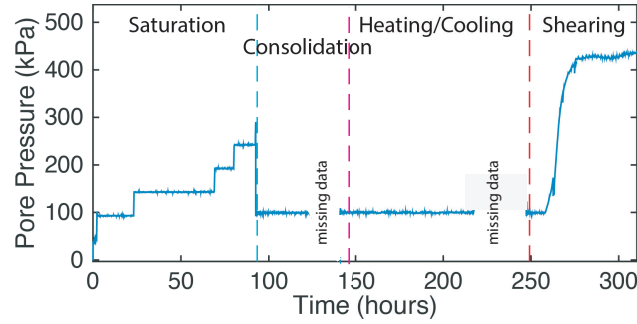


Figure 5.4: Pore Pressure during 5 cycle temperature profile applied to Durham Clay sample

It should be noted when considering the duration of Test 10-DC-5C on Durham Clay an experimental error in the early stage set up of the heating system meant that this test was conducted over a shorter time period when compared to the kaolin sample (full temperature data provided in Appendix A.5). However, when considering the results it can be seen that this has had minimal impact on the results and an equilibrium was reached at the maximum heating and minimum heating points, ensuring that the total water relative volume of water was expelled from or absorbed by the sample. If the period had been maintained for a longer duration, it is likely that very little additional water would have been expelled or adsorbed from the sample.

5.1.3 Comparison

When comparing the cyclic temperature profile experimental results carried out on kaolin and Durham Clay, Figure 5.5, it can be seen that both samples provide an approximately regular pattern of water expulsion and adsorption. As identified in the elevated temperature testing, Durham Clay has been observed to expel a higher volume of water in comparison to kaolin, however the impact of cycle 1 on the overall volume variation required further understanding. Mitigating the initial error in the Durham Clay sample shows that Durham Clay becomes relatively stable in

its expulsion and adsorption of water across the 5 cycles unlike the kaolin sample which continues to have a positive net relative volume of water drained following each cycle. Due to the experimental errors of the Durham Clay tests, it cannot be determined if this positive net relative volume of water drained continues beyond 5 cycles of temperature variation, however due to the regularity of water expelled and adsorbed from cycle 4 to 10 in the 10 cycle temperature variation test, it is unlikely an equilibrium will have been reached similar to that of Durham Clay, over the 10 cycles of temperature variation for kaolin, therefore a ratcheting effect would still be present.

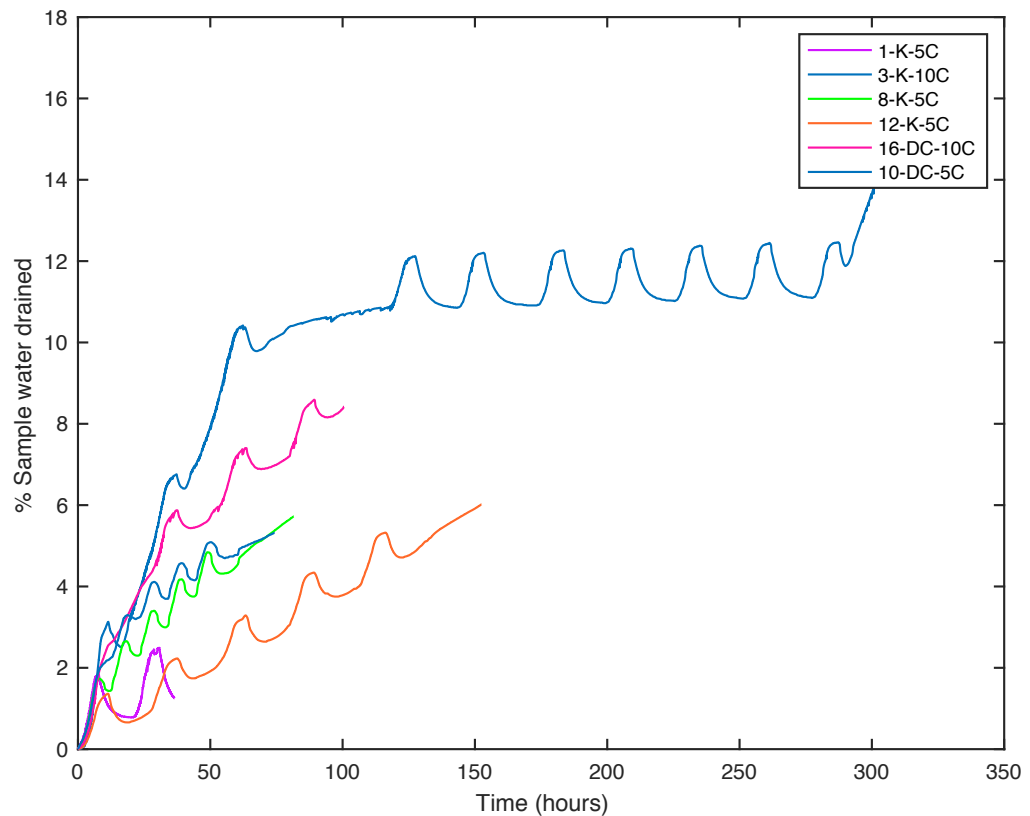


Figure 5.5: Volume of water drained from kaolin and Durham Clay during cyclic temperature variation

5.2 Stiffness

The stiffness of the samples tested following cyclic temperature variation with the deviator stress vs. deviator strain results given in Figure 5.6. It can be observed

that due to an experimental error, the sample of Durham Clay was unloaded at approximately 2% axial strain. However, as the results continue at the same gradient, this error appears to have had minimal impact on the overall stress strain behaviour and no impact on the small-strain stiffness results.

Figure 5.7 has been plotted with the secant modulus taken for small strain stiffness calculation. It can be seen that for Durham Clay, a docking error has been observed, therefore a secant modulus has been taken from 0.03 to 1.03 %. Docking errors typically occurred where the top cap mis-aligned with the load cell in the first instance, logging the start of shearing occurring too early.

The results of small strain stiffness have been plotted in Figure 5.8, which shows the secant shear modulus of kaolin and Durham Clay. Limited data points are available for this comparison. It can be seen that the lower plasticity Durham Clay has a greater stiffness than that of higher plasticity kaolin.

In comparing the results to literature, Burghignoli et al. (2000) found that in a sample which had previously been exposed to relatively higher temperatures a stiffening effect occurred. This can be seen in the 5 cycle kaolin test where the sample is stiffer than that tested at 60 °C. In the case of the 10 cycle kaolin test, it can be seen that there is a reduction in stiffness. However, this value could potentially be influenced by the leak within the cell, as previously discussed in reviewing the heating stage results.

5.3 Critical state

The results in this section show the critical state friction angle findings for the kaolin Test 3-K-10C and 12-K-5C and Durham Clay Test 10-DC-5C.

5.3.1 Kaolin

The results of the CSL for the kaolin tested by applying 5 cycles and 10 cycles of temperature are shown in Figure 5.9. The results show that the sample sheared

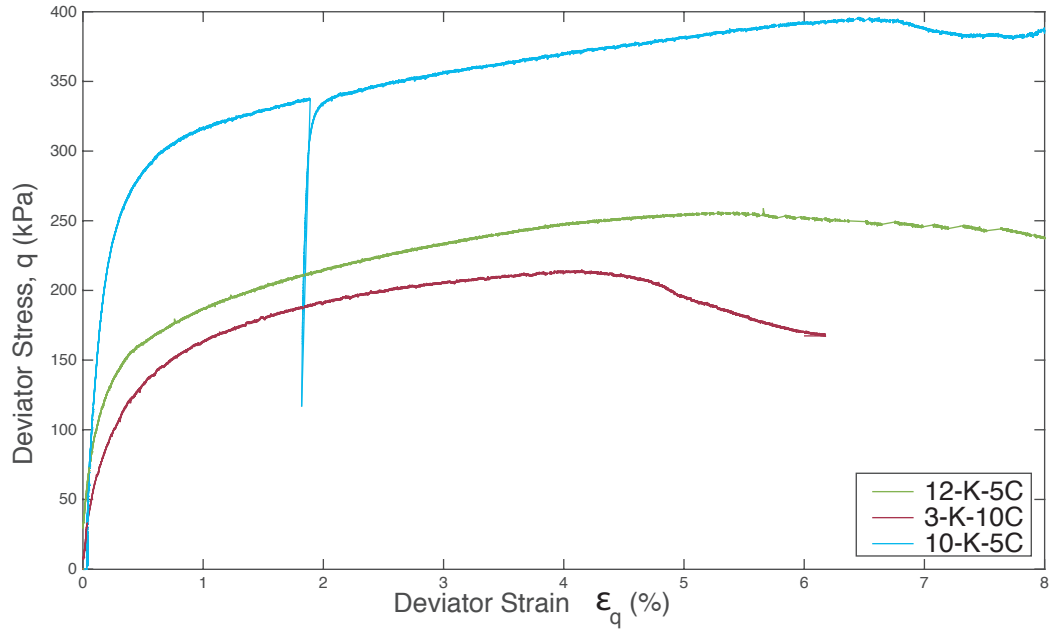


Figure 5.6: Deviator stress vs. deviator strain for kaolin and Durham Clay samples tested following cyclic temperature variations

following 5 cycle temperature variations had an effective friction angle, $\phi' = 22^\circ$ and the sample sheared following 10 cycles $\phi' = 20^\circ$. Therefore it can be seen that when compared to a sample tested following zero temperature variation ($\phi' = 21.37^\circ$) there is an increase in friction angle following 5 cyclic temperature variations. Comparing the result of 5 cycle temperature variations to that of the 10 cycle temperature variation, it can be seen that there is a reduction in the friction angle following the additional 10 cycles.

5.3.2 Durham clay

The result of the CSL for the Durham Clay sample tested by applying a 5 cycle temperature profile is presented in Figure 5.10. The results show that the sample sheared following a 5 cycle temperature variation has a friction angle $\phi' = 30^\circ$, this is an increase in friction angle from $\phi' = 28^\circ$ as calculated following the elevated tests in Section 4. It can also be seen that the sample undergoes a phase transition, as found in the elevated temperature samples.

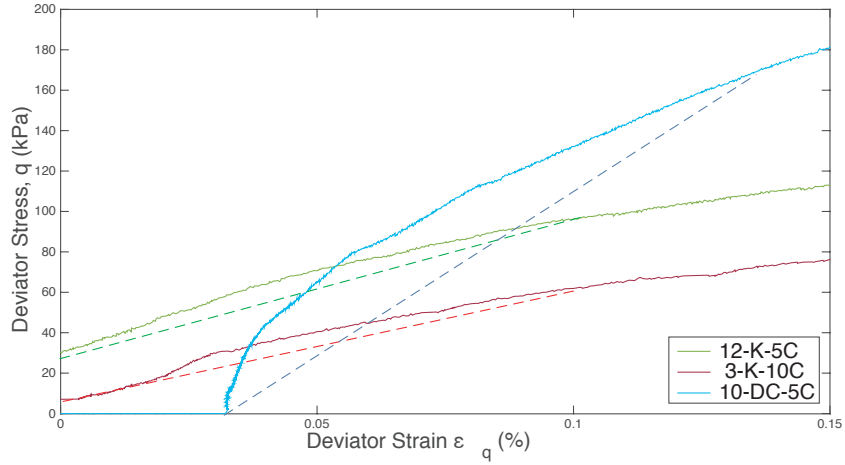


Figure 5.7: Small strain stiffness deviator stress vs. deviator strain for kaolin and Durham Clay samples tested following cyclic temperature variations. Dashed lines representing the secant modulus

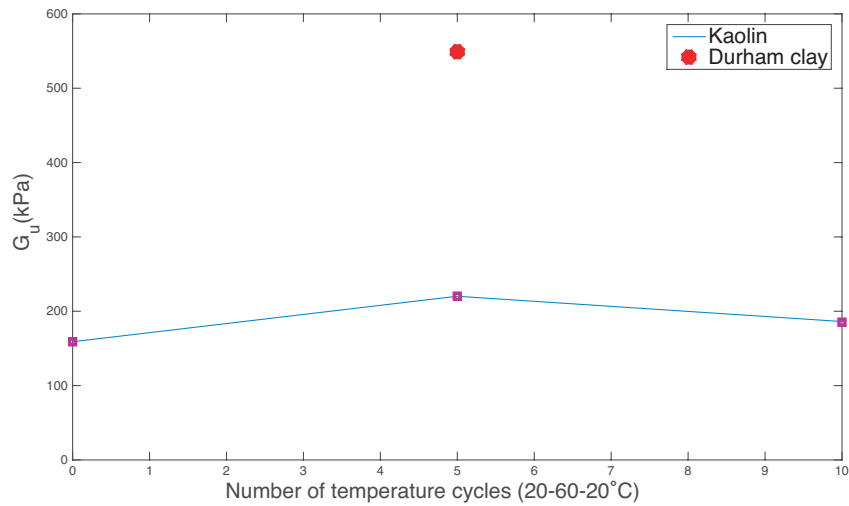


Figure 5.8: Shear modulus for cyclic temperature variaiton

5.3.3 Comparison

A comparison between the results of the kaolin and Durham Clay tests has been produced in Figure 5.11. Durham Clay continues to have the higher friction angle when compared with the results of kaolin. The response to cyclic temperature variation has been considered as part of a broader study by Cekerevac (2003) where it was found that cyclic temperature variation does impact on ϕ' . The results from this study are provided in Figure 5.11. The results from this study are consistent with the study by Cekerevac (2003) in which found that there is only 1° variation

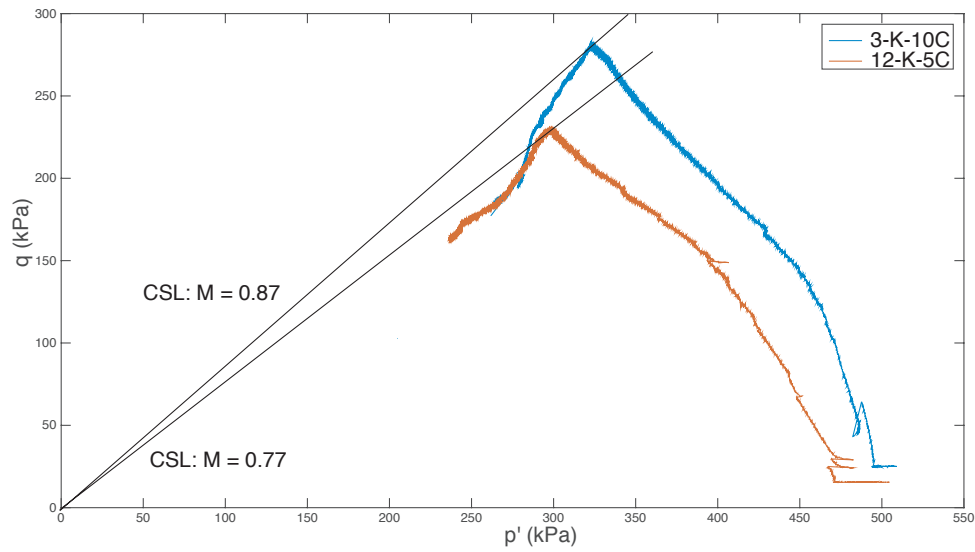


Figure 5.9: Post cyclic temperature variation q p' for kaolin Tests 3-K-10C and 12-K-5C

between zero cycles and five cycles, thus the 3 cycle test by Cekerevac (2003) falls within this range. The trend which is displayed here has been considered further in Chapter 6.

5.4 Summary

This chapter has presented the results of 5 and 10 cycle temperature variations on samples of kaolin and Durham Clay. The results of consolidated undrained triaxial testing following the temperature variations have shown:

- The initial heating period of a sample does not expel a significantly greater relative volume from the sample compared with later cycles for clays with the plasticities tested
- More regular expulsion and adsorption patterns are observed across both kaolin and Durham Clay in the later cycles
- The CSL friction angle increases following a 5 cycle temperature profile applied to a sample, this is evident in both kaolin and Durham clay

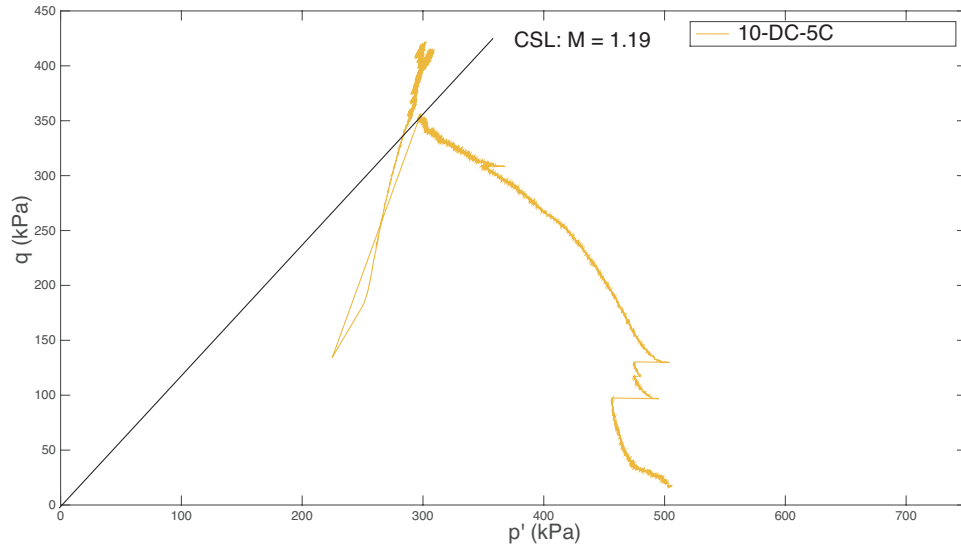


Figure 5.10: Post cyclic temperature variation p' vs. q for Durham clay Test 10-DC-5C

- The CSL friction angle decreases with an additional 5 cycles, following the application of a 10 cycle temperature variation profile for kaolin
- The secant stiffness of kaolin increases following a 5 cycle temperature variation
- The secant stiffness of kaolin following the application of 10 temperature cycles decreases from that observed following a 5 cycle temperature variation, in addition to that observed following the zero cycle test carried out at 24 °C, Test 6-K-20.

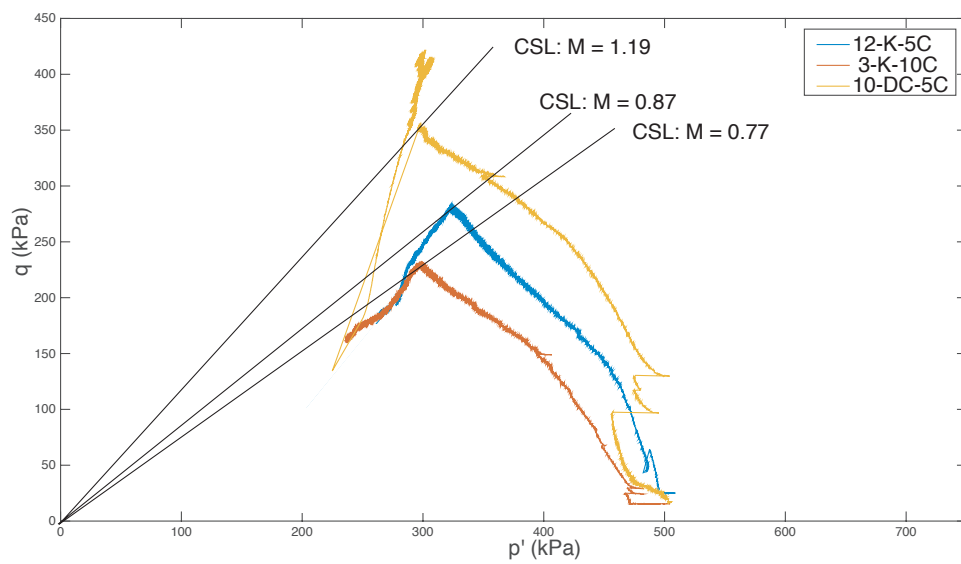


Figure 5.11: p' vs. q for kaolin 5 & 10 cycles and Durham Clay 5 cycles

Chapter 6

Understanding the Impact of Cyclic Temperature Variation

This section starts by drawing together the results found in Chapters 4 & 5, addressing the key trends and behaviours observed during testing. Following this, the heating stage and shear stage of testing have been considered in detail, bringing together areas of literature to provide evidence to support the rationale behind the findings. A conceptual model has been proposed, with evidence of its application to literature findings. This section finishes with a discussion on how the conceptual model impacts the work of industry and those designing pile foundation heat exchangers.

6.1 Summary of experimental results

Combining Chapters 4 & 5, this section draws together and summarises the main finding from experimental testing with regard to the relative percentage of sample volume drained, the observed friction angles and the clay stiffness during the application of elevated and cyclic temperature profiles.

6.1.1 Volumetric change

The result of the volume change of the sample is observed through the change in back volume during the heating of kaolin. This has been found to be closely proportional to the increase in sample temperature, shown in Figure 6.1. When considering the initial cycle on the cyclic temperature profiles against the relative percentage of sample volume drained during elevated temperature, it can be seen that there is a varied percentage drained in this first cycle between the cyclic and elevated tests, as shown in Figure 6.2. It can be seen for kaolin samples that the elevated temperature samples, heated for a shorter duration, drained a higher percentage of sample water. When considering the Durham Clay samples, it is important to note that the 5 cycle result, Tests 10-DC-5C and 16-DC-10C, includes an additional proportion of water drained due to previously discussed lack of re-absorption of drained water. This was due to experimental issues previously detailed. It could therefore be expected that without this additional pressure, the percentage of water drained in the initial heating stage for Durham Clay, would be lower than the percentage drained in the elevated temperature test.

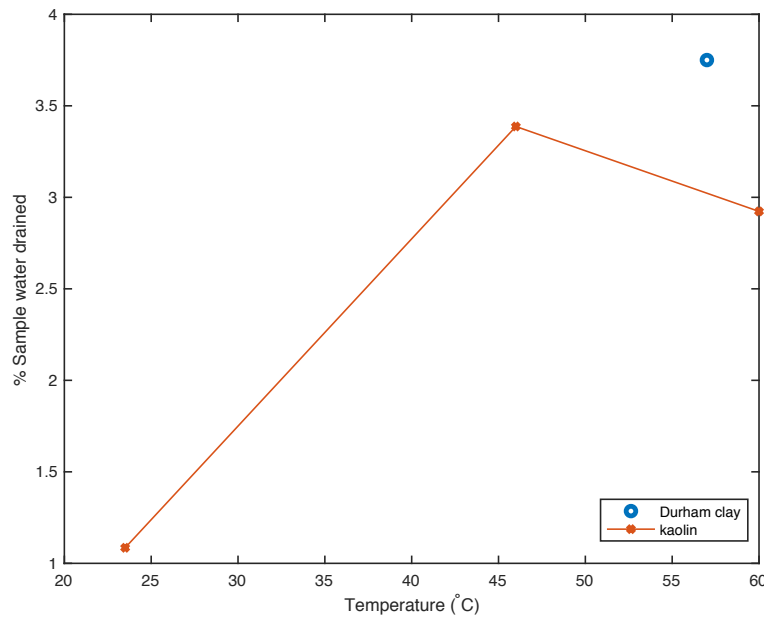


Figure 6.1: Percentage of original sample water drained against temperature for elevated temperature tests, taken 36 hours into the test stage

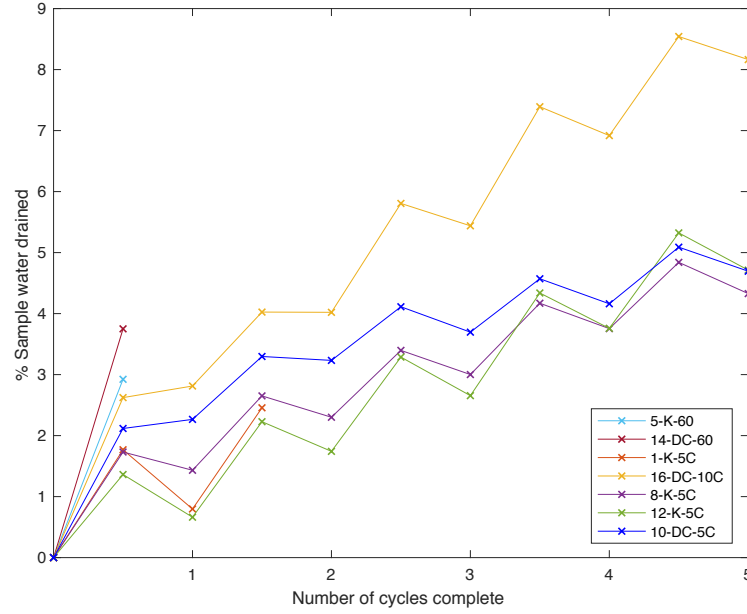


Figure 6.2: Percentage of original sample water drained against number of cycles complete for kaolin and Durham clay

6.1.2 Critical state friction angle

The results of critical state analysis for elevated and cyclic temperature variation produced the experimental values for the angle of friction (ϕ'), shown in Table 6.1. It can be seen that Durham Clay has a higher friction angle than kaolin when subject to both elevated and cyclic temperature profiles. Both the results of kaolin and Durham Clay are consistent with friction angles reported in literature, as provided in Table 6.1. When comparing the results of samples subject to an elevated temperature profile to those of a cyclic temperature profile, it can be seen that following 5 temperature cycles (Test 12-K-5C), the friction angle of kaolin increases, however by 10 cycles (Test 3-K-10C) the friction angle reduces to lower than the original friction angle. The variation in the 10 cycle friction angle, as previously discussed, has potential to be due to experimental errors. For Durham Clay the same trend of increasing friction angle from 60 °C (Test 14-DC-60) to 5 temperatures cycles (Test 10-DC-5C) has also been observed.

Table 6.1: Critical angle of friction values observed during testing

Test type	Material / Test	M value	ϕ' (°)
Elevated	Kaolin (20, 40, 60 °C)	0.83	21
	Durham Clay (40, 60 °C)	1.13	28
Cyclic	Kaolin - 5 cycles	0.87	22
	Kaolin - 10 cycles	0.77	20
	Durham Clay - 5 cycles	1.19	30
Ambient Temperature	Kaolin - 20 °C (Cekerevac 2003)	-	21
Cyclic	Kaolin - 3 cycles 20-90-20 °C (Cekerevac 2003)	-	21
Ambient Temperature	Durham Clay (Hughes et al. 2009)	-	27

6.1.3 Stiffness

The small strain stiffness analysis determined the experimental secant modulus of stiffness provided in Table 6.2. For the samples of kaolin, it can be seen that an increase in temperature increases the stiffness of the clay with a reduction of stiffness being observed following multiple cycles, this is illustrated in Figure 6.3. Due to the lack of experimental data for Durham Clay, the same relative comparison cannot be made.

Table 6.2: Small strain stiffness of clays tested. * potentially unrepresentative result, see Section 4.4.1.

Test type	Material / Test	G_u (kPa)
Elevated	Kaolin - 20	159*
	Kaolin - 40	213
	Kaolin - 60	248
Cyclic	Kaolin - 5 cycles	220
	Kaolin - 10 cycles	186
	Durham clay - 5 cycles	549

6.2 Rationale from literature

This section presents a summary of the theories and hypotheses presented in the literature surrounding the impact of temperature variations. Additional literature has been sourced to complement the understanding where required.

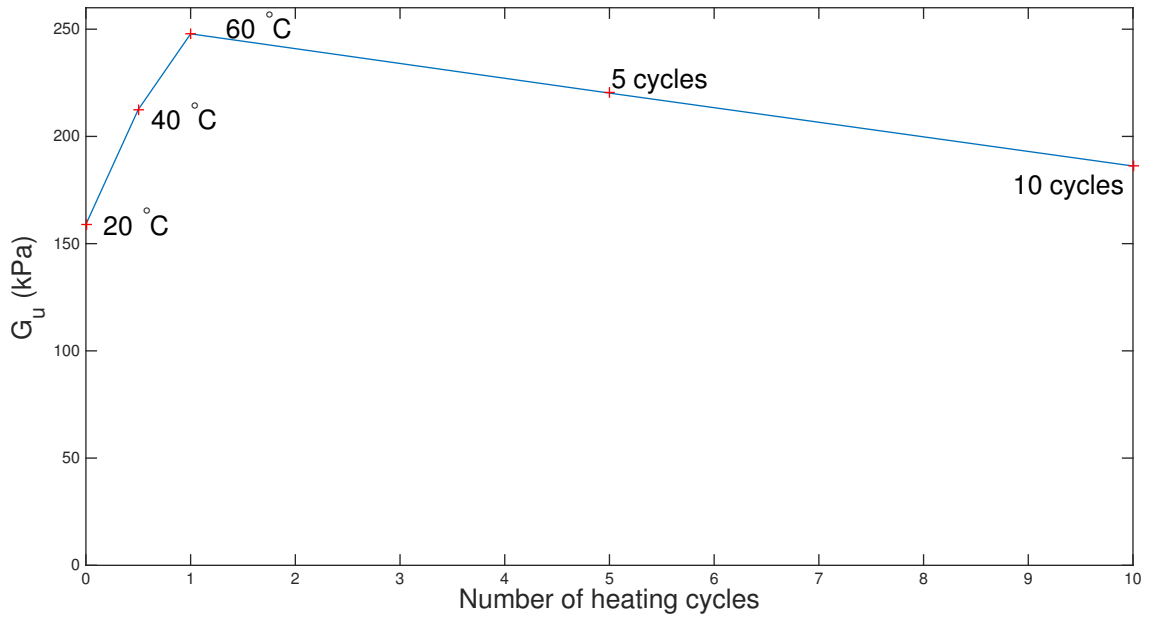


Figure 6.3: Change in stiffness (G_u) with number of temperature cycles for kaolin samples

6.2.1 Heating stage

This section will consider the heating stage of testing, considering evidence in the literature for the change in clay microstructure, which occurs in order to provide the bulk behaviour observed during testing.

Campanella & Mitchell (1968) determined that the volumetric change of clay in drained conditions was determined by the volumetric expansion of soil water, volume of pore water and the temperature change. Section 2.1 similarly discussed the three main elements of clay microstructure to be taken into account when considering thermal effects on saturated clays: clay particles; inter-particle water; and inter-aggregate water. This section will therefore consider the effect of heating on the clay particles, alongside the clay water, both inter-particle and inter-aggregate.

Particle and double layer response

As identified in Section 2.1.1 a clay particle is surrounded by a layer of water which is adsorbed to the clay particle surface. In considering how a clay particle responds to an increase in temperature, it is imperative to consider the role of this adsorbed

water in a clay's response.

A hypothesis published by Towhata et al. (1993) suggested that during heating between 20 °C and 90 °C, the molecules of water attracted to the clay's surface gain kinetic energy as the temperature increase. These molecules gain the opportunity to break free from the range of electric attractive force, once the energy is large enough, thereby becoming free water. The adsorbed double layer would therefore reduce in thickness, allowing the clay particles to move closer together or come into contact with one another. This further allows the bulk clay volume to decrease as the now inter-aggregate water is drained. This theory is however contradicted by the studies carried out by Gulgun (2011) & Wang et al. (1990), where it was found that the double layer adsorbed water remains constant up to a temperature of 400 °C for kaolin. During this temperature range, only the inter-layer water is lost from the sample, which once the particles were mixed with distilled water, this process of removing the inter-layers will have been reversed. It can therefore be determined that the physical properties of the clay particles, alongside the adsorbed double layer water, remain unchanged during the heating and cooling cycles.

In a study by Plum & Esrig (1969) an interpretation of the mechanical behaviour of soil during heating was made, suggesting that as the temperature of a sample is increased, the double layer water adsorbed to the clay particle expands, which in turn decreases the effective stress between particle contacts, thus permitting shear failure to occur at these contacts. This hypothesis was found to contradict the findings of Lambe (1959) where the clays studied were less active and interparticle contacts were less integral and Yong (2003) where the concentration of salts in the pore fluid promoted a face-to-face particle structure, causing the expansion of the double layer adsorbed water to produce a bulk sample expansion. The finding of Yong (2003) did not directly support the hypothesis that an expansion in double layer promotes a decrease in sample volume, due to the reduction in effective stress between the particles. This would be associated with a predominantly edge-to-face structure. The observations by Yong (2003) of an expanding sample with a predominantly

face-to-face structure do support the hypothesis of an expanding double layer. The face-to-face structure has already undergone permanent deformation and cannot reduce to a more compact state than they originally were like those studied by Plum & Esrig (1969). The expansion in a sample with a face-to-face particle structure is evidence of volumetric expansion in the adsorbed double layer water. It should be noted that a face-to-face particle structure is representative of a sample which has experienced very large mechanical stress or strain levels.

The hypothesis by Plum & Esrig (1969) supports the earlier hypothesis by Campanella & Mitchell (1968), which presents a theory that as the sample temperature increases, there is a volumetric expansion of the clay particles decreasing the shear strength between individual interparticle contacts resulting from this thermal energy. This acts in conjunction with the shear force at interparticle contacts, resulting in an increased probability of bond slippage or failure. In turn, this leads to a partial collapse of the soil structure with a decrease in void ratio until a sufficient number of additional contacts are formed by the particles to enable the soil to carry the additional stress imposed by the higher temperature. This has been compared to a secondary compression effect under an increase in mechanical stress.

Upon cooling of the sample, the reverse is applied to the volumetric shrinkage of the clay particles and water, promoting a relative suction pressure within the sample. This is thought to be true due to the temperature decrease promoting a strengthening of the soil structure, as the effective stress across the sample is reduced and therefore no further particle arrangement is required to carry the effective stress imposed on the sample once cooled.

A conclusion has been made that the adsorbed double layer does not lose or gain water molecules due to kinetic energy. The heating and cooling of clay particles and the adsorbed double layer leads to a thermal volumetric expansion and contraction. This volumetric expansion reduces the shear force (particle attraction) which subsequently leads to an increased number of bond slippages and failure. This leads to a collapse and reorientation of the particle structure, with suction occurring during

cooling due to the volumetric shrinkage of particles and adsorbed double layer water where drainage has been allowed. Overall, this leads to a permanent deformation of the particle structure.

Pore water response

In addition to the volumetric expansion of the clay particles and double layer water adsorbed to the clay particle, expansion of the (free) pore water within the sample, whether that be inter-particle/intra-aggregate or inter-aggregate, also occurs. To support the effect of pore water expansion on the pore size and shape, studies considering an increase mechanical load have been considered.

In a study by Yu et al. (2016) it was found that the most common particle structure of kaolin subject to sedimentation is that of unwashed clay with a predominant face to edge structure and therefore more voluminous structure, as shown in Figure 6.4 (b). The alternative clay structure is that of Figure 6.4 (a), which shows the particles fully parallel to one another with face to face contacts. Yu et al. (2016) found that during isotropic mechanical loading and unloading the typically open structure of kaolin was easily compressed, producing a large deformation within the sample. It can therefore be determined that the structure of consolidated clays falls somewhere between (a) and (b) depending on the degree of consolidation. This is supported by the work of Cetin & Gokoglu (2013) who found similar structures in clay samples pre-triaxial testing. Due to the test pressures used within this study, it is most likely that the particle structure tends to that of 6.4 (b).

Observations by Israelachvili (2011) produced a theory whereby the load applied to the sample at constant temperature overcomes the double layer repulsive forces, thus pushing the clay particles closer together. Once the load is reduced, the double layer repulsive forces work to return the particles near to their original state. It was determined that the deformation of the sample in response to loading is predominantly controlled by the changes in particle (including adsorbed double layer) rather than the compression of the adsorbed double layer.

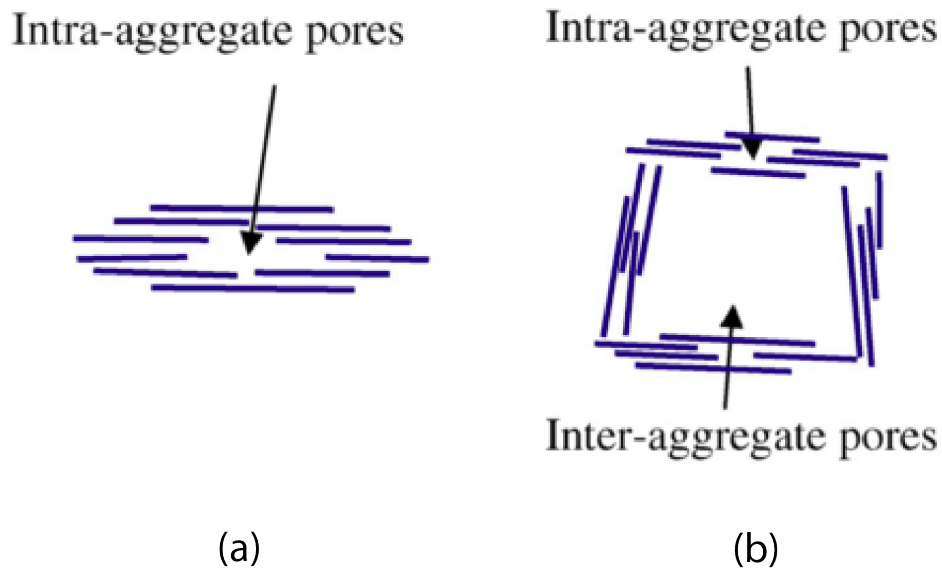


Figure 6.4: Typical particle structure found in natural cycles. (Yu et al. (2016))

The effect of loading was further studied by Yu et al. (2016) by conducting 1-D consolidation of kaolin samples. It was found during consolidation that large inter-aggregate pore spaces collapsed during loading up to an effective stress of 100 kPa.

The final point to note from the study by Yu et al. (2016) is that when oven drying (oven temperature not detailed) of saturated samples decreased the volume of pores with the sample, there was a major shift towards smaller pore sizes with inter-aggregate pores reducing in volume whilst intra-particle pores increased in volume.

In conclusion, it has been reported that during heating the expansion of pore water reduces the shear stress between the particles, promoting a collapse of the particles into the pore spaces. Pore spaces within the sample therefore reduce in size and number during heating.

6.2.2 Shearing stage

This section considers the shear stage of testing, considering the change in clay microstructure which occurs in order to provide the bulk behaviour observed during testing. Following the previous section focusing on heating stage, this section will

consider the response of the clay particle and double layer in addition to pore water. In current literature, there is limited hypotheses considering the effect of temperature on clay particles, double layer adsorbed water and pore water, however an appreciation of the effects can be determined through literature considering drained and undrained triaxial testing.

Particle and double layer response

As discussed in Section 2.2, Cetin & Gokoglu (2013) carried out a study to identify the orientation pattern of clays before, during and after, undrained and drained triaxial testing. In consolidated undrained triaxial testing, there were clear signs showing a change in particle orientation from the near random original particle orientations. The particles tended to orientate themselves towards the failure plane, becoming parallel to the shear plane. During shearing it was found that considerable preferred orientation occurred, which was thought to be due to particles becoming parallel to one another.

During drained tests, Cetin & Gokoglu (2013) observed a similar reorientation of the clay particles with the particles aligning themselves parallel to the shear plane as shearing progresses. Overall, it was concluded that the pressure within the sample induces a preferred orientation within the fabric elements.

In conclusion, similar to that of the heating stage, during shearing a collapse and re-orientation of the clay particles occurs as the load is increased.

Pore water response

Through studying the pore sizes before and after drained triaxial testing, Yu et al. (2016) found that the shearing process reduced the size of the inter-aggregate pores, whereas the intra-aggregate pores ($< 0.17 \mu\text{m}$) remained almost unchanged. This observation corresponds with the effect consolidation has on the pores, providing further evidence that the predominant pore space within kaolin is the aggregate to aggregate pore spaces which provide the mechanical response. These findings are

supported by the work of Cetin & Gokoglu (2013), who found that the orientation pattern of clay particles before shearing is nearly random, with some degree of particle re-orientation caused by the previous overburden pressure applied during sample consolidation.

It could be interpreted that the decrease in inter-aggregate pores is due to an increase in pore water pressure with increase in axial load, expanding and collapsing the pores. For an undrained sample, the increase in axial load would lead to an increase in pore water pressure, which with reduced shear strength between the clay particles, would lead to an expansion of inter-aggregate pores until a collapse of the surrounding particles occurred, reducing the pore space.

In conclusion, during shearing there is a further reduction in pore number and size as the particles re-orientate themselves to withstand the applied mechanical load.

6.3 Proposed conceptual model

When considering the effect of temperature on the microstructure of clay during the heating stage and shearing stage, it can be seen that there is a running theme by means of an increase in pore water pressure within a sample, promoting a re-orientation of clay particles, whether that be due to the heating of a sample or during the shearing of a sample, to support the applied load. This increase in stress, whether mechanically or thermally induced, has also been shown to break down the pores within a sample. Following the observations and hypothesis discussed in the previous two sections, a combined conceptual model can be proposed.

6.3.1 Heating stage

For an increase in sample temperature the following combined hypothesis is proposed:

- As sample temperature increases, there is an increase in pore water pressure

within the clay sample due to the thermal expansion of the clay particle, absorbed double layer water and pore water both inter-particle and intra-aggregate

- The expansion of the double layer water adsorbed to the clay particle promotes a decrease in shear resistance between the individual clay particles. This reduced shear resistance increases the probability of bond slippage and failure
- The expansion of pore water increases the shear force on the already weakened bonds between clay particles, leading to the collapse of the relatively weaker inter-aggregate pores
- The collapse of inter-aggregate pores leads to a relatively consolidated clay structure
- Where drainage is permitted, the pore water pressure of the sample is reduced through the expulsion of pore water
- The collapse of inter-aggregate pores continues until the clay particles form a structure, which can withstand the effective stress induced from sample heating and the draining of pore water is reduced

6.3.2 Cooling stage

When considering a decrease in sample temperature, the following combined hypothesis is proposed:

- As the sample temperature decreases, the pore water pressure within the clay sample is reduced due to the contraction of the clay particles, adsorbed double layer water and pore water both inter-particle and intra-aggregate
- The contraction of the absorbed double layer increased the attraction between clay particles

- This induces a suction within the sample, with the initial cooling promoting an increase in effective stress on the sample prior to the suction of water back into the sample to oppose this effect, where drainage is permitted
- The combined effect of contraction of clay particle, adsorbed double layer and pore water create further tension and therefore negative pore water pressure within the sample allowing previously drained water to return to the sample to neutralise the negative pore pressure
- A re-structure of the clay particles occurs during sample cooling as the particles under volumetric contraction, however this is relatively small when compared to the restructure induced by sample heating
- There is a net reduction in pore water volume within the sample as not all the original pore water is reabsorbed into the sample in order to neutralise the negative pore pressures. In order to reabsorb all water during cooling, additional energy would be required in order to modify the soil structure, which has been stabilised during the heating period.
- A change in structure has been achieved, with an increased number of particle contacts in a reduced volume

6.3.3 Subsequent cycles

For the second and subsequent cycles, many of the above stages are repeated, with variations occurring due to the reduced pore water volume. The following conceptual model is proposed for the heating stages:

- As sample temperature increases, there is an increase in pore water pressure within the clay sample due to the thermal expansion of the clay particles, adsorbed double layer water and pore water both inter-particle and intra-aggregate. This causes a decrease in the effective stress.

- The expansion of the double layer water adsorbed to the clay particle promotes a decrease in shear strength between the individual clay particles. As the number of particles remains constant within the sample, the percentage of water within the sample which forms the double layer adsorbed water also remains relatively constant, therefore the same decrease in shear force occurs as the initial temperature increases.
- There is a decrease in shear strength between particles, increasing the probability of bond slippage and failure. However, as this is the second temperature increase, the likelihood compared to the initial temperature increase is significantly lower given the particle restructuring which has already occurred in the initial cycle. This can be described as within the ‘elastic range’ of the clay, with a temperature increase beyond that of the original temperature increase promoting a ‘more plastic’ deformation of the sample.
- The expansion of pore water increases the shear force on the bonds between clay particles leading to the collapse of the relatively weaker inter-aggregate pores. However, as there is now a reduced volume of pore water, the reduction in shear force is less when compared to the force in the initial temperature cycle
- The collapse of any inter-aggregate pores leads to a relatively consolidated clay structure. Due to the decrease in applied shear force from the expansion of pore water there is a smaller number of inter-aggregate pores which collapse
- Where drainage is permitted, the effective stress of the sample is reduced through the expulsion of pore water. A smaller volume of water is drained during subsequent cycles due to the reduced increase in pore water caused by a reduction in the pore water volume
- As the clay has been subject to the induced pore water pressures previously, limited particle restructuring is required to withstand the load applied to the sample

As the clay sample temperature is reduced, the following conceptual model is proposed:

- A thermal contraction of the clay particle, adsorbed double layer water and pore water both inter-particle and intra-aggregate. This induces a negative pore water pressure within the sample, with the initial cooling promoting an increase in effective stress on the sample prior to the suction of water back into the sample to oppose this effect
- The volume of water drawn back into the sample due to suction is relatively consistent to the volume of water drained during the second temperature cycle caused by the now elastic behaviour of the sample
- The clay particle attraction increases as the double layer decreases in volume and distance between particles reduces

It can therefore be concluded from these hypotheses that a clay's response to temperature is determined by:

- The initial plasticity, and therefore the water content of the sample, thus the amount of free water expanding to increase the pore water pressure upon heating
- The initial structure, i.e. the number, nature and size of the pores within the sample
- The temperature increase the clay is subject to, and thus the magnitude of the particle, adsorbed and free water expansion

An additional conclusion can be detailed with regard to an elastic temperature behaviour within the clay. The initial temperature increase causes permanent temperature deformation of the clay microstructure, with the clay returning to a different particle structure following a temperature decrease. For the second and subsequent cycles, the behaviour of the clay represents elastic temperature deformation as a relatively equal amount of water is drained and reabsorbed to the sample

during heating. This relatively equal amount of drainage and reabsorption can be expected to continue for all subsequent temperature cycles, permitted the temperature does not exceed that of the original temperature increase.

When considering this in the context of a PFHX, it should be noted that the sample will not instantaneously heat a fixed volume of clay. Instead a thermal front will form and move out from the pile, dependent on the heating profile of the pile. This is similar to the thermal gradient which the clay sample experienced, with the outside of the sample heating and cooling ahead of the centre of the sample. To further understand the thermal gradient across the samples, further testing with embedded samples would be required.

6.4 Application of conceptual model to experimental results

This section has considered the results of the experimental testing carried out as part of this study in light of the proposed conceptual model to assess the robustness of the model.

6.4.1 Volume change

The simplified comparison of the relative percentage of sample volume drained and therefore sample volume change is shown in Figure 6.6. As previously discussed, the 5 cycle Durham Clay initial heating cycle has been found to be unrepresentative due to experimental errors, however the following cycles provide evidence to support the proposed conceptual model.

From the kaolin results, it can be seen that for both the 5 and 10 cycle samples, a relatively regular volume of water is drained and re-absorbed to the sample during each heating and cooling cycle. The lack of significantly larger initial percentage of water drained from the sample is an indication that kaolin is not as high plasticity and therefore there is not a large volume of pore water available at the beginning of

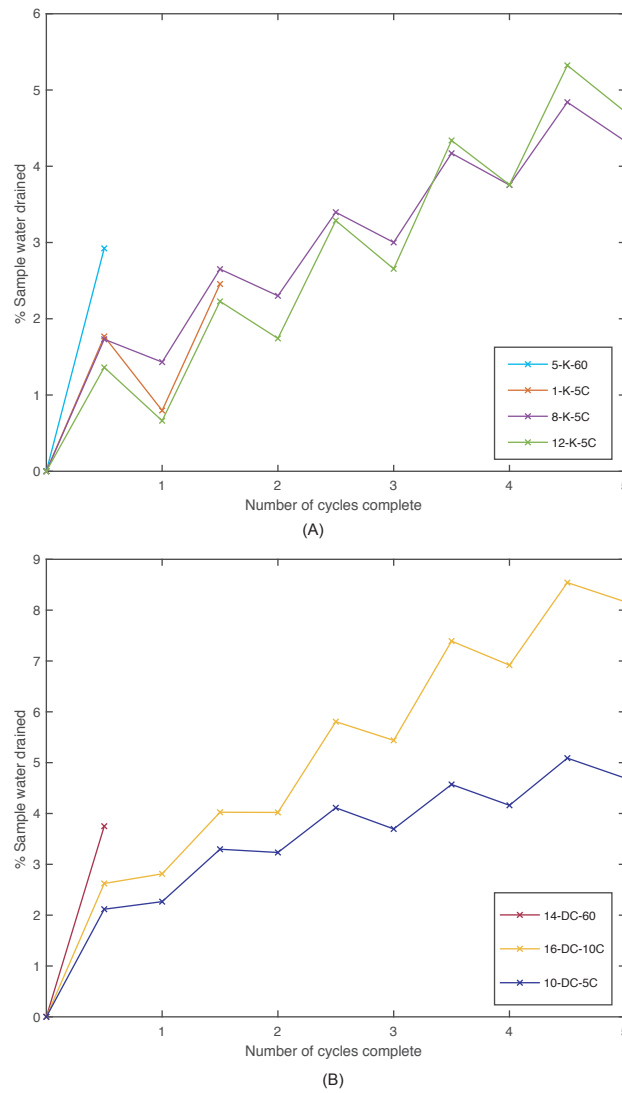


Figure 6.5: Percentage of sample volume drained during heating cycles for: (a) kaolin, (b) Durham Clay. Note: Varying y-axis scale used to demonstrate the cyclic trend

the cycles to expand and generate a large amount of increased pore water pressure, which would promote a significant particle restructure and therefore large permanent deformation within the sample. There is however a net amount of water drained following each heating and cooling cycle, which is an indication that the clay particle structure is not fully ready to withstand the induced increase in shear stress between the particles upon heating. It can be seen that there is a reduction in this net loss with each cycle, indicating that for undrained clays a significantly large percentage of their sample volume on the first cycle, the reorientation of the particle structure is an

iterative process occurring over the cycles. When considering the second and third temperature cycles of the Durham Clay sample, it can be deemed that this iterative process is complete by the third cycle whereby there is a relatively insignificant different net percentage of sample water drained following the cycle.

It can therefore be determined that the experimental results for volume change support the conceptual model proposed. This concept has also been tested alongside the results of Campanella & Mitchell (1968), discussed later in this section.

6.4.2 Critical state friction angle

The critical state friction angle was found to be independent of the elevated temperatures for both kaolin and Durham Clay. From the conceptual model, it would be expected that due to the expansion of the elements within the sample and therefore increased shear stress between the clay particles, a re-orientation of the clay particle created a change in the fabric of the clay and a further change in the critical state friction angle.

When considering the critical friction angle for the cyclic temperature testing, it can be seen that there is a slight increase of 1° following 5 cycles and then a reduction of 2° following 10 cycles leading to a net reduction in 1° from zero to 10 cycles. This suggests an increase in strength over 5 cycles, but a net decrease in strength over 10 cycles. This goes against the conceptual model as it would be expected that there would be a strength increase due to the re-orientation of the particles during the first temperature cycles, with subsequent cycles having minimal impact on the strength as the temperature remains within the thermal elastic range. It should be noted that the 10 cycle kaolin sample was subject to experimental errors and therefore is potentially not representative of a 10 cycle tested sample.

For the Durham Clay, an increase in 2° is observed following 5 temperature cycles, this complies with the conceptual model that the re-orientation of particles during temperatures cycle produces a strengthening of the clay structure.

When assessing the results against the conceptual model, due to the degree of

error across the test equipment, it is difficult to support and reject the conceptual model. It has been found that these results tend to support the conceptual model, with respect to the change in temperature over 5 cycles. With regard to the elevated temperature, it could be deemed that the increase in strength within the sample is too low to be identified by the experimental equipment.

6.4.3 Stiffness

For the experimental results for kaolin, it was found that the small strain stiffness increased when tested at elevated temperatures. This finding is supported by the conceptual model, by applying the same elements as for the critical state friction angle. With increasing temperature, the clay particles are required to re-structure in order to withstand an increasing pore water pressures within the sample and therefore an increasing shear stress between the particle bonds.

When applying the conceptual model to the small strain stiffness, at 60 °C during elevated temperature testing, the clay particles have re-structured to withstand the increased shear stress imposed between the clay particles, whilst experiencing the lowest shear force between the particles due to the thermal expansion of the adsorbed double layer water remaining. The clay particle structure is therefore restructured to withstand the highest shear stress between the particles, with the lowest levels of particles attraction. As the temperature decreases, the shear stress between the particles reduces, as the particle attractive forces increasing due to the decreasing in volume of the adsorbed double layer, allowing particles to move closer to one another. At the same time, the pore water undergoes thermal volumetric contraction, resulting in what could be described as a thermally overconsolidated sample. During subsequent temperature cycles, the conceptual model states that relatively small amounts of particle re-structuring will occur as the structure is already in a state to withstand the increased shear stress between the clay particles. From this, it could be determined that the clay would have a similar, or slightly greater small strain stiffness independent of the number of cycles complete. No evidence of this

is seen in the experimental results of this study with respect to the kaolin results. Unfortunately, due to previously discussed experimental errors a comparison cannot be determined for Durham Clay.

It should be noted that for the elevated temperature tests, the results provided are at temperature (sample temperature at 60 °C test), therefore mid-temperature cycle, opposed to the cyclic temperature results where testing was carried out after whole temperature cycle (sample temperature 24 °C). The difference of 24 kPa observed between the result of the 5 cycle test and 10 cycle test, has potentially been influenced by the pore water leakage detailed in Section 5.1.1. In comparing the experimental results to the conceptual model, there is support for the conceptual model with regard to the elevated temperature results, however this support is reduced when considering the cyclic temperature results. This is potentially due to the temperature at which the testing was conducted not allowing for a true comparison, in addition to an element of experimental errors. However, due to the results of the cyclic temperature variation falling between those of the 20 and 60 °C testing, it can be determined that the conceptual model would hold true to this understanding.

6.5 Application of conceptual model to literature results

When considering the results of literature, there are three seminal studies which have been conducted within this area, in addition to one major field study within the UK. In order to further consider the proposed conceptual model, it will be applied to the results of these studies to explain the findings of each in turn.

6.5.1 Campanella & Mitchell (1968) - Volume change

In a study of an illite sample through temperature variations as previously discussed, it was observed that an initial temperature variation resulted in a relatively large

amount of pore water being drained from the sample. The results of Campanella & Mitchell (1968) have been plotted alongside the results of kaolin and Durham Clay in Figure 6.6.

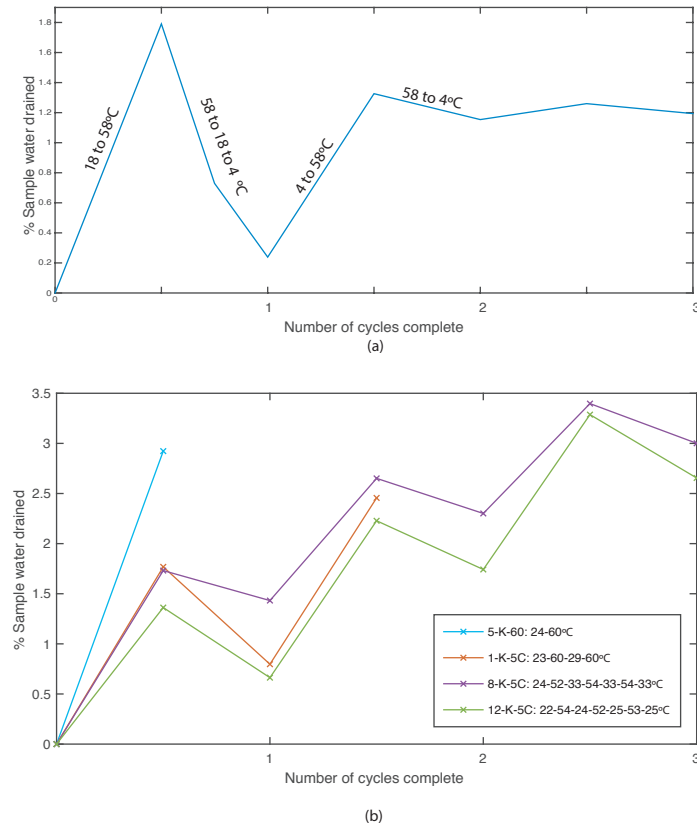


Figure 6.6: Percentage of sample volume drained during heating cycles for: (a) illite, taken from (Campanella & Mitchell 1968), (b) kaolin. Note: Varying y-axis scale used to demonstrate the cyclic trend

When comparing the plasticity of these samples, shown in Figure 6.7, illite has a relatively higher plasticity index to kaolin. As higher plasticity clays contain a greater volume of pore water, this can be attributed to the larger comparative volume of water being drained during the initial cycle when compared to subsequent cycles.

The conceptual model can further be tested on the second cycle of illite where an increased temperature differential is applied to the sample. During the initial cycle the sample was subjected to a temperature increase and decrease of 40 °C which, according to the conceptual model, will have resulted in a permanent deformation of the clay structure. For the second temperature cycle, the change in temperature was 54 °C, which is beyond that of the original temperature increase, thus promoting

further permanent deformation of the clay structure.

When considering the initial cooling period, the sample was subject to a 54 °C decrease in temperature following the 40 °C increase. In applying the conceptual model to this situation, it can be expected that a greater volume of water is re-absorbed into the sample during the cooling cycle, to account for the additional reduction in pore water pressure due to the increased temperature differential. As this is an increase in the suction of the sample, it could be expected that no further particle reorientation occurs due to this.

During the third and subsequent cycles, it can be seen that there is an insignificant net percentage of water drained from the sample, with the percentage drained approximating the percentage re-absorbed. Applying this conceptual model, this observation is due to the heating and cooling occurring within the elastic range of the sample as the temperatures do not exceed those which the sample has previous been subject to.

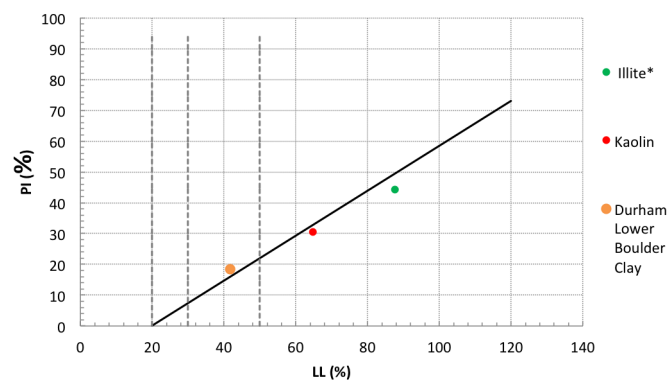


Figure 6.7: Plasticity chart for kaolin and Durham Clay tested within this study, in addition to illite studied in Campanella & Mitchell (1968)

It can therefore be determined that the proposed conceptual model supports the results of Campanella & Mitchell (1968).

6.5.2 Plum & Esrig (1969) - Lower void ratio with an increase in stress

The effect of heating to 50 °C and subsequent recooling to 24 °C has been investigated by Plum & Esrig (1969) through consolidometer testing of illite (PI = 84 %) with the results shown in Figure 6.8. At 24 °C the reduction in void ratio with increased vertical pressure followed that of a normal compression line, however during the heating of the illite, the void ratio of the sample decreased whilst the applied vertical pressure remained static. Upon cooling, the void ratio slightly increased before subsequently decreasing with increased applied vertical pressure. Upon completion of the cooling cycle, it was observed that a greater stress was now associated with a lower void ratio, when compared to that of the original normal consolidation line. The same effect was observed when the heating and cooling cycle was repeated at higher applied vertical pressure.

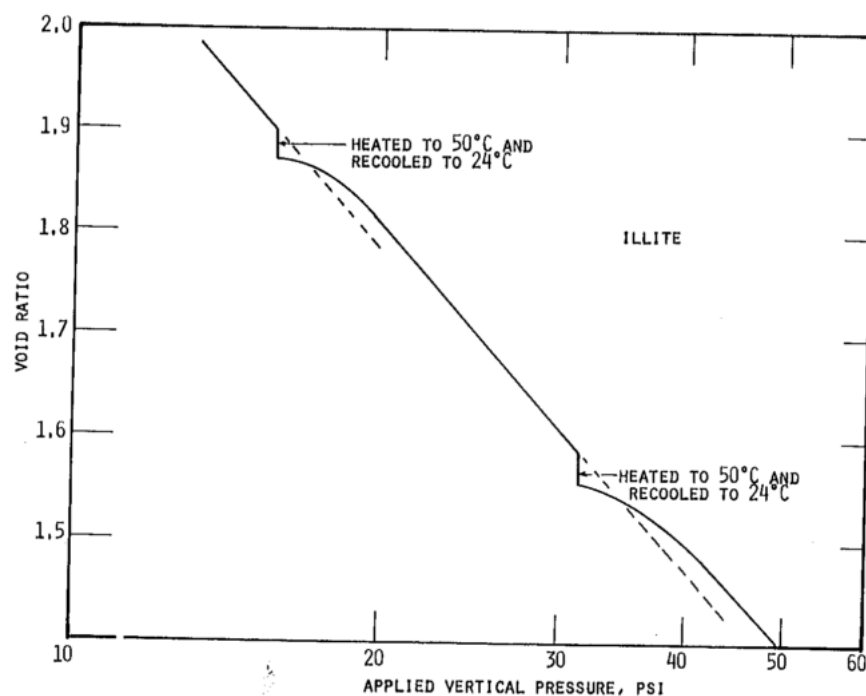


Figure 6.8: Effect on stress-strain behaviour in consolidometer of heating and cooling illite. (Plum & Esrig (1969))

Applying the conceptual model to this experimental data, it can be seen that during the initial temperature increase, the clay particles, adsorbed water and pore

water expand due to thermal volumetric expansion. An excess pore water pressure is induced whilst the shear force between the particles reduces, and shear stress within the sample increases. As pore water drains from the sample to neutralise the excess pore water pressure, a restructuring of the clay particles occurs to withstand the additional shear stress induced. A reduction in void ratio is therefore produced, which is what is observed in the experimental results. During cooling all elements of the clay contract, increasing the shear force between the particles with a reducing shear stress within the sample. A small increase in void ratio is observed as suction re-absorbs water to the sample to mitigate the suction of pore water pressures. The clay structure has now been strengthened, due to the temperature cycle, and can thus withstand a greater applied vertical pressure at a lower void ratio, as observed in the experimental results. It can therefore be determined that the proposed conceptual model supports the results of Plum & Esrig (1969).

6.5.3 Cekerevac et al. (2013) - Effect of overconsolidation ratio

As previously discussed, Cekerevac et al. (2013) found that in drained heating, normally consolidated clays contract, lightly over consolidated clays dilate before later contracting and highly overconsolidated clays only dilate upon heating from 22 to 90 °C, shown in Figure 6.10. Applying the conceptual model, it can be deemed that for the normally consolidated clays the clay particles are yet to experience a higher stress state and therefore a relatively large volume of pore water residing within the sample. Upon heating, this pore water expands, increasing the pore water pressure, thus promoting a drainage of pore water, with a reduction in sample volume. As this occurs, the clay particles are decreasing their shear force between one another, whilst the shear stress on the particles is increase causing a reorientation of the clay particles to support this higher stress state.

For the highly overconsolidated clay ($OCR = 12$), the opposite is true. The clay particles of a highly overconsolidated have previously existed at a higher shear stress

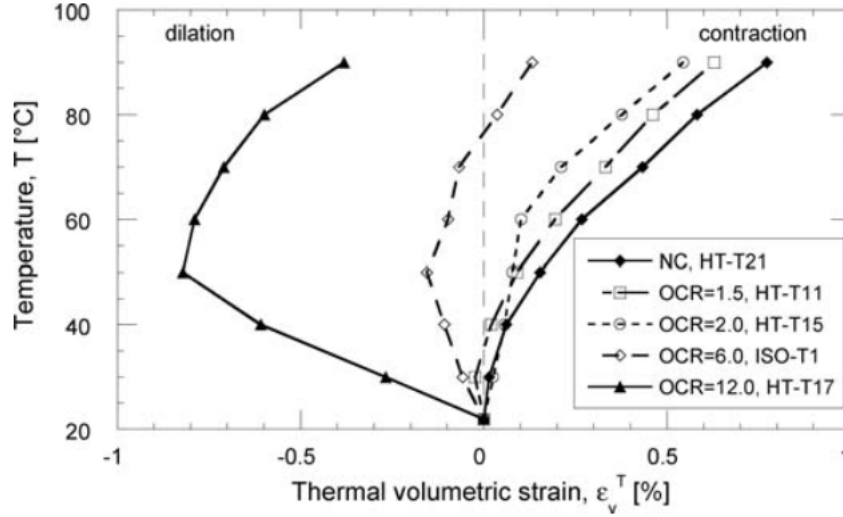


Figure 6.9: Volumetric strain of kaolin, at varying OCR, during heating from 22 to 90 °C. (Cekerevac et al. (2013))

state due to the mechanical loading during consolidation. This higher mechanical loading has previously increased the pore water pressure, promoting drainage of the pore water to mitigate this effect. It can therefore be deemed that the increase in temperature from 22 to 90 °C acts within the elastic range of the clay particle structure due to prior mechanical loading. A dilation of the sample therefore occurs as a result of the clay particle, adsorbed double layer and remaining pore water thermally dilating with temperature.

At higher temperatures, it can be observed that a reversal of the dilation occurs. Applying the conceptual model, at temperatures beyond 50 °C a pore water pressure, beyond that induced by the prior mechanical loading, is developed leading to the sample now behaving as a normally consolidated sample. This concept can also be applied to the lightly overconsolidated clay (OCR= 6) whereby normally consolidated behaviour occurs also occurs at a temperature of 50 °C. The lightly consolidated clay has a net contraction following the temperature increase, which is due to a reduction in the initial amount of thermal dilation at lower temperatures. The initial dilation of the lightly overconsolidated clay is relatively less than that of the highly overconsolidated clay. Following the conceptual model, this observation is due to the particle structure of the highly overconsolidated clay being in a more

compact structure having previously re-orientated to withstand a higher shear stress between particles. Therefore the particles in the overconsolidated clay do not re-orientate during heating; the particles and their adsorbed water, alongside remaining pore water, simply expand. For the lightly overconsolidated clays, the particles still have the ability to re-structure to withstand the increasing shear stress between the particles. There is a less profound effect of heating due to the re-structuring of the clay particles as the particles, adsorbed water and pore water expand. This theory could be simplified to the particles in the lightly overconsolidated clay being more active in their response to increasing temperature and therefore shear stress between the particles, whereas the highly overconsolidated clay particles are stagnant in their response, having previously re-structured to withstand the shear stress induced by temperatures up to 50 °C. The particles and pore water therefore remain in the same orientation whilst undergoing thermal volumetric expansion. It can therefore be determined that the proposed conceptual model supports the results of Cekerevac et al. (2013).

6.5.4 Bourne-Webb et al. (2009) - Field study

Within the field study produced by Bourne-Webb et al. (2009), previously discussed in Section 2.5, the pile head displacement is monitored during a period of pile cooling with a fluid temperature of -6 ° pile heating with a fluid temperature of 40 ° and daily temperature cycles between -6 and 40 °, shown in Figure 6.10. It should be noted that a fluid temperature of -6 ° does not lead to a 6° reduction in ground temperature and the concrete pile performs a role to insulate the heat exchanger loops, with a thermal gradient occurring across the pile radius.

On the first day of the cooling stage, there was a settlement of the pile head to a value of approximately 5 mm, once at 5 mm the level of the pile head remained constant for the duration of the cooling period. When the temperature of the pile was reversed and heated to 40 °, on the first day of heating the settlement of the pile head is reduced to approximately 3 mm, a net uplift of 2 mm in pile head

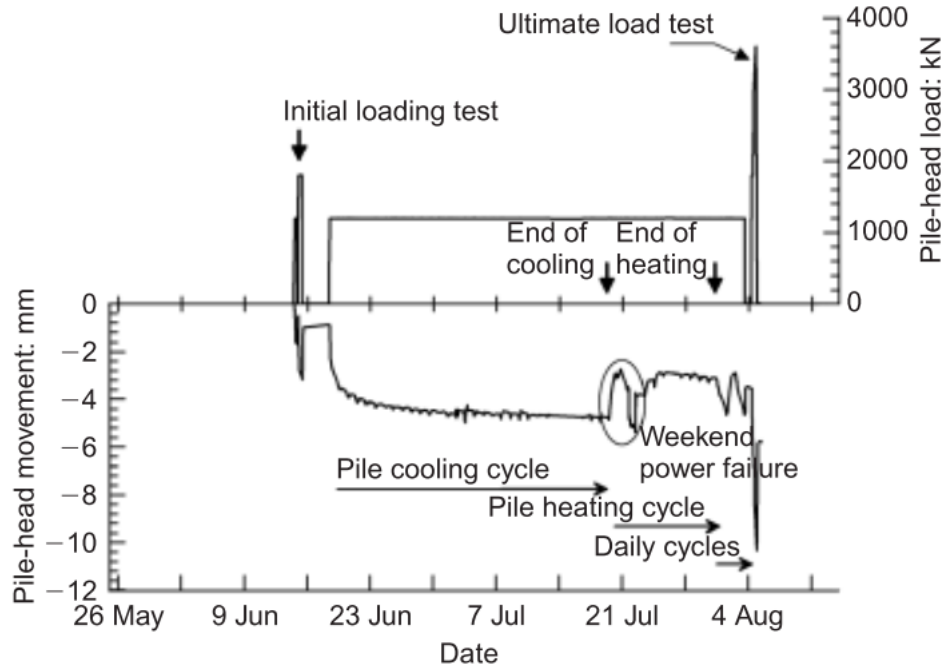


Figure 6.10: Load control and pile-head displacement through test period for PFHX installed at Lambeth College. (Bourne-Webb et al. (2009))

displacement. This net uplift was maintained for the duration of the heating period. During the final stage of testing the daily temperature cycles induced an oscillating pile head movement of 1 mm coinciding with the daily change in temperature.

When applying the conceptual model to these results it can be determined that the reduction in temperature ground temperature promoted a contraction of the pore water within the clay, in addition to a contraction of the clay particle and adsorbed double layer. This contraction reduced the shear stress whilst increasing the attractive forces between the particles, leading to a net reduction in volume.

During the heating stage, the increase in temperature promotes an increase in pore water pressure and therefore shear stress between the particles through the thermal volumetric expansion of pore water. The thermal expansion of the adsorbed water reduced the attractive force between clay particles. The excess pore water pressure is dissipated throughout the body of clay as the clay particles re-structure themselves in response to the additional shear stress within the sample. Once re-structuring of the clay particles has occurred, there will be very limited volume change of the sample. This corresponds to the results of the heating period of the

field study whereby the pile head movement remained constant following the initial reduction in displacement.

For the daily temperature cycling, between -6 and 40 °C, the clay is operating within the thermal elastic region of the clay, therefore the only factors which induce a volume change are due to the thermal volumetric expansion of the clay elements. As the clay particle structure has previously re-organised to withstand an increase in shear stress, no further orientation is required. This corresponds to the 1 mm daily variation in pile head displacement during the daily cycling of the pile temperature. From these results, it can be determined that the conceptual model supports the finds of the study by Bourne-Webb et al. (2009).

6.6 Summary of conceptual model

Following the comparison of experimental studies and a field study, the proposed conceptual model has been verified to represent the microstructural behaviours and therefore bulk behaviour of clays subject to cyclic temperature variation. The now confirmed conceptual model has been illustrated in Figures 6.11 and 6.12 in order to provide clarity on the impact of single heating and cooling cycle.

With regard to subsequent temperature variations, subject to a sustained period of elevated temperature being allowed to ensure the excess pore water pressures are dissipated, the clay will behave in a thermoelastic manner. The volume change experience in subsequent samples will be a product of the thermal expansion of the clay particles, adsorbed double layer water and pore water.

In cases whereby a sustained period of elevated temperature is not permitted, the clay is required to undergo multiple temperature cycles. This will allow for a particle re-organisation to be complete in order to withstand the increased shear stress applied to the particles at its maximum temperature. With subsequent cycles, the the differential in volume change due to the thermally induced pore water pressure would reduce with each cycle until it was fully dissipated, and therefore a regular, elastic volumetric change would occur. The difference between an initial significant

period of sustained heating and a reduced duration is illustrated in Figure 6.13.

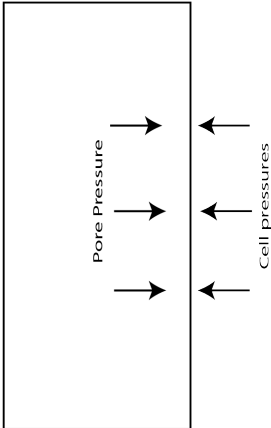
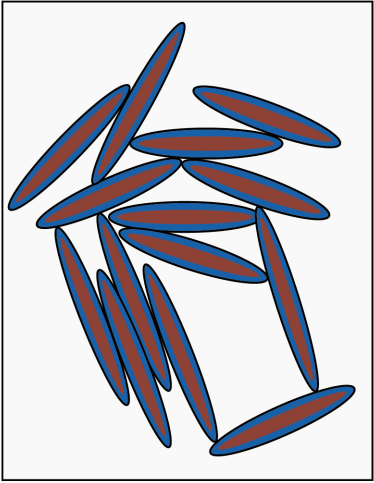
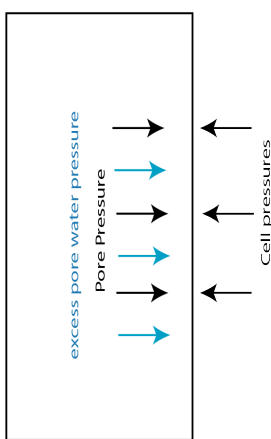
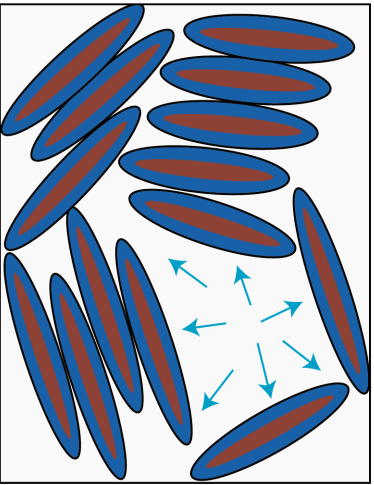
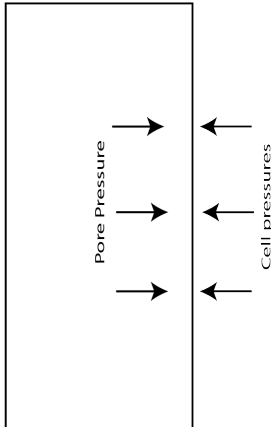
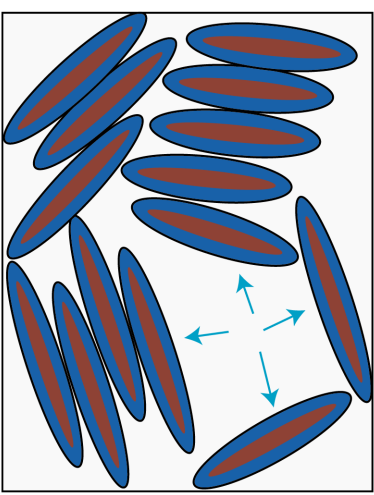
	Bulk Observations	Microstructure Observations	Brief Description
20 °C			<ul style="list-style-type: none"> - Particles and adsorbed double layer water in neutral state - Cell pressure and pore pressure inducing an effective stress on the sample
20 to 60°C - no drainage			<ul style="list-style-type: none"> - At the immediate point of temperature increase, no drainage occurs - Particles and adsorbed double layer water and pore water undergo thermal volumetric expansion - Distance between particles increase, shear strength reduces - Particle attractive forces decreases - Pore water pressure increases, reducing the sample effective stress - Shear force between particles increase, increasing probability of bond slippage or failure
20 to 60°C - drained			<ul style="list-style-type: none"> - Pore water pressure dissipates through drainage of pore water - Pressure within pore space reduces - Particles and adsorbed water remain at their increased volume - Effective stress increases as water drains towards the original effective stress present at 20°C - Particles restructure to withstand the now increasing effective stress - Distance between particles remains greater than at 20°C

Figure 6.11: Diagram of conceptual model for clay heating showing the bulk and microstructural behaviours

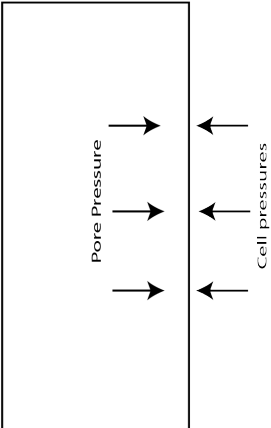
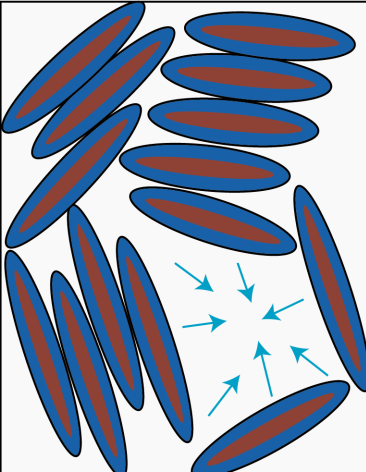
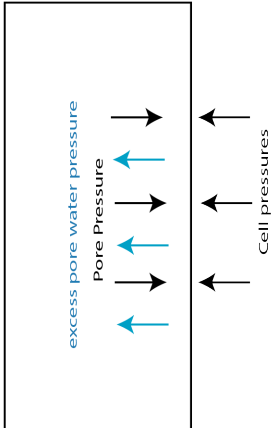
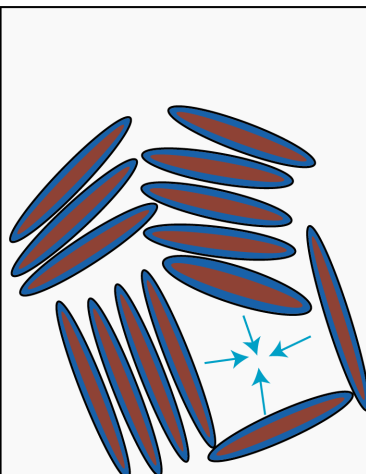
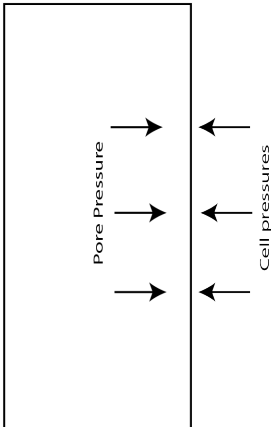
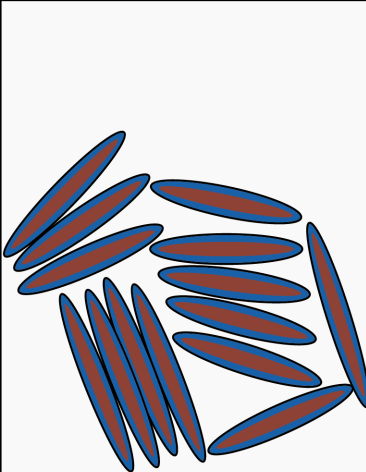
	Bulk Observations	Microstructure Observations	Brief Description
60 to 20°C - no drainage			<ul style="list-style-type: none"> - At the immediate point of cooling water adsorption does not occur - Particles, double layer adsorbed water and pore water undergo thermal volumetric contraction - Pore water pressure reduces - Effective stress increases, beyond that of at 20°C - Distance between particles increase, increasing shear strength between particles - Particle attractive forces increase
60 to 20°C - drained			<ul style="list-style-type: none"> - Negative pore water pressure is equalised through suction drawing water back into the sample - Pore water pressure decreases, reducing the effective stress of the sample to that of 20°C - Particles, adsorbed water and pore water reduce to their original volume - A net volume of water is drained from the sample - Particles do not restructure as there is no increase in effective stress
20 °C			<ul style="list-style-type: none"> - Particles and adsorbed double layer water returned their original volume - Pore water returns to it's original volume - State of original effective stress - Reduction in number and size of pore within sample

Figure 6.12: Diagram of conceptual model for clay cooling showing the bulk and microstructural behaviours

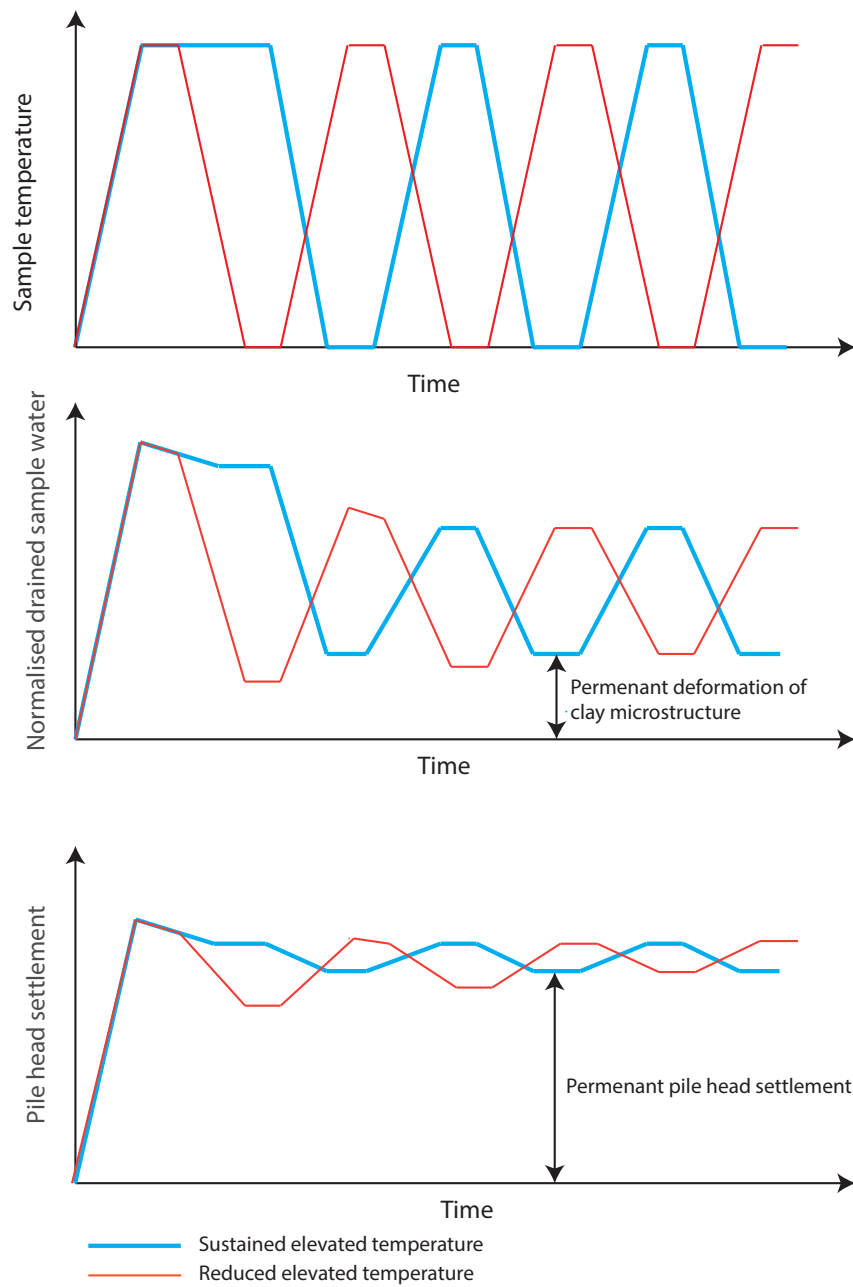


Figure 6.13: Illustration of the variation in cycle volume change with variation duration of initial heating

6.7 Application of conceptual model

In applying the conceptual model to the application of PFHX the effect has been defined with respect to a clay's plasticity.

For *high plasticity clays* the higher water content leads to a significantly increased pore water pressure during the initial temperature cycle. This is especially significant in clays with low permeabilities whereby drainage occurs at a slower rate. It could be determined that for low permeability clays, if the maximum temperature is not maintained for a long enough duration for the excess pore water to drain and dissipate this water, multiple temperature cycles will be required before the temperature cycle variation behaves elastically.

For *low plasticity clays* there is a relatively small difference in volume change between the first and subsequent cycles due to the lower water content of low plasticity clays. For lower plasticity clays, the volume change during cyclic heating and cooling is dependent on the expansion and contraction of the clay particles, adsorbed water and pore water within the samples, which behaves elastically across the temperature cycles.

It can be determined for all clays, that once the initial pore water pressures have been dissipated either by repeated number of cycles or a period of elevated temperature, an elastic thermal behaviour will be maintained, permitted the temperature increase does not exceed that of the original temperature increase. If the temperature is increased beyond that of the initial temperature increase, an excess pore water pressure will be induced, leading to further permanent deformation of the sample. This would apply across any differential, theoretically up to 300°C, the point where double layer water is released, and therefore not limited to the experimental temperatures within this study.

As an example, a PFHX installed in kaolin with an effective stress of 500 kPa, subject to a temperature increase from 22 °C to 80 °C would observe an increase in relative volume of sample water drained during heating when compared to that of this study. This is in response to an increase in pore water pressure due to

the additional thermal expansion of clay particles, adsorbed water and pore water. Holding the temperature of the clay at 80 °C until the volume of water drained from the sample tended to zero, allows for the permanent re-structuring of clay particles to occur to withstand the increase in shear stress between the particles. From this point onwards, the clay would operate within a thermally elastic range, whereby its volume expansion and contraction would not increase or decrease more than that observed in the heating and cooling of the first temperature cycle. For a clay of higher plasticity, an extended period of elevated temperature would be required before the volume of water drained tended to zero, in addition to a greater increase and decrease occurring during the initial period of heating and cooling.

Chapter 7

Conclusion

This thesis has considered the impact of cyclic temperature on pile foundations used as heat exchanges through consideration of current literature, experimental studies and the development of a conceptual model of how the microstructure of clay responds to cyclic temperature variation and the bulk behaviour this leads to. The following conclusions have been made in the following areas.

This work supports the current literature on PFHX in the areas of:

- the understanding on the energy performance achievable through PFHX
- the variations in structural properties with temperature
- the individual observations made during thermal testing of clays

7.1 Experimental study

Through the development of a thermal triaxial cell testing, testing was carried out on two clays of different plasticities. Samples of kaolin and Durham Clay were tested at an effective stress of 500 kPa at elevated temperatures up to 60 °C and following 5 cyclic temperature variations from 20 °C to 60 °C. Through testing, the following has been found:

- Higher plasticity clays drain a relatively higher volume of water than clays of a lower plasticity

- There is a net loss of water drained from a sample following a heating and cooling cycle
- The critical state friction angle of clays tested at elevated temperatures remains constant. The critical state friction angle for kaolin was found to be 21° and for Durham Clay was 28°
- The small strain stiffness of kaolin increases with temperature for clay tested at elevated temperature
- The small strain stiffness of kaolin increases following 5 temperature cycles

7.2 Conceptual model

By drawing together the understanding from literature and the finding of experimental work, a conceptual model has been constructed which considers the role of clay particles, adsorbed double layer water and the pore water within a clay. It can be seen by the conceptual model that there are two opposing effects due to:

- The thermal expansion and contraction of the clay particles and their adsorbed double layer water
- The increase and decrease of pore water pressure with the thermal expansion and contraction of pore water

The effects contribute to the overall bulk behaviour of the clay which has been found to vary in its response to temperature, according to:

- **The initial temperature increase:** The initial temperature increase dictated the maximum pore pressures within the sample and defines the thermal range over which the clay will subsequently behaviour ‘elastically’
- **Plasticity of the clay:** The plasticity of the clay defines the initial water content of the clay. This provides an indication of the required duration of

initial heating required for permanent deformation to occur within the clay particles or the number of reduced duration cycles that are required for permanent deformation to be complete.

- **Overconsolidation ratio:** The overconsolidation ratio provides an indication of amount of thermally induced shear stress which the particles of the clay can withstand before further permanent deformation will occur within the clay.

Further details of this conceptual model are provided in Section 6.6.

7.3 Application to PFHX design

In applying this conceptual model to the design of PFHX the following consideration should be made, with respect to the behaviour of the clay:

- There is no limit to which the clay can be heated. This conceptual model applies to clay up to 400 °C where chemical changes are observed in the clay
- The plasticity of the clay indicates the amount of pile head settlement which will occur in the initial seasons
- Greater consideration should be given to the design of PFHX for use in high plasticity clays. It would be advised that thermal triaxial testing is conducted on site specific undisturbed samples to identify the degree of volume change induced and therefore initial pile settlement
- In low plasticity clays, the induced volume change of the clay is small. This will pose minimal impact on the overall settlement of the pile foundation

Due to the volume changes observed within this study and those of literature, a conservative estimate can be made that for low plasticity, normally consolidated clays a volume change of less than 0.5% is to be expected, with higher plasticity clays experiencing a volume change less than 1%.

7.4 Recommendations for future research

To further understand the behaviour of clay subject to cyclic temperature variation, the following additional areas should be pursued:

- Produce evidence that, for clays heated and cooled within the temperature range which the clay has previously been subject to, the behaviour of clay is elastic. Whereby, once a clay has returned to its original temperature, the clay returns to its pre-heated state.
- Equate the increase in stress which is produced during temperature increase of the clay to an associated mechanical stress. This would allow a mechanical over-consolidation ratio to be determined following the application of temperature cycles to clays.
- Identify if it's possible to relate the secondary volumetric creep constant to temperature induced consolidation.
- Evidence how a thermal gradient moves through the clay using additional embedded thermocouples, either through triaxial or oedometer testing.

Bibliography

- Abuel-Naga, H. M., Bergado, D. T. & Lim, B. (2007), ‘Effect of temperature on shear strength and yielding behaviour of soft bangkok clay’, *Japanese Geotechnical Society* **47**(3), 423–436.
- Agar, J. G., Morgenstern, N. R. & Scott, J. D. (1986), ‘Thermal expansion and pore pressure generation in oil sands’, *Canadian Geotechnical Journal* **23**(3), 327–333.
- Amis, T. & Loveridge, F. (2014), ‘Energy piles and other thermal foundations for GSHP – Developments in UK practice and research’, *REHVA Journal* (January), 32–35.
- Baldi, G., Hueckel, T. & Pellegrini, R. (1988), ‘Thermal volume changes of mineral water system in low porosity clay soils’, *Canadian Geotechnical Journal* **25**(4), 807–825.
- Banks, D. (2008), *An Introduction to Thermogeology Heating and Cooling*.
- Bourne-Webb, P. J., Amis, T., Soga, K., Davidson, C., Payne, P. & Amatya, B. (2009), ‘Energy pile test at Lambeth College, London: geotechnical and thermodynamic aspects of pile response to heat cycles’, *Géotechnique* **59**(3), 237–248.
- Bourne-Webb, P. J., Soga, K. & Amatya, B. (2011), ‘A framework for understanding energy pile behaviour’, *Proceedings of the ICE - Geotechnical Engineering* pp. 1–8.
- Brandl, H. (2006), ‘Energy foundations and other thermo-active ground structures’, *Géotechnique* **56**(2), 81–122.

- Buildings Research Establishment (2016), Study on Energy Use by Air- Conditioning : Final Report BRE Client Report for the Department of Energy, Technical Report June.
- Burghignoli, a., Desideri, A. & Miliziano, S. (2000), ‘A laboratory study on the thermomechanical behaviour of clayey soils’, *Canadian Geotechnical Journal* **37**(4), 764–780.
- Burland, J. B. (1990), ‘On the compressibility and shear strength of natural clays’, *Géotechnique* **40**(3), 329–378.
- Busby, J., Lewis, M., Reeves, H. & Lawley, R. (2009), ‘Initial geological considerations before installing ground source heat pump systems’, *Quarterly Journal of Engineering Geology and Hydrogeology* **42**(3), 295–306.
- Campanella, R. G. & Mitchell, J. K. (1968), ‘Influence of temperature variations on soil behaviour’, *ASCE* **94**(3).
- Carbon Trust (2007), Air Conditioning. Maximising comfort, minimising energy consumption, Technical report, UK.
- Cekerevac, C. (2003), Thermal effects on the mechanical behaviour of saturated clas, PhD thesis, Ecole Polytechnique Federale de Lausanne.
- Cekerevac, C. & Laloui, L. (2004), ‘Experimental study of thermal effects on the mechanical behaviour of a clay’, *International Journal for Numerical and Analytical Methods in Geomechanics* **28**(3), 209–228.
- Cekerevac, C., Laloui, L. & Vulliet, L. (2013), ‘A Novel Triaxial Apparatus for Thermo-Mechanical Testing of Soils’, *Geotechnical Testing Journal* **28**(2), 1–10.
- Cetin, H. & Gokoglu, A. (2013), ‘Soil structure changes during drained and undrained triaxial shear of a clayey soil’, *Soils and Foundations* **53**(5), 628–638.
- Evidence Directorate (2009), *Ground source heating and cooling pumps – state of play and future trends*.

- Finn, F. N. (1952), The Effect of Temperature on the Consolidation Characteristics of remolded clau, *in* ‘Symposium on Consolidation Testing of Soils’, pp. 65–71.
- Glendinning, S. & Hughes, P. (2014), ‘Construction , management and maintenance of embankments used for road and rail infrastructure : implications of weather induced pore water pressures’, pp. 799–816.
- Gulgun, Y. (2011), ‘The effects of temperature on the characteristics of kaolinite and bentonite’, *Scientific Research and Essays* **6**(9), 1928–1939.
- Houston, S. L. & Lin, H. (1987), ‘A thermal consolidation model for pelagic clays’, *Marine Geotechnology* **7**(2), 79–98.
URL: <http://dx.doi.org/10.1080/10641198709388209>
- Hueckel, T. (2002), ‘Reactive plasticity for clays during dehydration and rehydration. Part 1: Concepts and options’, *International Journal of Plasticity* **18**(3), 281–312.
- Hueckel, T. & Pellegrini, R. (1992), ‘Effective stress and water pressure in saturated clays during heating-cooling cycles’, *Canadian Geotechnical Journal* **29**, 20–25.
- Hughes, P., Glendinning, S., Mendes, J., Parkin, G., Toll, D., Gallipoli, D. & Miller, P. (2009), ‘Full-scale testing to assess climate effects on embankments’, *Engineering Sustainability* **162**(ES2), 67–79.
- Israelachvili, J. N. (2011), *Intermolecular and surface forces*, Academic Press.
- Kenney, T. (1966), Shearing resistance of Natural Quick Clays, PhD thesis, University of London.
- Korson, L., Drost-Hansen, W. & Millero, F. J. (1969), ‘Viscosity of water at various temperatures’, *The Journal of Physical Chemistry* **73**(1), 34–39.
- Laloui, L., Nuth, M. & Vulliet, L. (2006), ‘Experimental and numerical investigations of the behaviour of a heat exchanger pile’, *International Journal for Numerical and Analytical Methods in Geomechanics* **30**(8), 763–781.

- Lambe, T. (1959), A Mechanistic Picture of Shear Strength in Clay, *in* 'ASCE Research Conference on Shear Strength of Cohesive Soils', Boulder, Colorado, pp. 116–130.
- Lambe, T. W. (1953), The structure of inorganic soils, *in* 'American Society of Civil Engineering', p. 315.
- Lambe, T. W. (1958), 'The structure of compacted clay', *Journal of the Soil Mechanics and Foundations Division* **1654**(SM2), 1–34.
- Leonards, G. & Girault, P. (1961), A Study of the One-Dimensional Consolidation Test, *in* 'Proc. Fifth Int. Conf. on Soil Mechanics and Found. Eng, Paris', pp. 116–130.
- Likitlersuang, S., Teachavorasinskun, S., Surarak, C., Oh, E. & Balasubramaniam, A. (2013), 'Small strain stiffness and stiffness degradation curve of Bangkok Clays', *Soils and Foundations* **53**(4), 498–509.
- Loveridge, F. & Powrie, W. (2012), Pile heat exchangers : thermal behaviour and interactions, *in* 'Proceedings of the Institution of Civil Engineers'.
- McConnachie, I. (1974), 'Fabric changes in consolidated', *Geotechnique* (2), 207–222.
- Mitchell, J. K. (1993), *Fundamentals of Soil Behaviour*, John Wiley & Sons Inc., New York, USA.
- Olmo, C. D., Fioravante, V., Gera, F., Hueckel, T., Mayor, J. C. & Pellegrini, R. (1996), 'Thermomechanical properties of deep argillaceous formations', *Engineering Geology* **41**, 87–102.
- Plum, R. L. & Esrig, M. I. (1969), Some temperature effects on soil compressibility and pore water pressure, *in* 'Highway Research Board, Special Report 103, Conference on the Effect of Temperature and Heat on Engineering Behaviour of Soils', pp. 231 – 242.

- Reeves, G., Sims, I. & Cripps, J. (2006), *Clay materials used in construction*, Geological Society, London.
- The Engineering Toolbox (n.d.), ‘Water - Thermodynamic Properties’.
- URL:** http://www.engineeringtoolbox.com/water-thermal-properties-d_162.html
- Towhata, I., Kuntiwattanakul, P., Seko, I. & Ohishi, K. (1993), ‘Volume change of clays induced by heating as observed in consolidation tests’, *The Japanese Geotechnical Society NII-Electronic Library Service* **33**(4), 170–183.
- Wang, M. C., Benway, J. M. & Arayssi, A. M. (1990), ‘The Effect of Heating on Engineering Properties of Clays’, *Physico-Chemical Aspects of Soil and Related materials* pp. 1139–1158.
- West, T. R. (1995), *Geology Applied to Engineering*, Waveland Press Inc., Long Grove, USA.
- Yavari, N., Tang, A. M., Pereira, J. M. & Hassen, G. (2016), ‘Effect of temperature on the shear strength of soils and soil/structure interface’, *Canadian Geotechnical Journal* **53**(7), 1186–1194.
- Yilmaz, G. (2011), ‘The effects of temperature on the characteristics of kaolinite and bentonite’, **6**(9), 1928–1939.
- Yin, Z. Y., Xu, Q. & Hicher, P. Y. (2013), ‘A simple critical-state-based double-yield-surface model for clay behavior under complex loading’, *Acta Geotechnica* **8**(5), 509–523.
- Yong, R. N. (2003), ‘Influence of microstructural features on water, ion diffusion and transport in clay soils’, *Applied Clay Science* **23**(1-4), 3–13.
- Yu, C. Y., Chow, J. K. & Wang, Y. H. (2016), ‘Pore-size changes and responses of kaolinite with different structures subject to consolidation and shearing’, *Engineering Geology* **202**, 122–131.

Yu, C., Yin, Z. & Zhang, D. (2014), ‘Micromechanical modelling of phase transformation behaviour of a transitional soil’, *Acta Mechanica Solida Sinica* **27**(3), 259–275.

Appendix A

Test data

A.1 Overview

An overview of all tests, including the sample moisture content, void ratio and comments relating to the test is provided in Table A.1.

A.2 Triaxial data

Triaxial data is provided for each of the tests detailed in Table A.1. This data is the raw data which has been taken directly from the GDS measurements recorded during the saturation, consolidation, heating and shear stage.

For each of the test, a commentary is provided:

- Test 1_K_5C (Figure A.1) failed after the second heating cycle, therefore the shear stage was not reached.
- Test 2_K _10C - no results shown as leak occurred during saturation stage.
- Test 3_K _10C (Figure A.2) shows a complete test.
- Test 4_Brass, no results shown as this test was used to verify thermal expansion of the system. The test however failed, with leaking occurring between the sample and cell water.

Table A.1: Sample properties and laboratory testing overview

Test Name	Material	Moisture Content before test (%)	Void Ratio, e	Consolidated?	Test Type	Temperature profile (°C)	Comments
1_K_5C	Kaolin	30.59	1.15	Yes	5 Cycles	23 - 60 - 29 - 60 - X	Test failed after 2nd heating cycle
2_K_10C	Kaolin	-	-	-	-	-	Leak occurred during saturation stage
3_K_10C	Kaolin	29.14	1.04	Yes	10 Cycles	21 - 59 - 23 - 59 - 24 - 59 - 23 - 60 - 24 - 60 - 24 - 60 - 24 - 60 - 24 - 60 - 24	Complete test
4_Brass	Brass	-	-	Yes	-	-	Leak during heating stage
5_K_60	Kaolin	30.23	1.11	Yes	Elevated to 60C	24 - 60	Complete test
6_K_20	Kaolin	30.73	1.16	Yes	Bench mark	23.5 (average)	Complete test
7_K_40	Kaolin	30.83	1.28	Yes	Elevated to 40C	23 - 46	Complete test
8_K_5C	Kaolin	30.02	1.10	Yes	5 Cycles	24 - 52 - 33 - 54 - 33 - 54 - 33 - 53 - 33 - 54 - 24	Local LVDT failure
9_DC_20	Durham Clay	-	-	-	-	-	Leak during saturation
10_DC_5C	Durham Clay	20.90	0.66	Yes	5 Cycles	24 - 50 - 35 - 50 - 33 - 49 - 33 - 49 - 24	Complete test
11_DC_10C	Durham Clay	-	-	-	-	-	Leak during saturation
12_K_5C	Kaolin	27.68	1.00	Yes	5 Cycles	22 - 54 - 24 - 52 - 25 - 53 - 25 - 54 - 24 - 54 - 22	Radial LVDT fell off
13_DC_40	Durham Clay	-	-	-	-	-	Leak occurred during saturation stage, peak state data included
14_DC_60	Durham Clay	20.54	0.62	Yes	Elevated to 60C	22 - 57 (average)	Complete test
15_DC_10C	Durham Clay	20.21	0.63	Yes	-	-	Leak occurred during first heating cycle - consolidation stepped to prevent LVDT's dislodging
16_DC_10C	Durham Clay	20.00	0.61	Yes	10 Cycles	24 - 60 - 26 - 59 - 26 - 58 - 25 - 59 - 25	Leak occurred after 4 heating cycles. Consolidation stepped to prevent LVDT's dislodging
17_K_40	Kaolin	-	-	-	-	-	Leak occurred during saturation stage
18_DC_40	Durham Clay	-	-	-	-	-	Leak occurred during saturation stage
19_K_40	Kaolin	-	-	Yes	Elevated	22 - 41 (average)	Local LVDT's failed & missing moisture test results
20_DC_40	Durham Clay	-	-	-	-	-	Cracked cell
21_DC_40	Durham Clay	-	-	-	-	-	Fault occurred in GDS unit midway through consolidation, making multiple file test. Consolidation and heating unrepresentative.
22_DC_40	Durham Clay	20.41	0.64	Yes	Yes	23 - 42 - 45 (20 hours) - 42	Leak from cell to atmosphere
23_DC_40	Durham Clay	-	-	-	-	-	Sample heated only
24_DC_40	Durham Clay	-	-	-	-	-	
25_K_Verify	Kaolin	25.85	0.89	-	Elevated	22 - 53 - 24	

- Test 5_K_60 (Figure A.3 shows a complete test.
- Test 6_K_20 (Figure A.4) shows a complete test.
- Test 7_K_40 (Figure A.5) shows a complete test.
- Test 8_K_5C (Figure A.6) shows a complete test.
- Test 9_DC_20, leak occurred during saturation, no results shown.
- Test 10_DC_5C (figure A.7) shows a complete test.
- Test 11_DC_10C, leak occurred during saturation, no results shown.
- Test 12_K_5C (Figure A.8) complete test, however local radial LVDT detached from sample
- Test 13_DC_40, leak occurred during saturation, no results shown.
- Test 14_DC_60 (Figure A.9) shows a complete test.
- Test 15_DC_10C (Figure A.10) shows results with a leak occurring during first heating cycle. In the results, it can be observed that consolidation was carried out in stages to mitigate potential for local LVDT's becoming detached during this stage.
- Test 16_DC_10C (Figure A.11) shows a leak occurring during heating stage. As Test 15_DC_10C, consolidation occurred in stages to prevent local LVDT's detaching from sample.
- Test 17_K_40, leak occurred during saturation, no results shown.
- Test 18_DC_40, leak occurred during saturation, no results shown.
- Test 19_K_40, complete test results shown. It should be noted that moisture test results were lost due to samples being misplaced in the oven. Void ratio results have therefore not been calculated.

- Test 20_DC_40, triaxial cell cracked during saturation stage, no results shown.
- Test 21_DC_40 results shown are combined tests 21, 22, 23 and 24 due to errors occurring in the GDS system. Despite these errors, a complete test was achieved.
- Test 24_K_Verify, no results shown as this test was a temperature calibration.

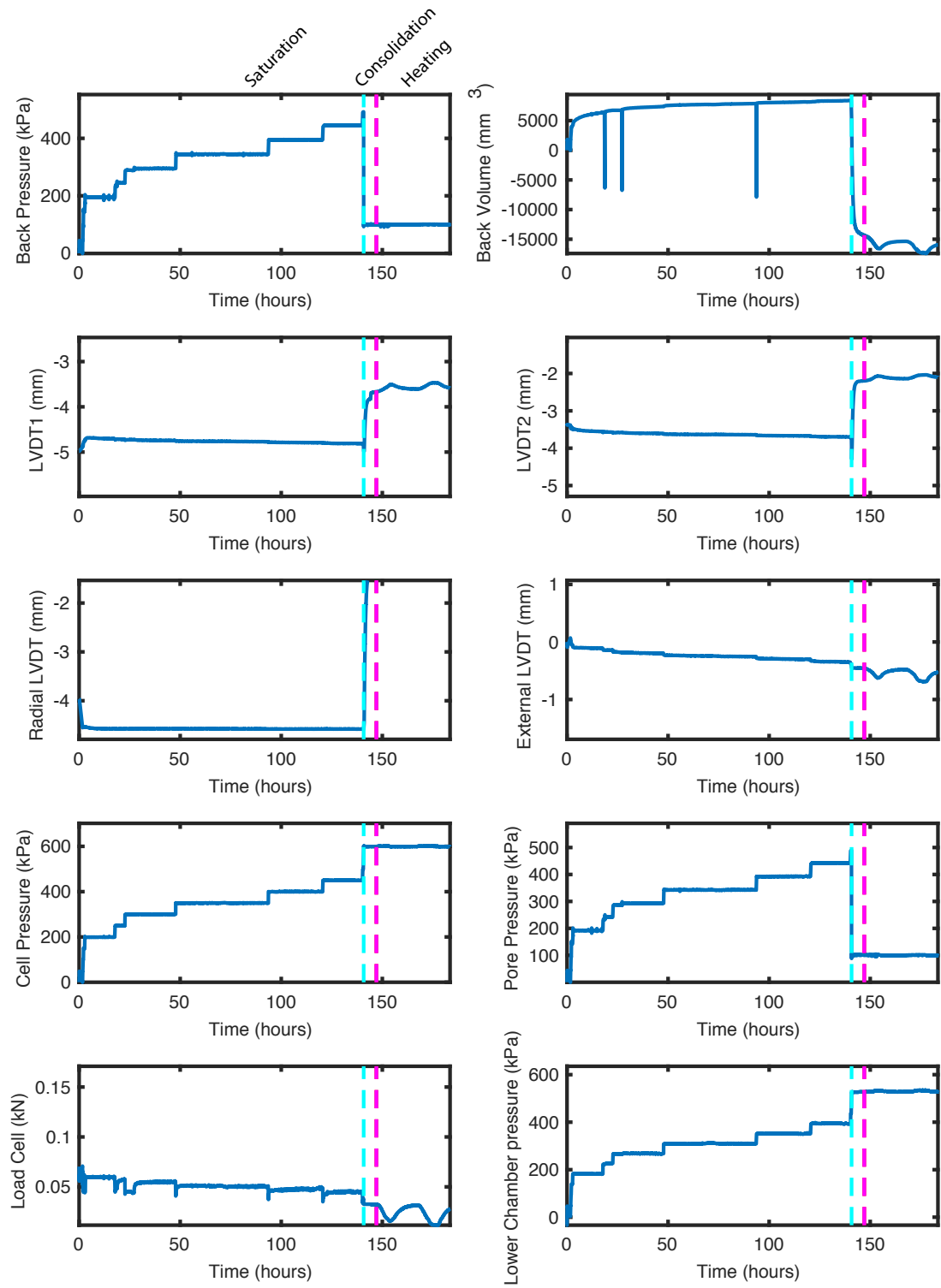


Figure A.1: Test 1_K_5C triaxial test data

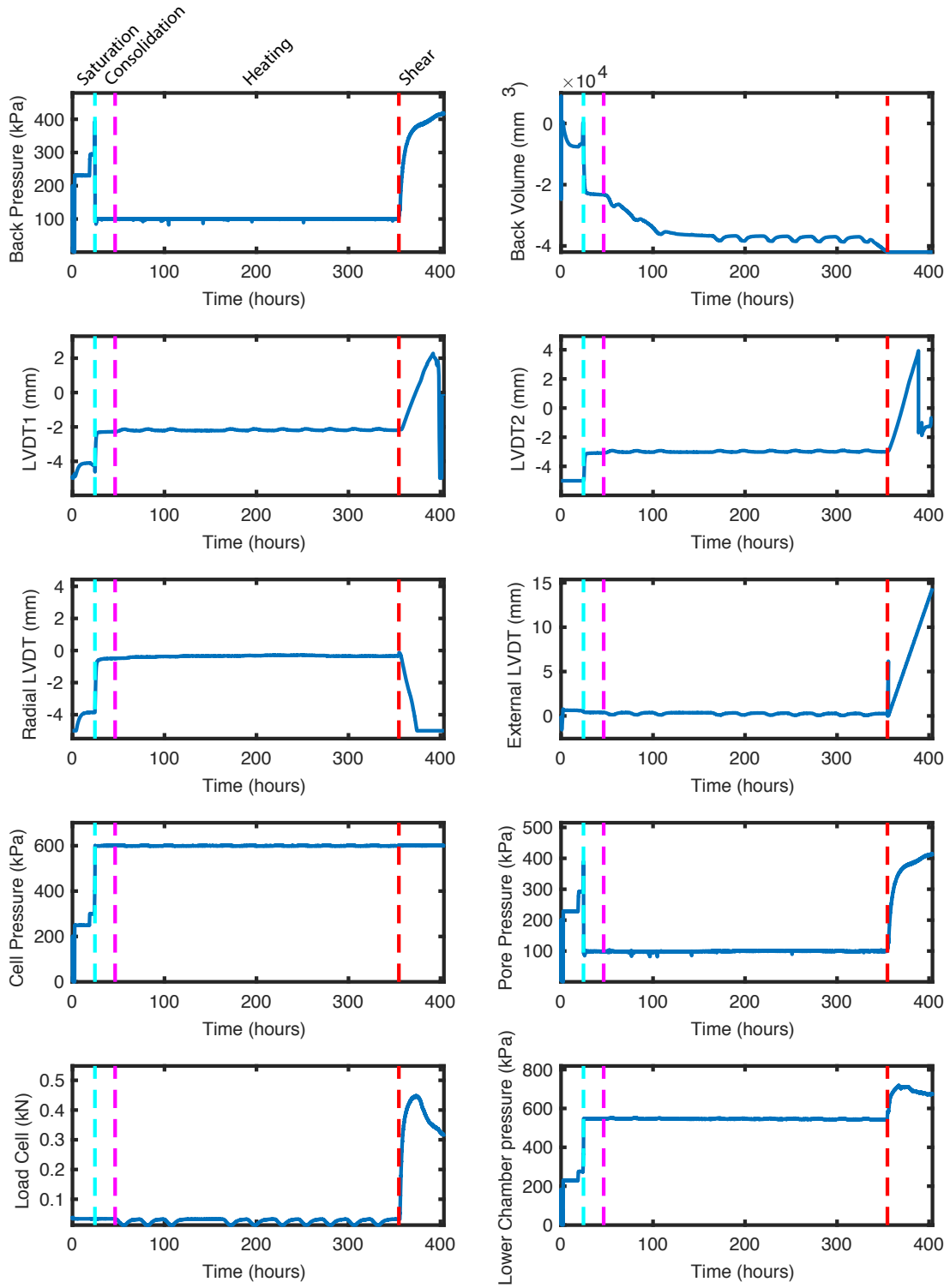


Figure A.2: Test 3_K_10C triaxial test data

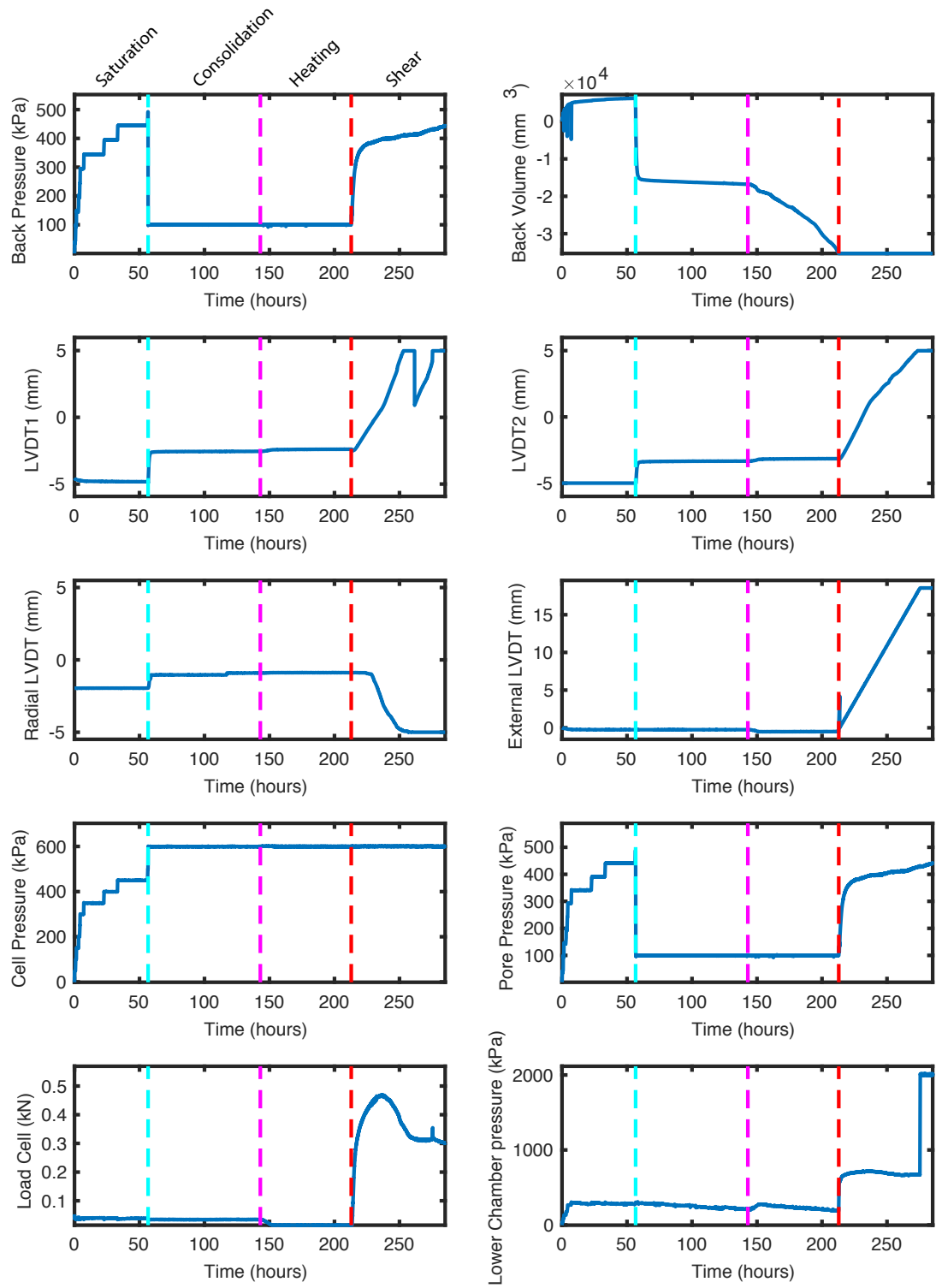


Figure A.3: Test 5_K.60 triaxial test data

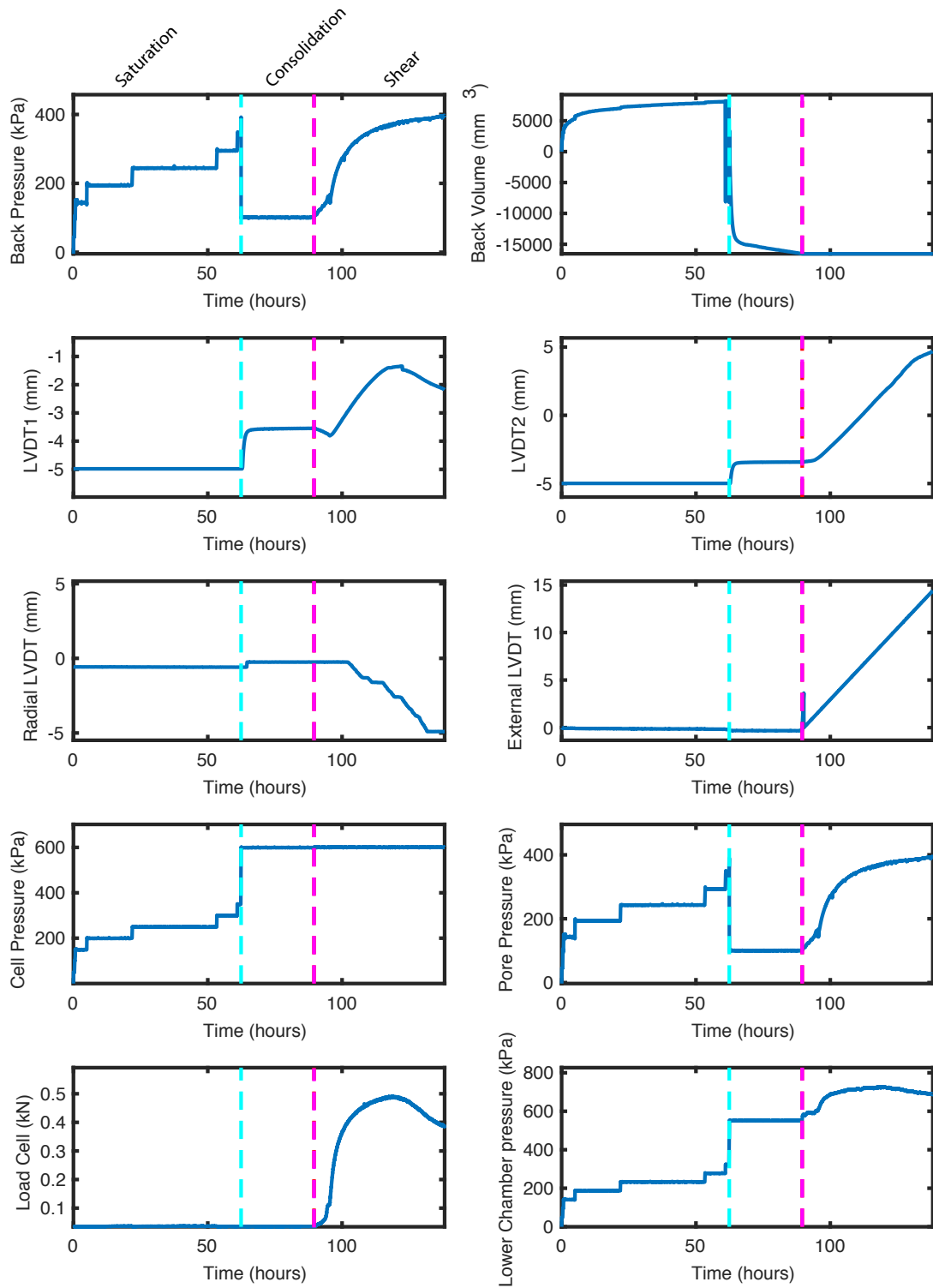


Figure A.4: Test 6_K.20 triaxial test data

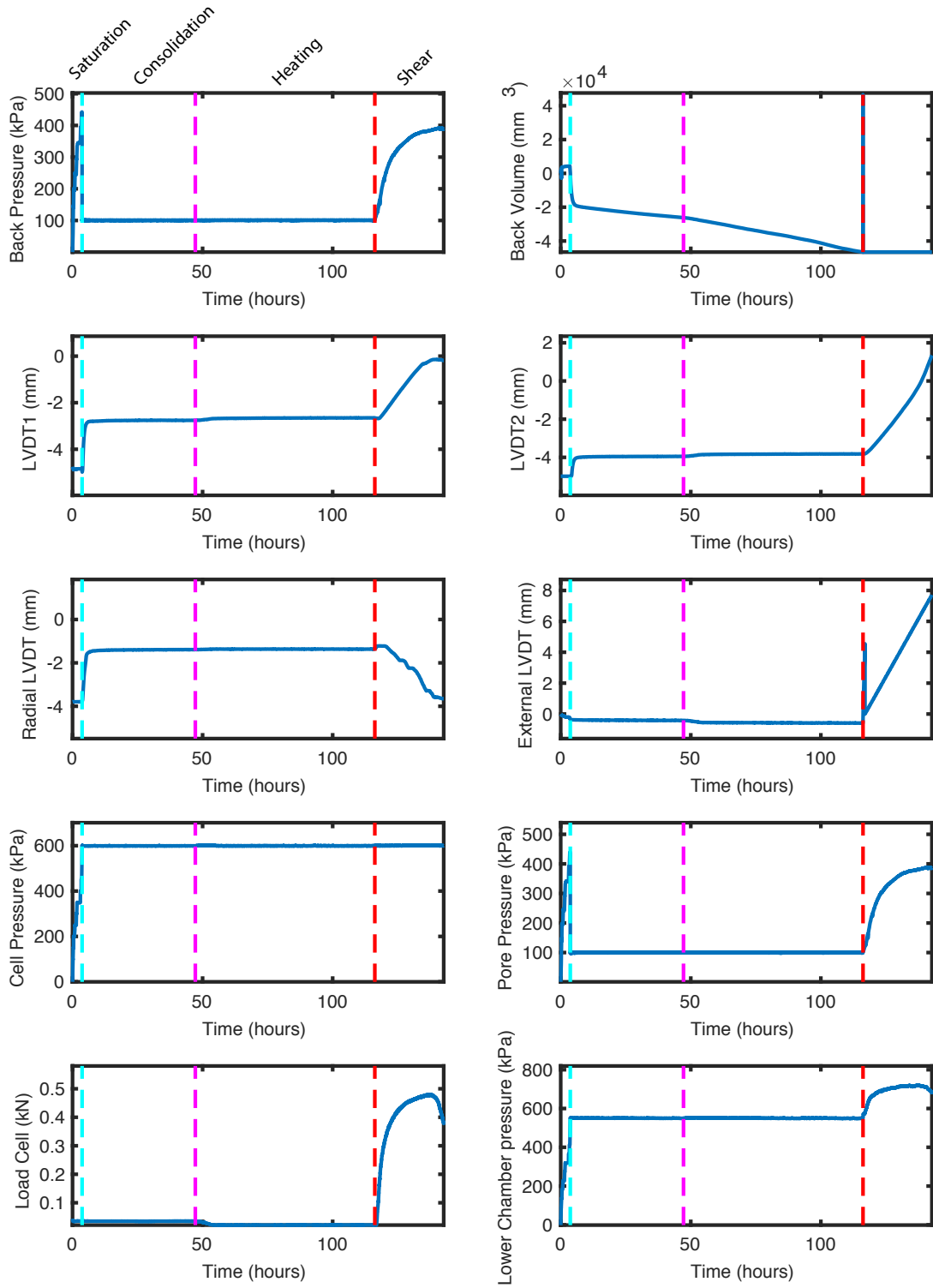


Figure A.5: Test 7_K.40 triaxial test data

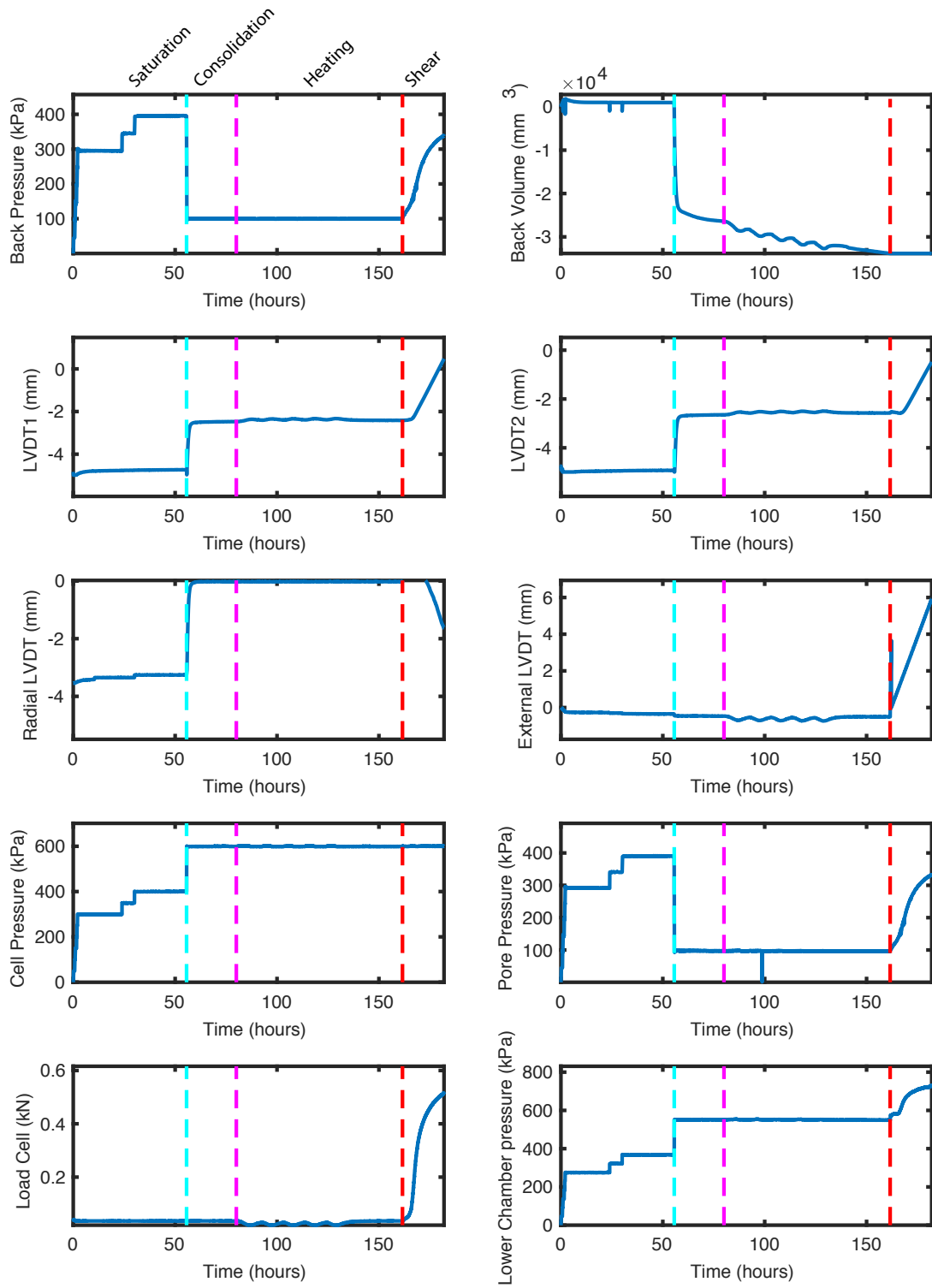


Figure A.6: Test 8_K_5C triaxial test data

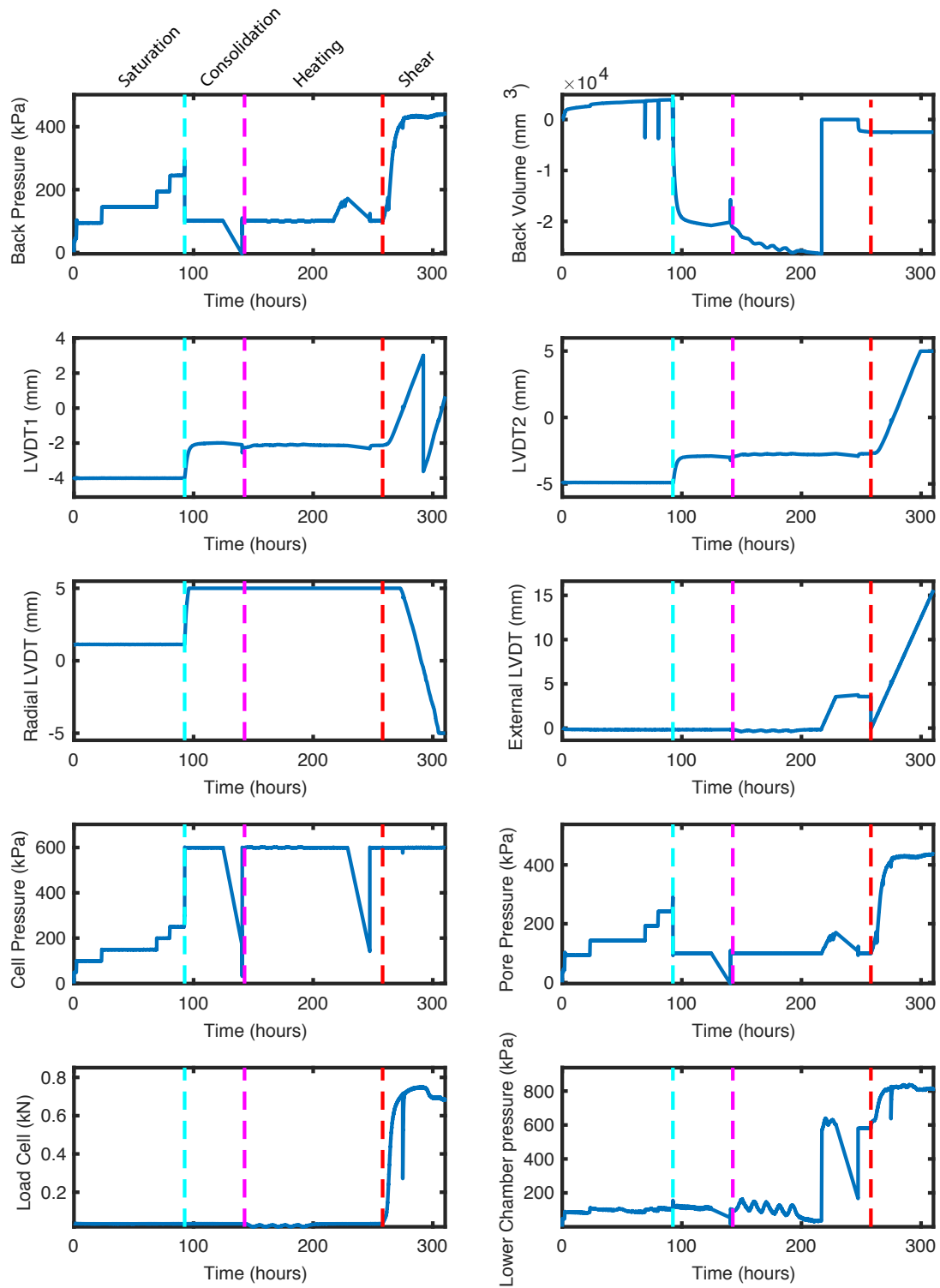


Figure A.7: Test 10_DC_5C triaxial test data

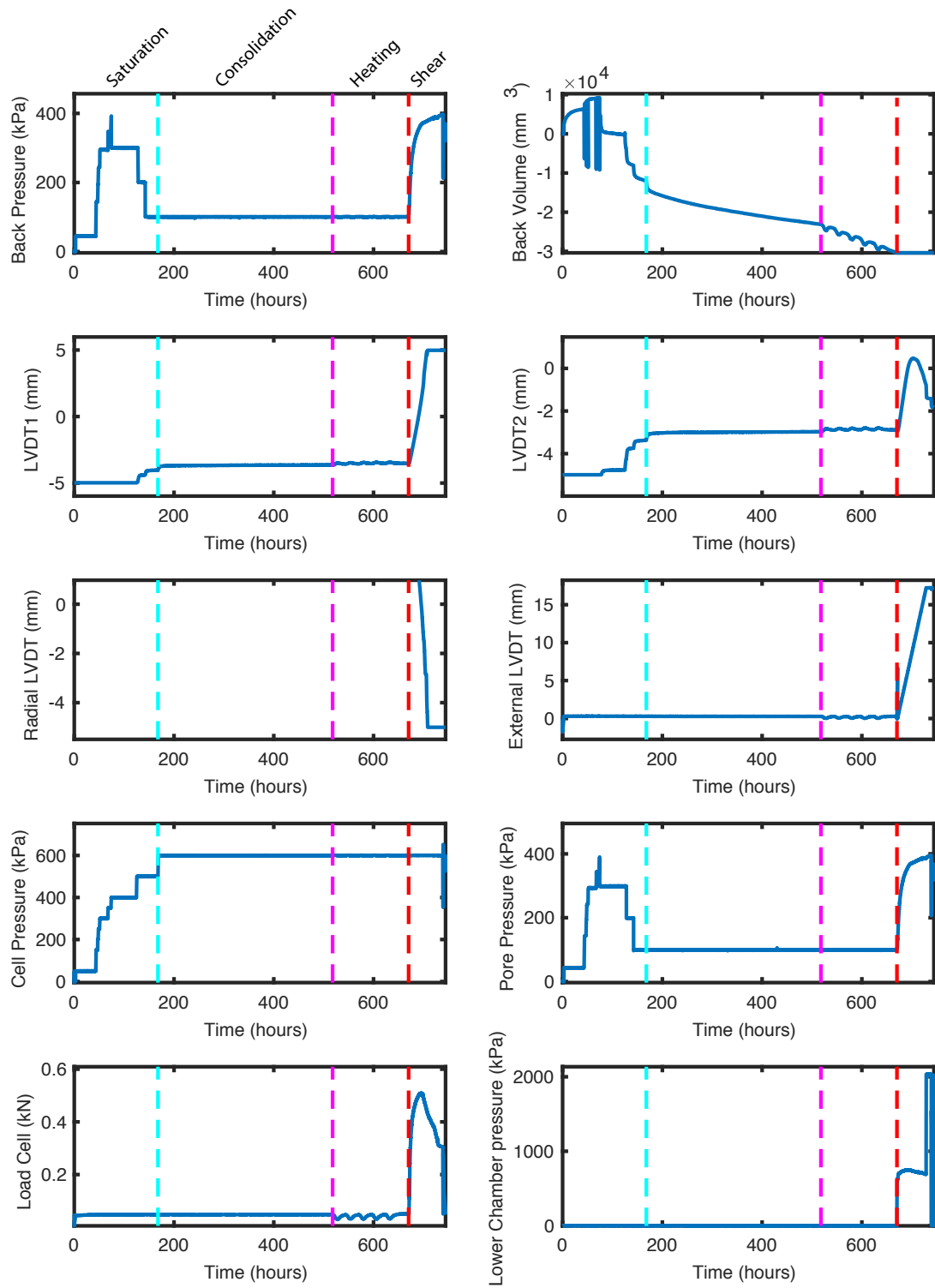


Figure A.8: Test 12_K_5C triaxial test data

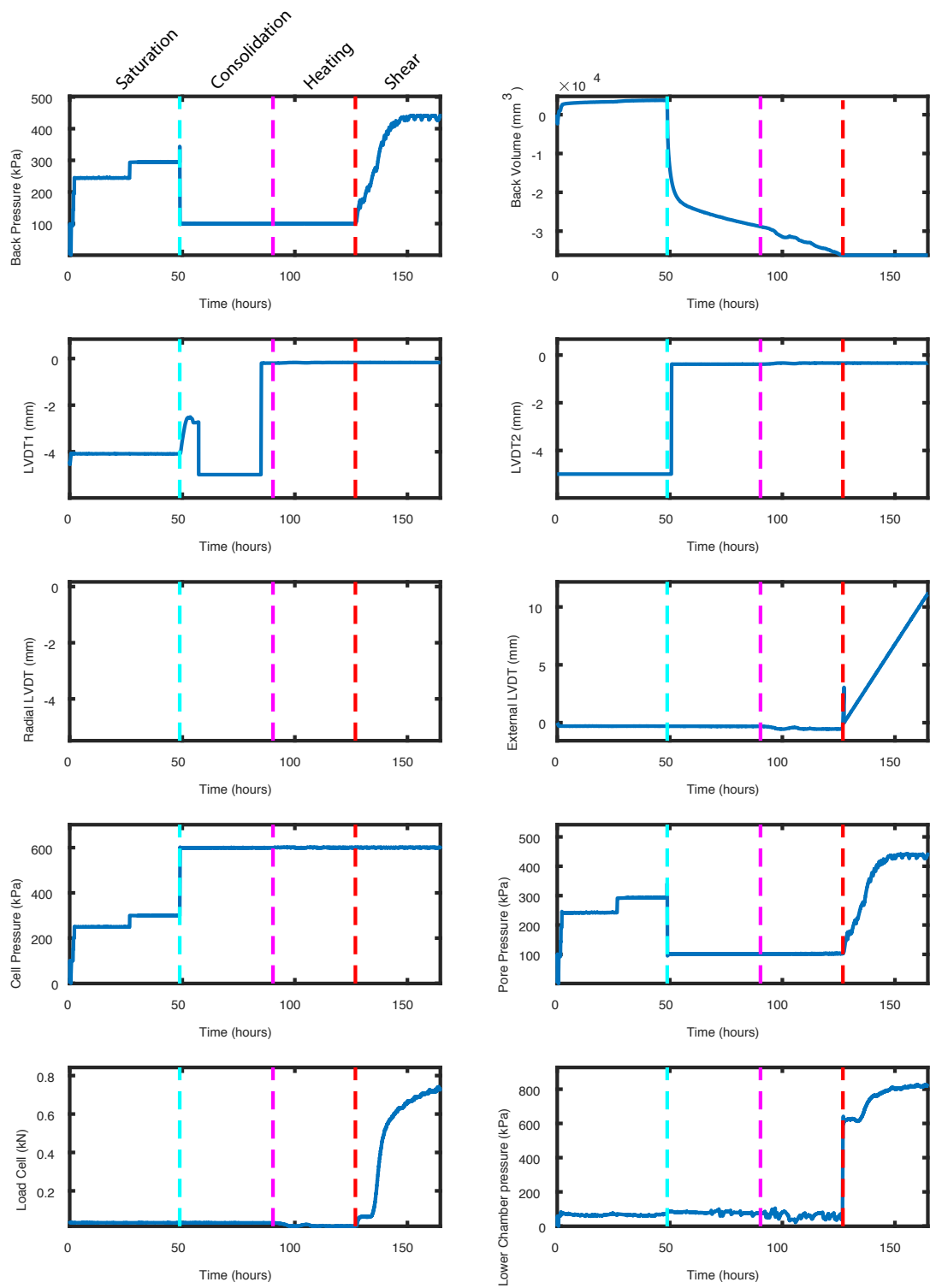


Figure A.9: Test 14_DC.60 triaxial test data

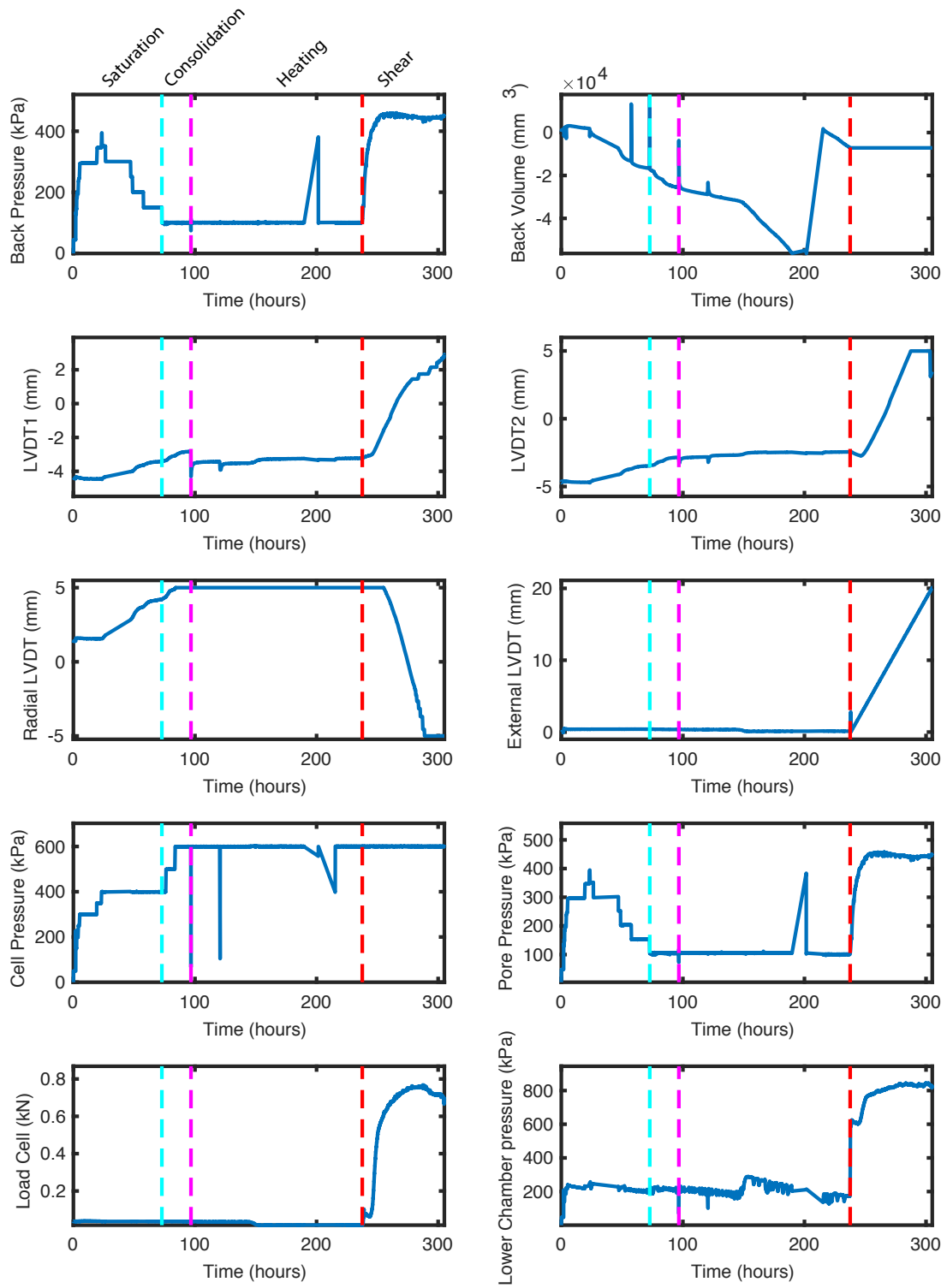


Figure A.10: Test 15_DC_10C triaxial test data

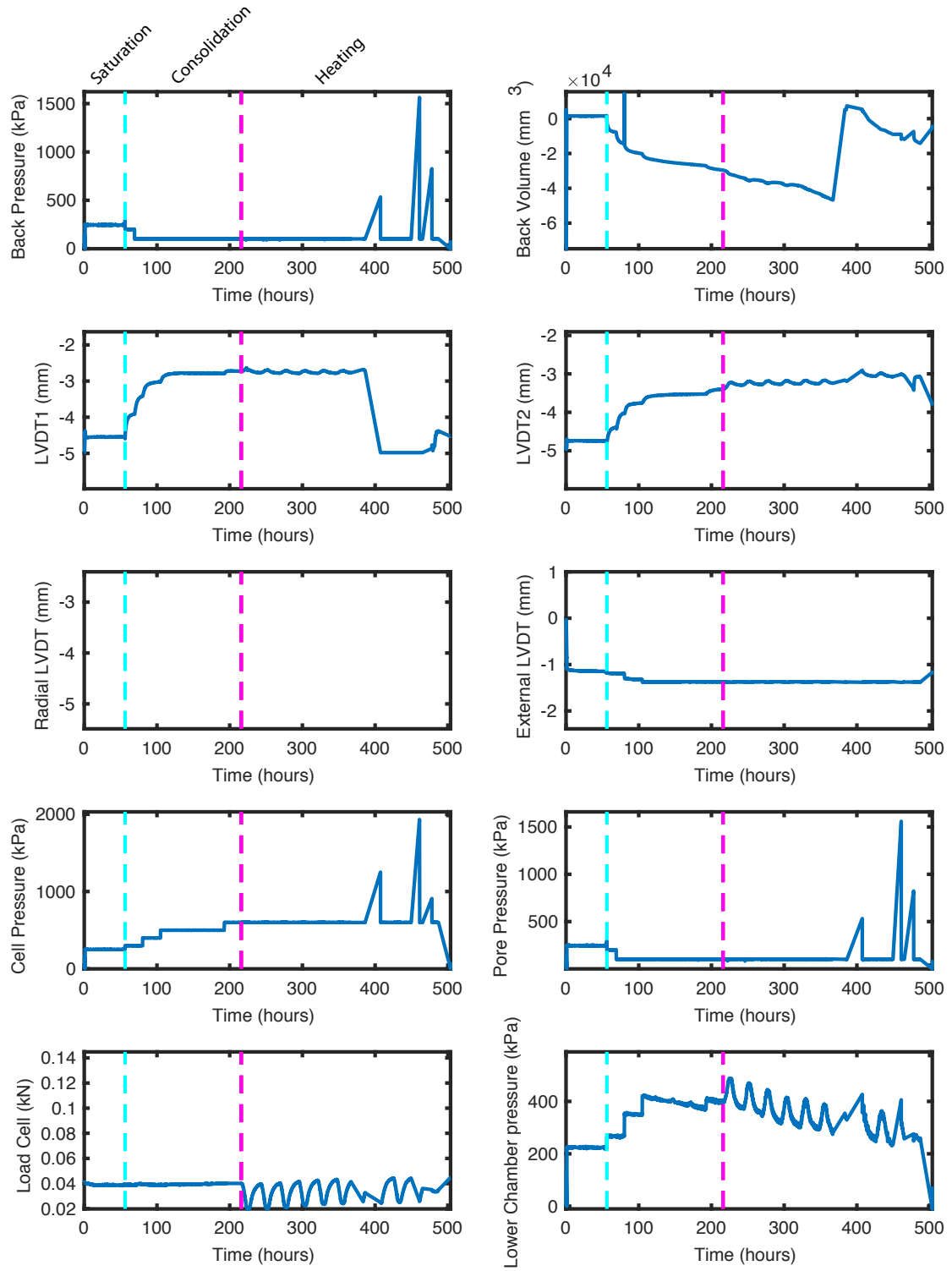


Figure A.11: Test 16_DC_10C triaxial test data

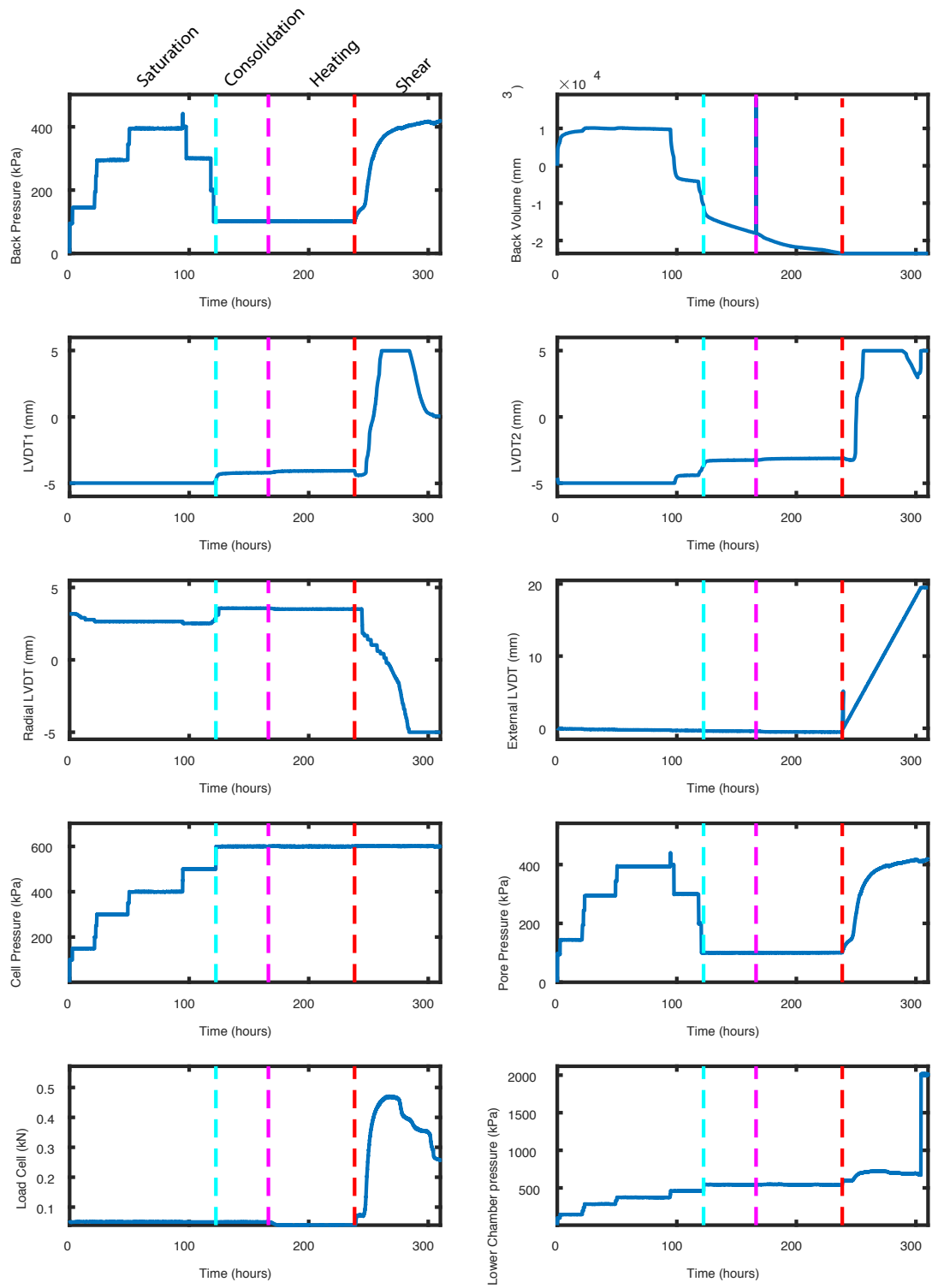


Figure A.12: Test 19_K.40 triaxial test data

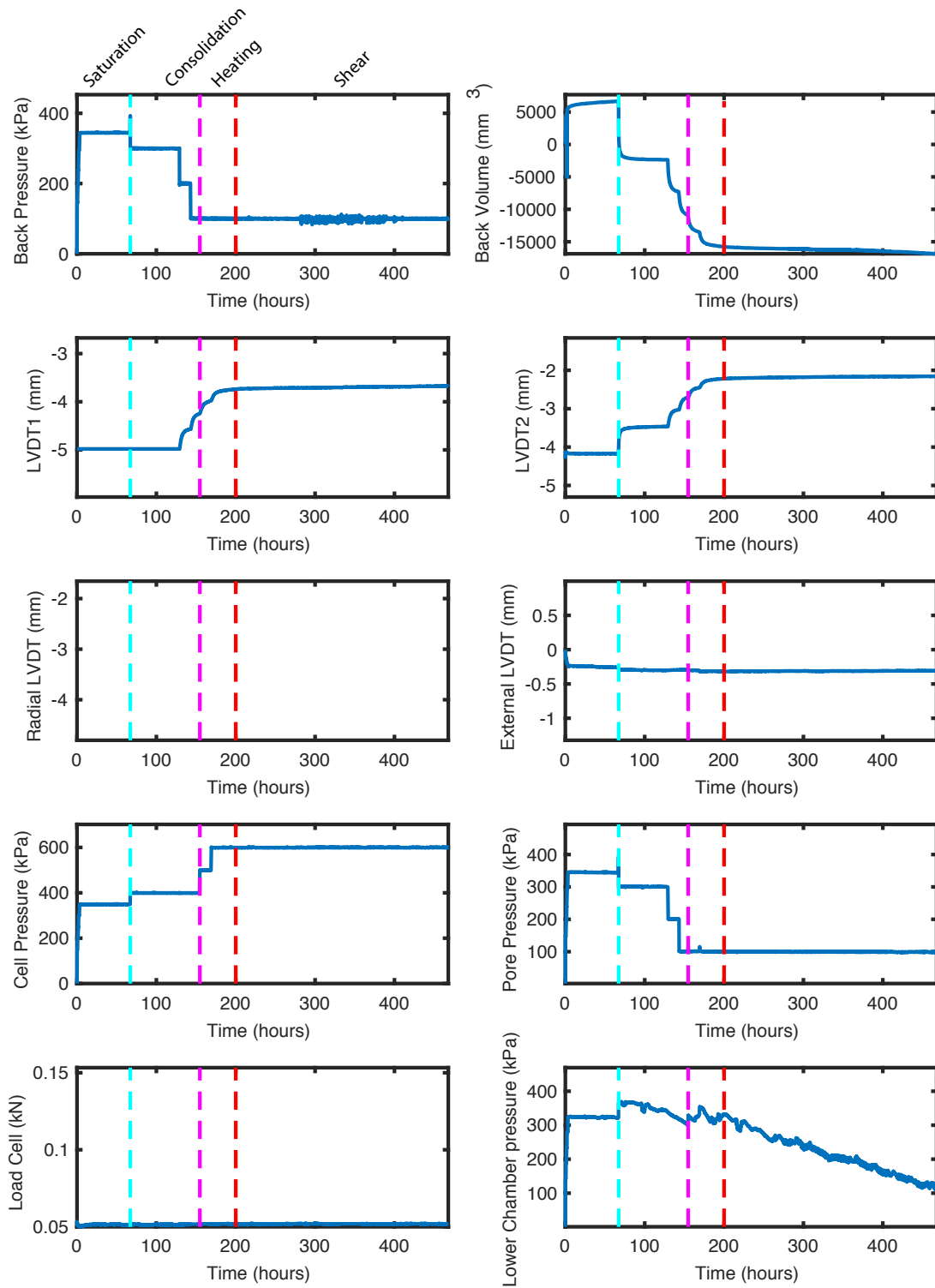


Figure A.13: Test 21_DC_40 triaxial test data

A.3 Consolidation data

The following pages present the results of the consolidation stage across all tests. Figure A.14 and A.15 show the consolidation stage for all kaolin and Durham Clay samples, with Figure A.16 and A.17 providing individual test results.

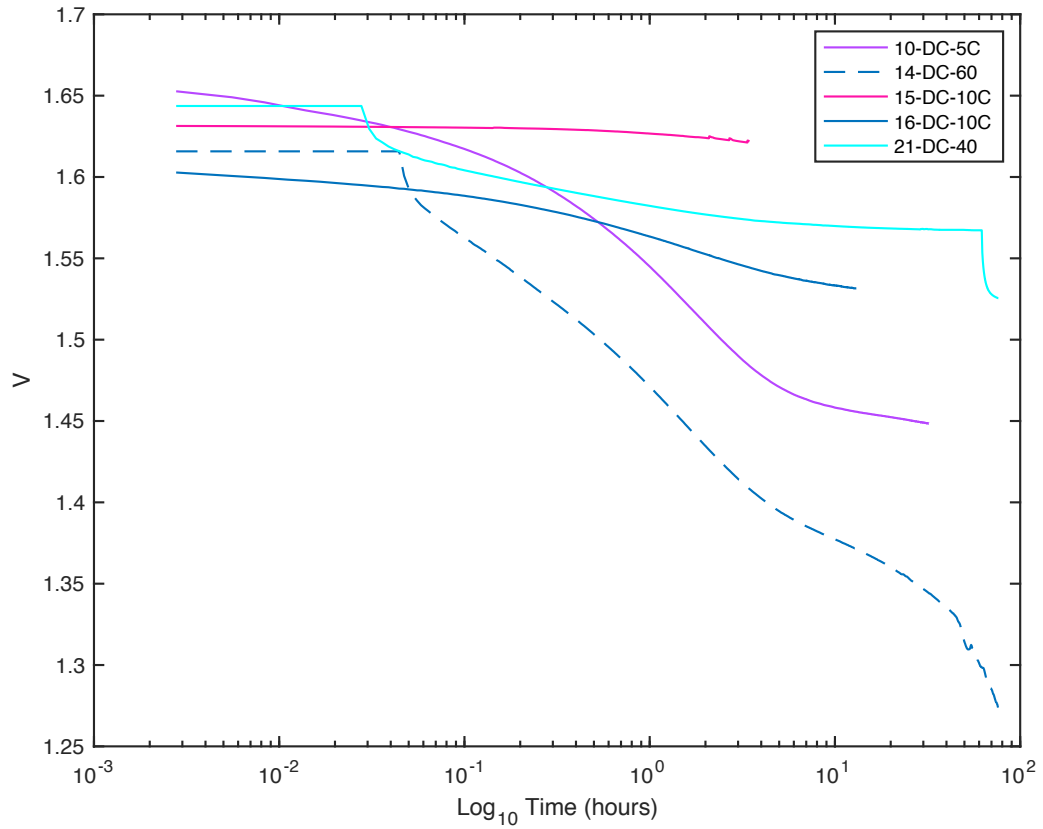


Figure A.14: Specific volume vs. log time - Durham Clay samples

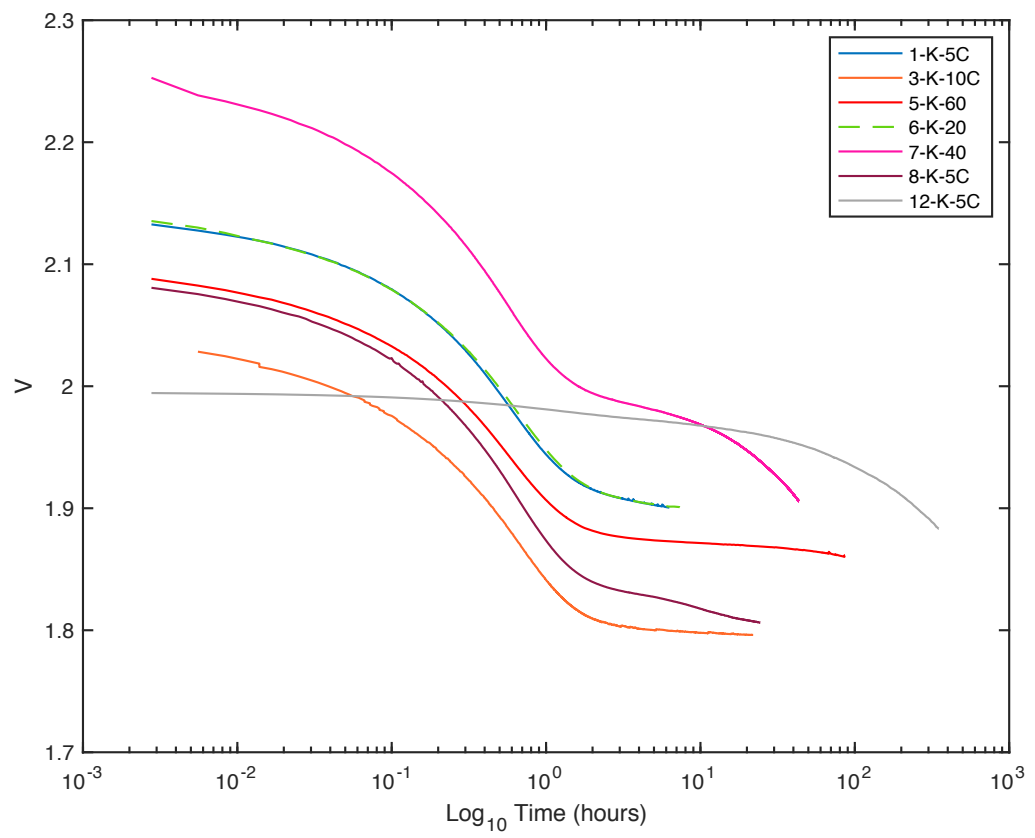


Figure A.15: Specific volume vs. log - kaolin samples

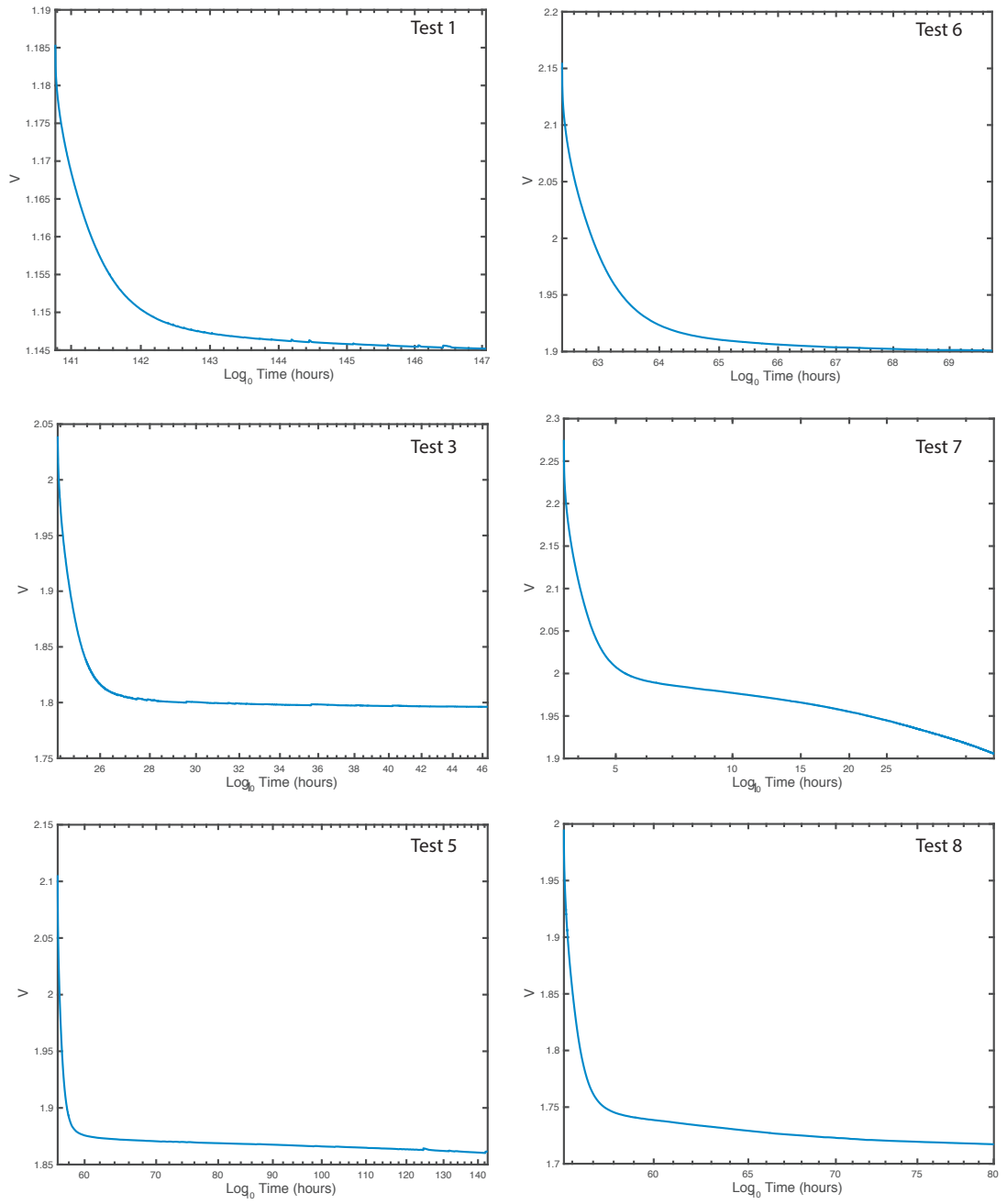


Figure A.16: Specific volume vs. log time for Tests 1 to 8

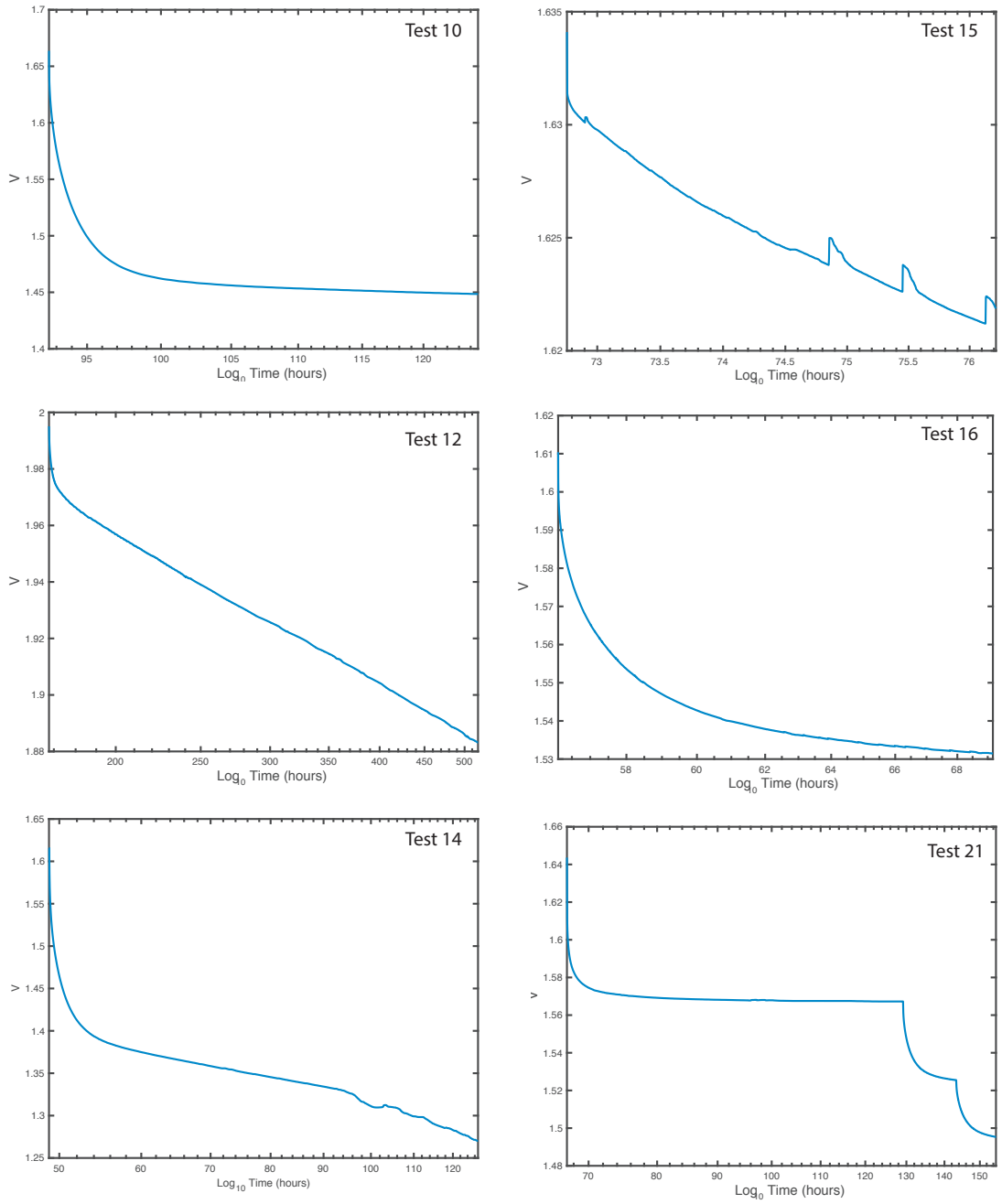


Figure A.17: Specific volume vs. log time for Tests 10 to 21

A.4 Back volume data during heating stage

The following pages present an overview of the percentage of the pre-heating sample volume drained during heating stages for each of the tests, shown as kaolin test in Figure A.18, Durham clay in Figure A.19 and combined in Figure A.20. The

absolute volumes of water drained for each test are then presented in Figures A.21 and A.22

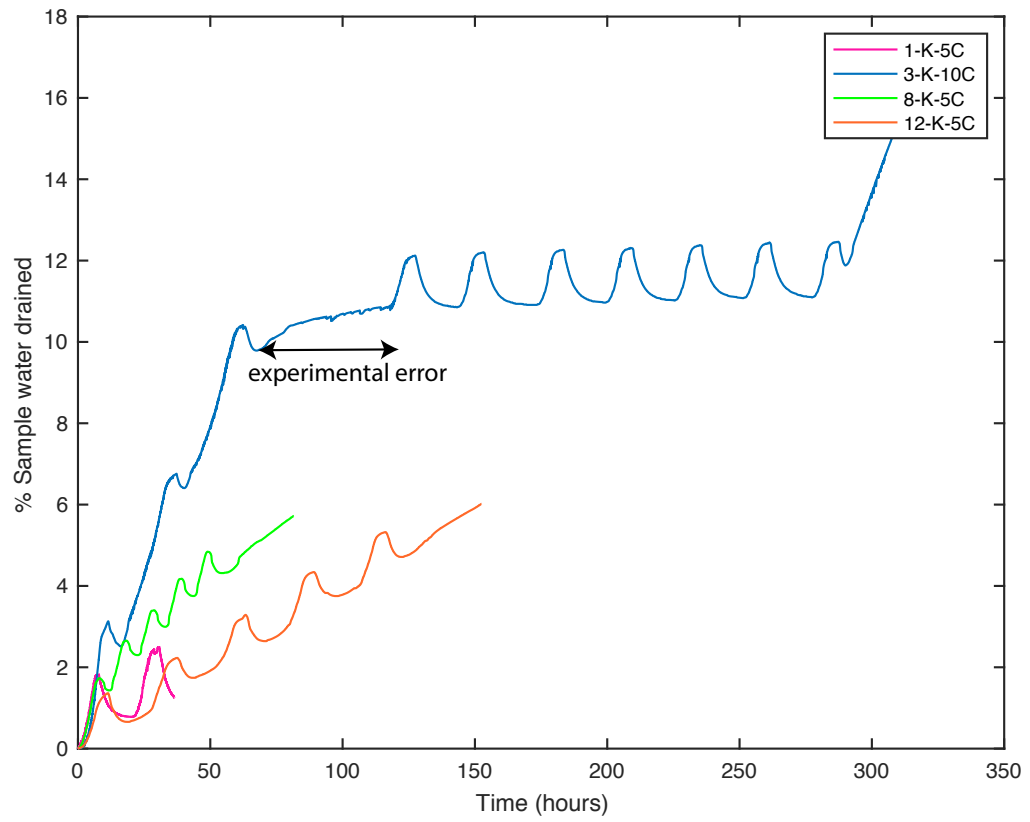


Figure A.18: Percentage of sample volume drained during heating stage, kaolin tests

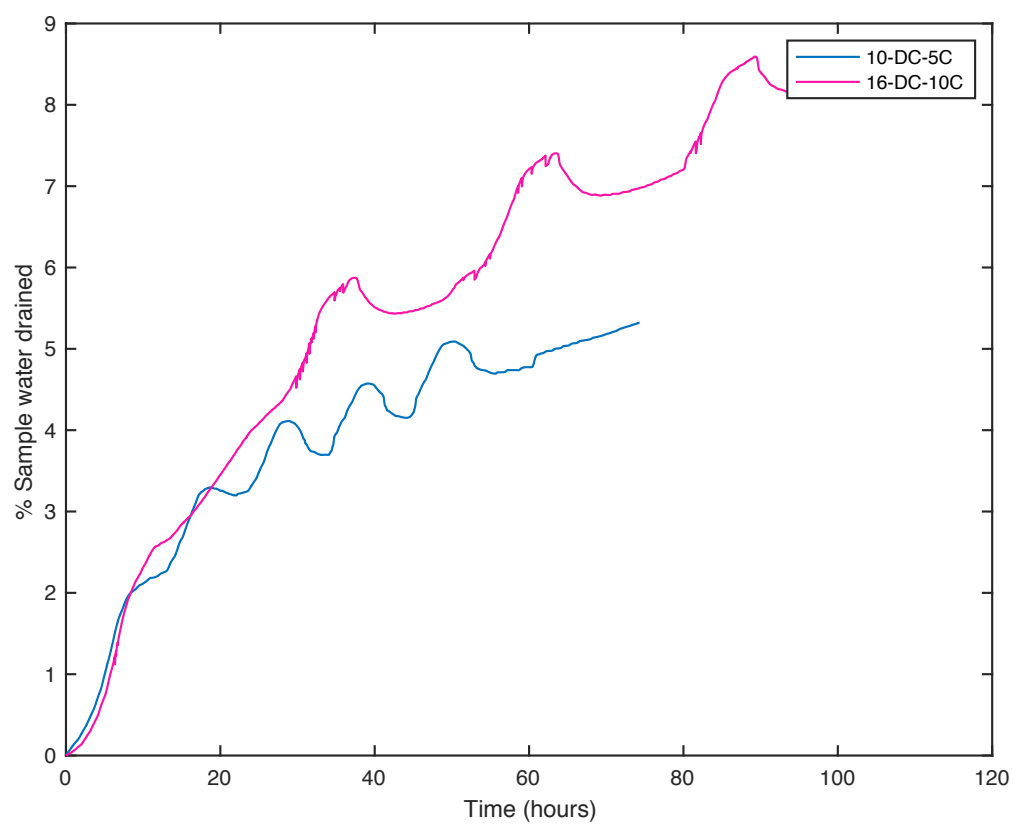


Figure A.19: Percentage of sample volume drained during heating stage, Durham clay tests

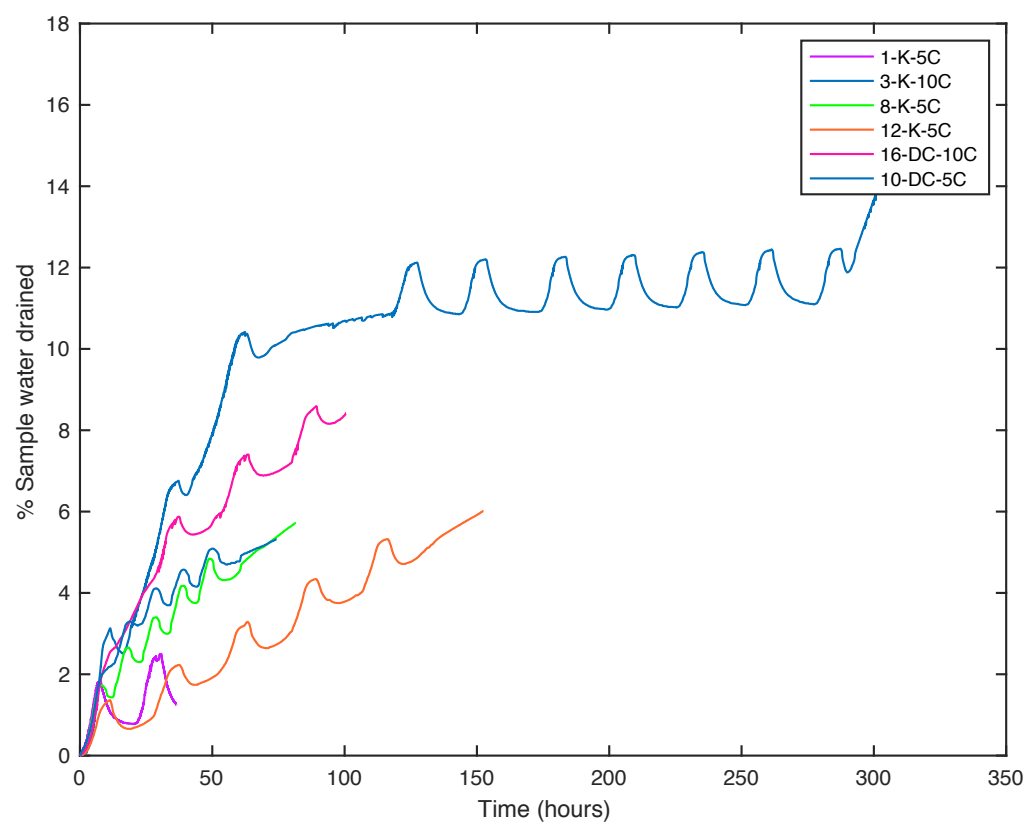


Figure A.20: Percentage of sample volume drained during heating stage, all tests

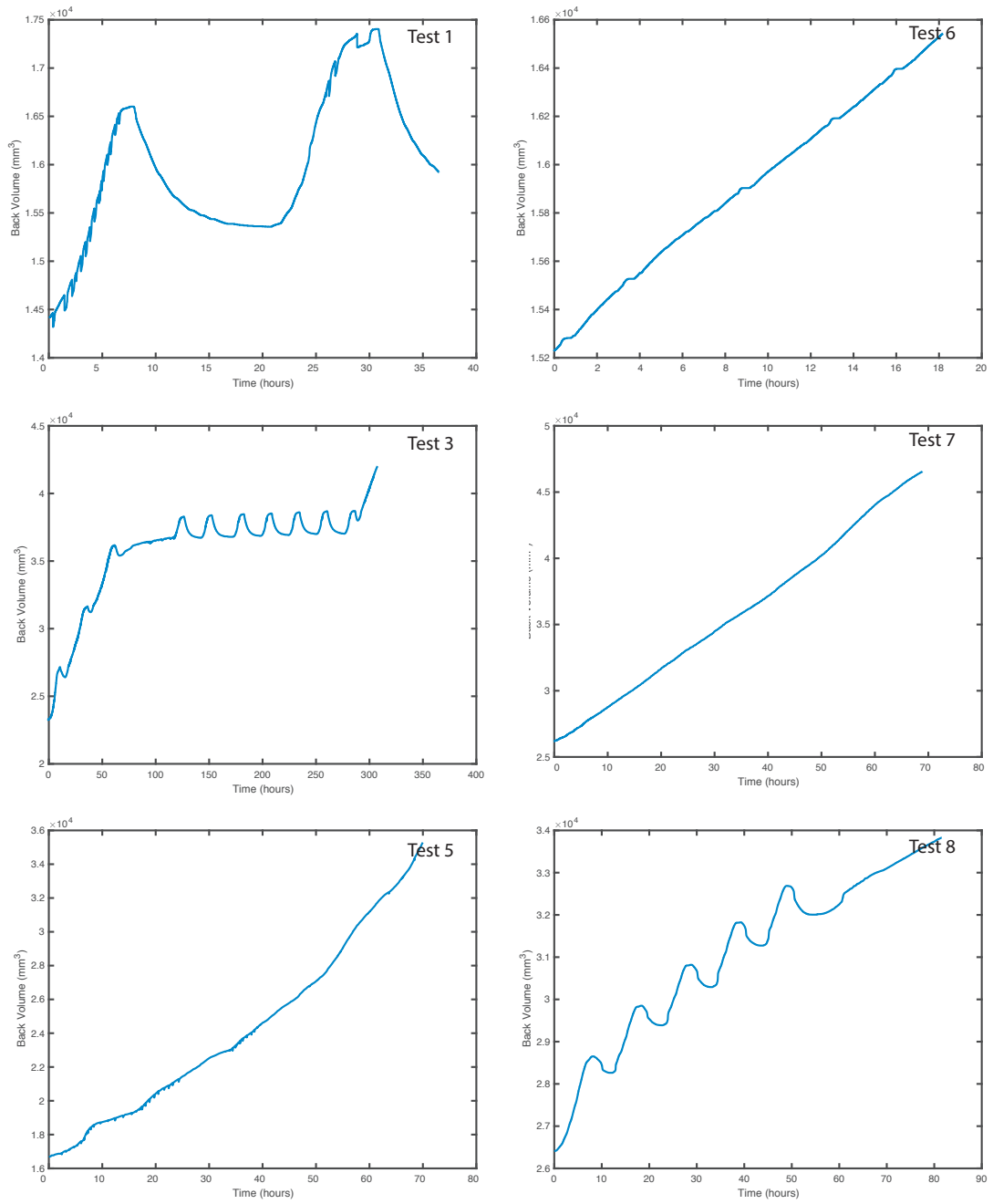


Figure A.21: Back volume drained during heating vs. time for Tests 1 to 8

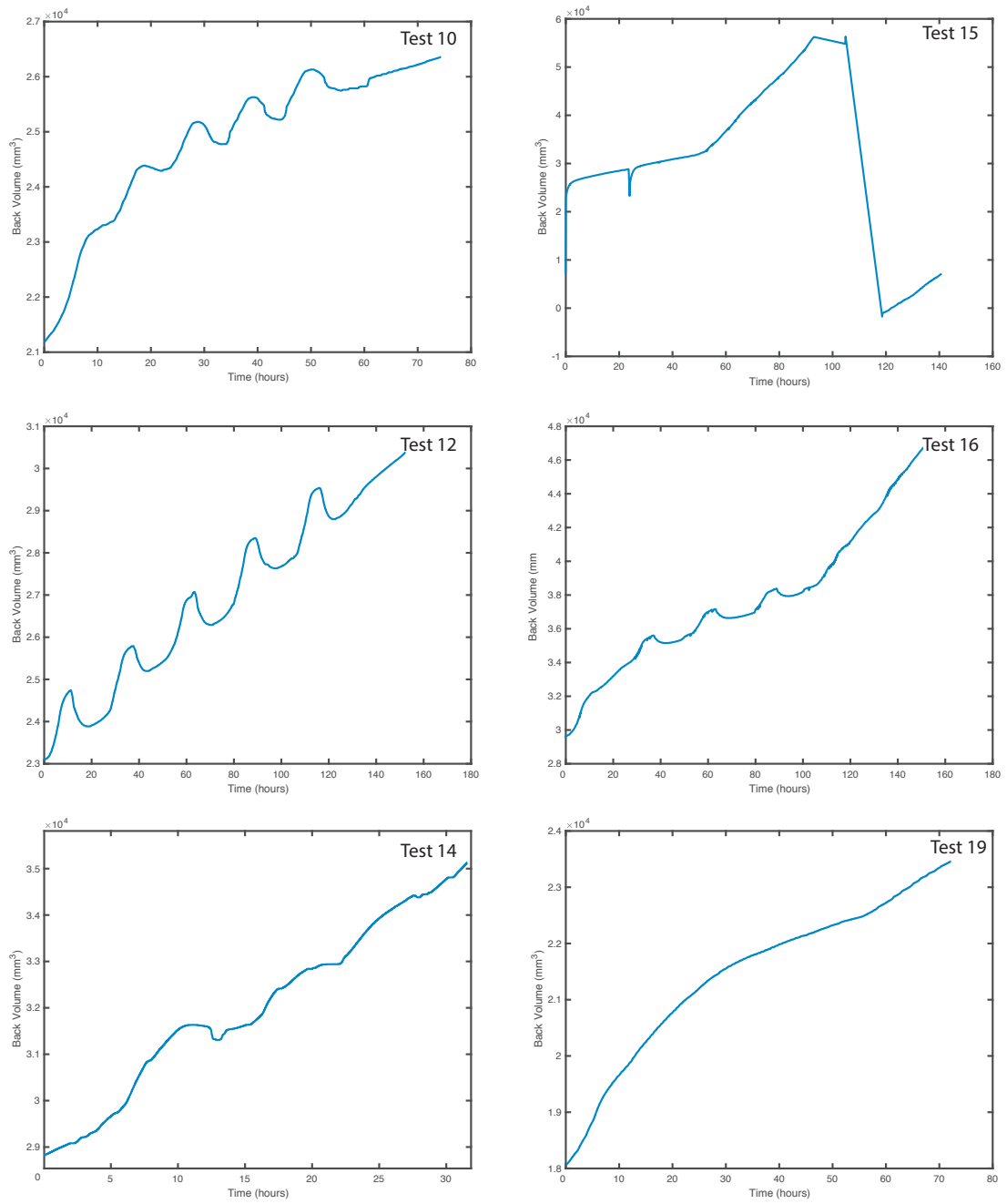


Figure A.22: Back volume drained during heating vs. time for Tests 10 to 19

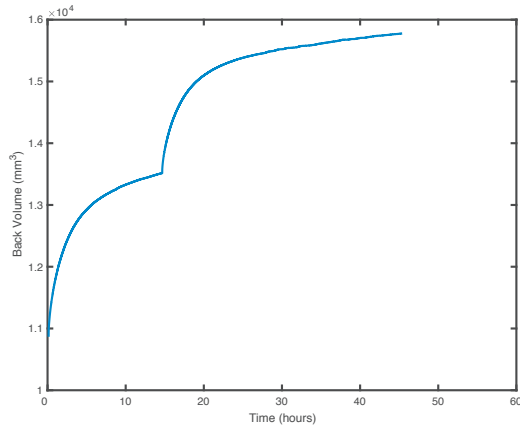


Figure A.23: Back volume drained during heating vs. time for Test 21

A.5 Temperature data

The temperature profiles which have been applied to the samples are detailed within this Appendix, along with details of any experimental errors which occurred during testing.

- Test 1-K-5C: Figure A.24: The 5 cycle temperature profile was applied, with the water bath elevated to 80 °C during the heating stage and naturally cooled during the cooling stage.
- Test 3-K-10C: Figure A.25: The 10 cycle temperature profile was applied using the same profile as the 5 cycle, with the water bath elevated to 80 °C during the heating stage and naturally cooled during the cooling stage.
- Test 5-K-60: Figure A.26: In order to maintain a temperature of approximately 60 °C, the water bath temperature was held at a constant 80 °C.
- Test 6-K-20: Figure A.27: For the 20 °C temperature profile, laboratory temperature water was circulated in order to maintain consistency throughout all testing. The relatively small variation in temperature can be attributed to the air conditioning system switching on and off to maintain laboratory temperature in addition to the door of the laboratory being opened and closed.

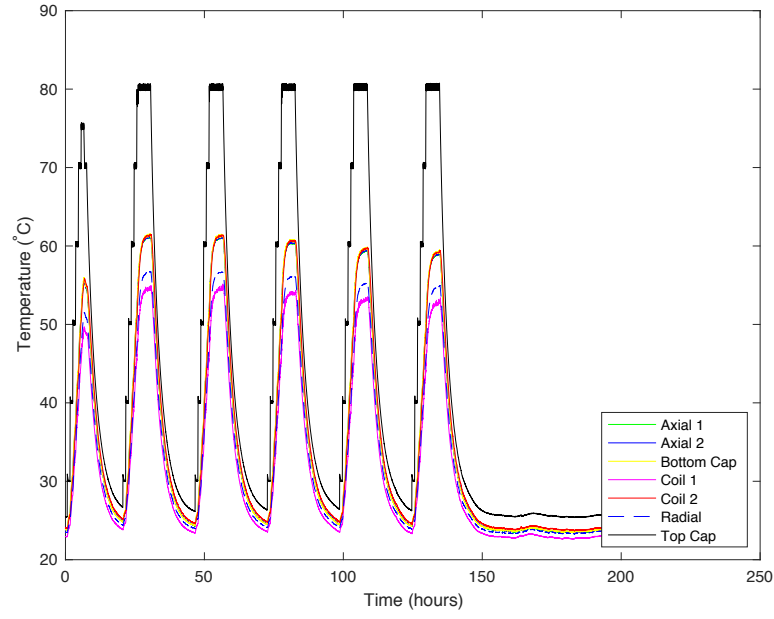


Figure A.24: Kaolin 5 cycles Temperature Profile. Test 1-K-5C

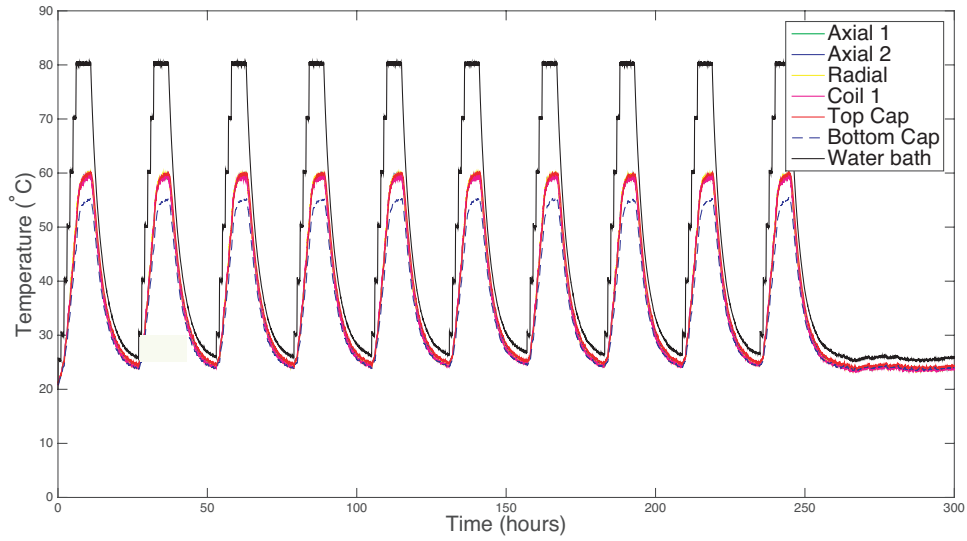


Figure A.25: Kaolin 10 cycles Temperature Profile. Test 3-K-10C

- Test 7-K-40: Figure A.28: To maintain a temperature of approximately 40 °C, following a staged temperature increase, the temperature of the water bath was held at a constant temperature of 60 °C.
- Test 8-K-5C: Figure A.29: The 5 cycle temperature profile was applied, with the water bath elevated to 80 °C during the heating stage and naturally cooled

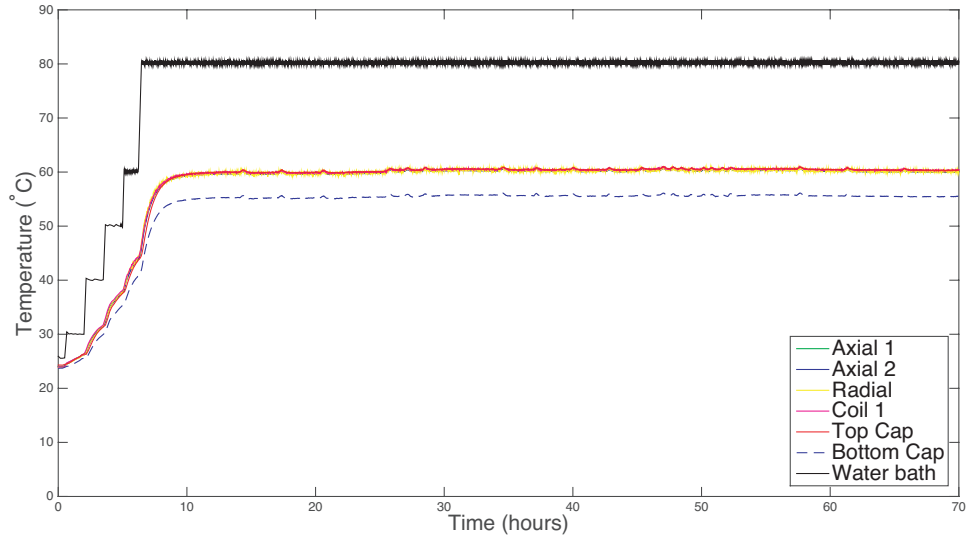


Figure A.26: Kaolin 60 °C Temperature Profile. Test 5-K-60

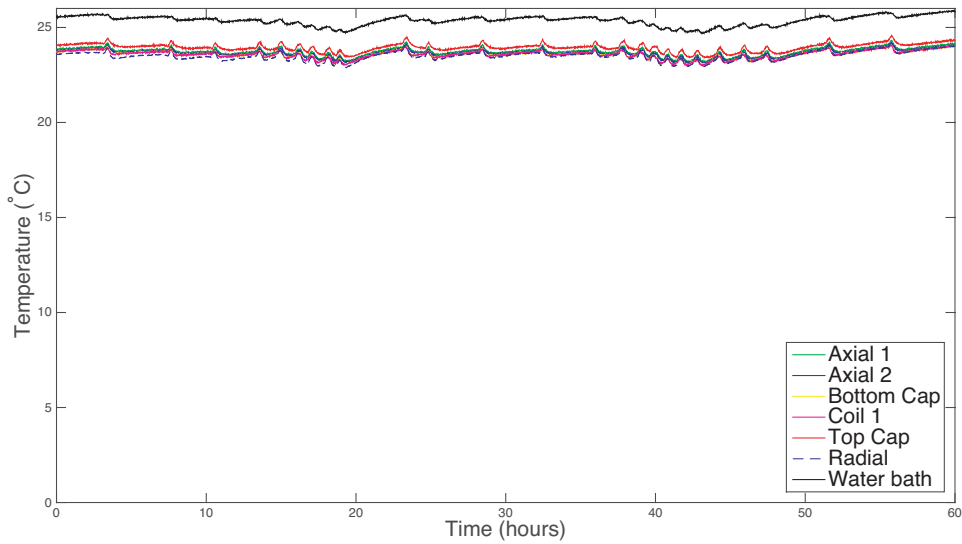


Figure A.27: Kaolin 20 °C Temperature Profile. Test 6-K-20

during the cooling stage.

- Test 10-DC-5C: Figure A.30: Due to a technical error in the programming of the cycles, the 5 cycle profile for Durham Clay was conducted at half the duration of the kaolin heating profile. Due to the shorter heating and cooling period, it can be seen that the sample reaches only 50 °C.
- Test 12-K-5C: Figure A.31: For the 5 cycle temperature profile it can be seen

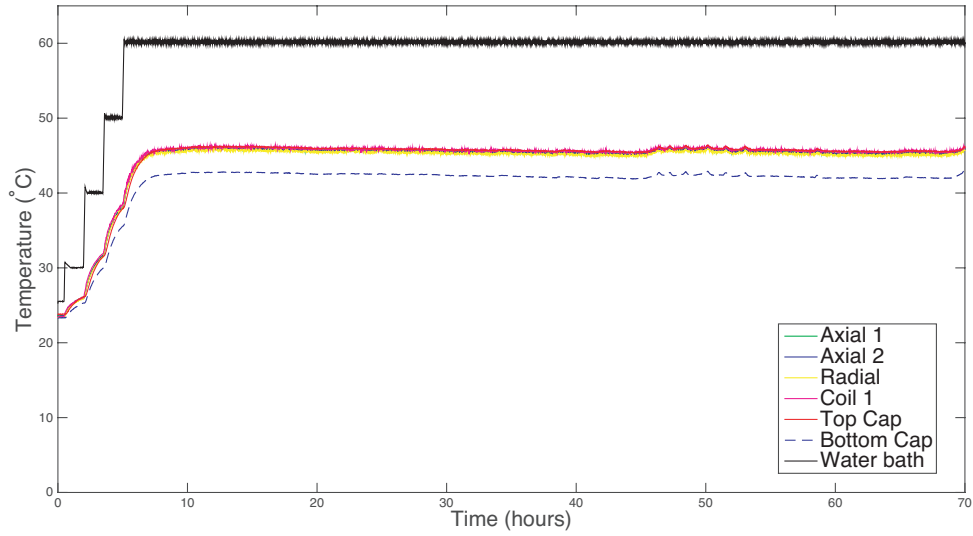


Figure A.28: Kaolin 40 °C Temperature Profile. Test 7-K-40

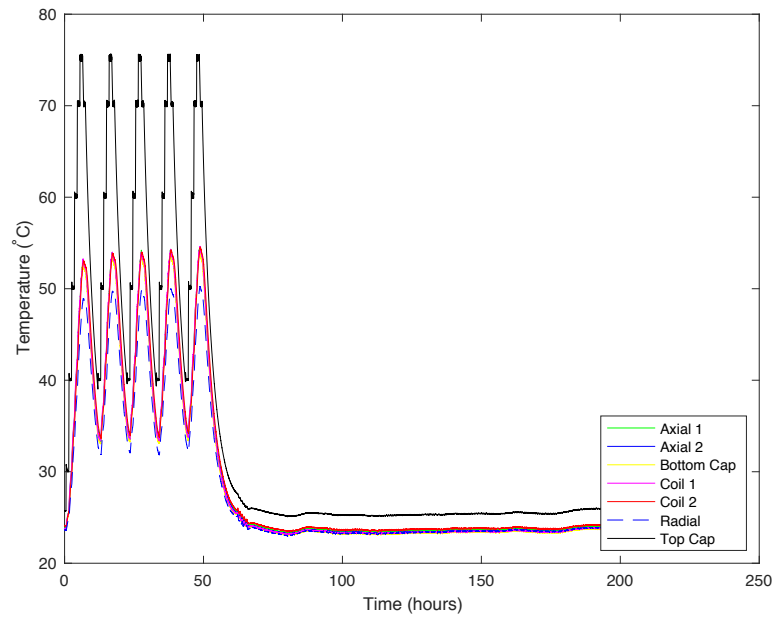


Figure A.29: Kaolin 5 cycles Temperature Profile. Test 8-K-5C

following a stage temperature increase the sample temperature was held constant at 80 °C prior to a natural temperature decrease occurring. During this period the water bath heater was switched off, and the temperature naturally decreased until laboratory temperature was established.

- Test 13-DC-40: Figure A.32: During the application of the 40 °C temperature profile it can be seen that around the 30 - 40 hours period there was a small

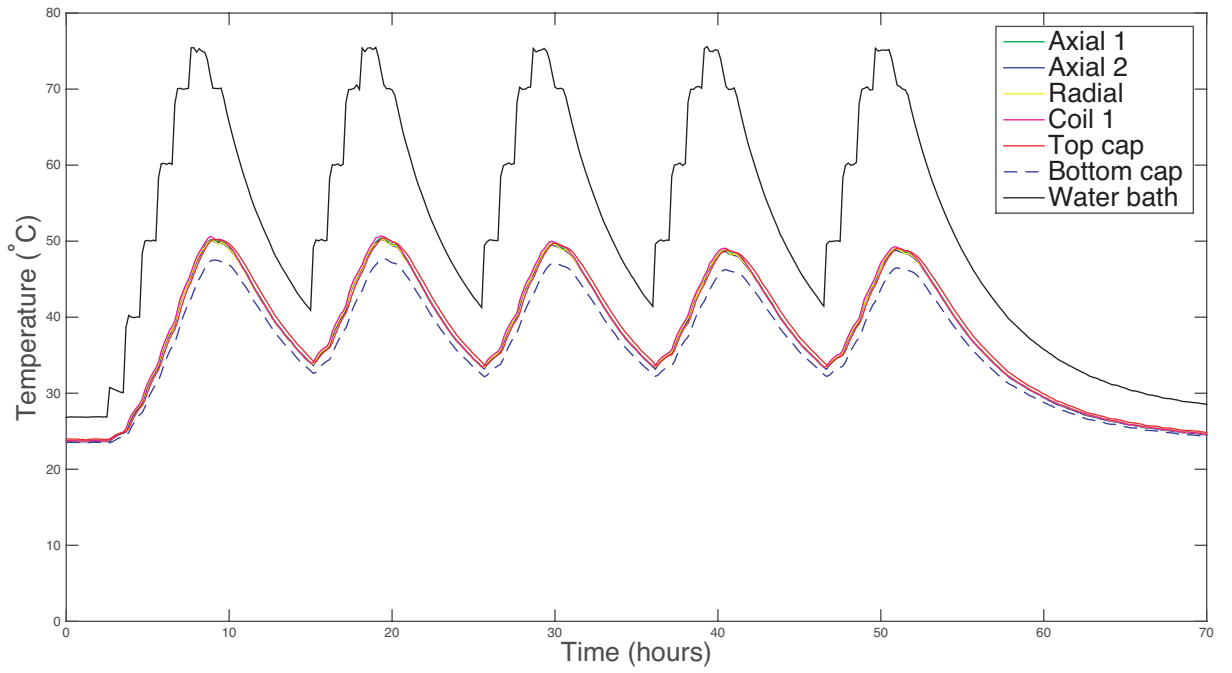


Figure A.30: Durham Clay 5 cycles Temperature Profile. Test 10-DC-5C

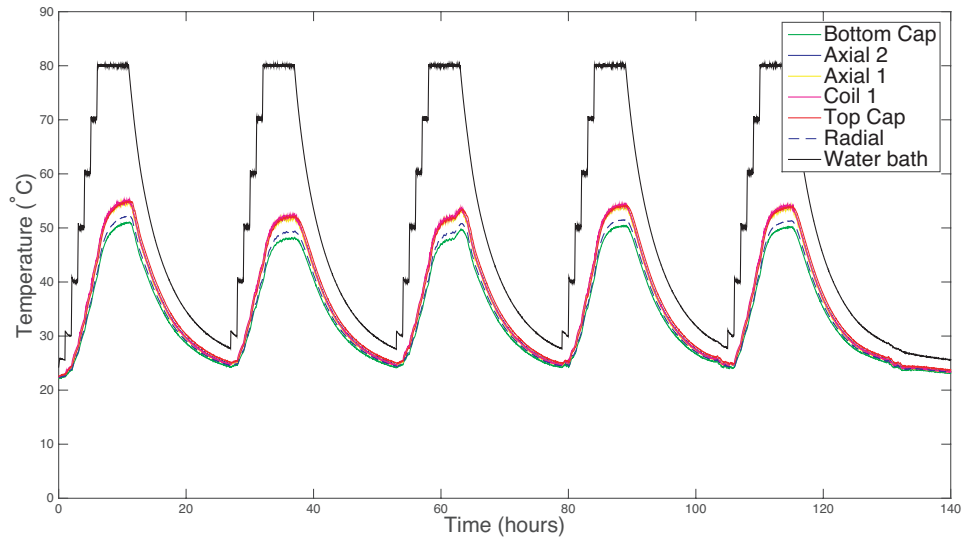


Figure A.31: Kaolin 5 cycles Temperature Profile. Test 12-K-5C

temperature increase in the sample. This temperature increase was due to a fault with the laboratory air conditioning system leading to a slight increase in the laboratory temperature, leading to a reduced heat loss across the system.

- Test 14-DC-60: Figure A.33: During the period of elevated temperature it can be seen that there were 2 occurrences during which the temperature of

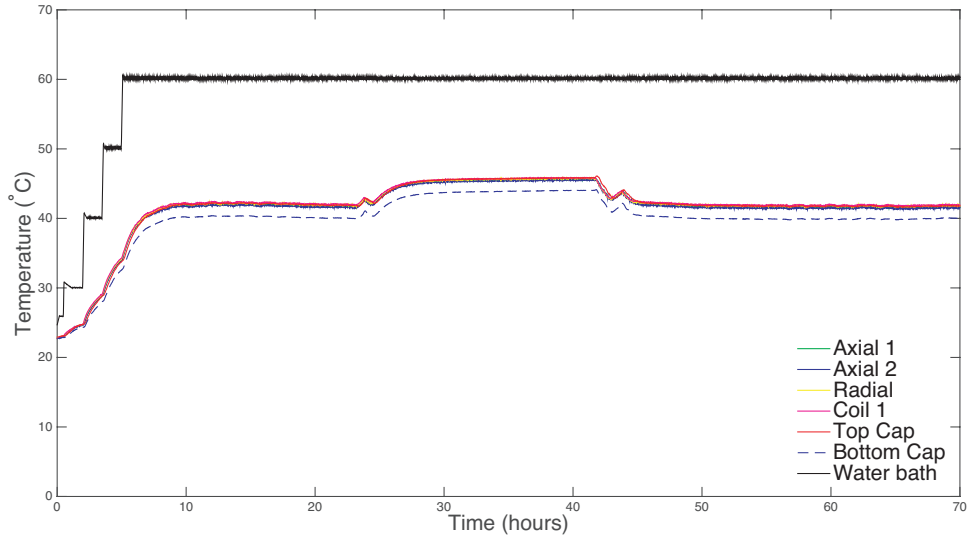


Figure A.32: Durham Clay 40 °C Temperature Profile. Test 13-DC-40

the water bath reduced. On the first instance at approximately 15 hours, this was due to the water level in the water bath dropping below the float switch and therefore turning off the heater due to an inbuilt safety feature. At approximately 22 hours, a computer update automatically restarted the computer, temporarily switching off the computer responsible for maintaining the heating system.

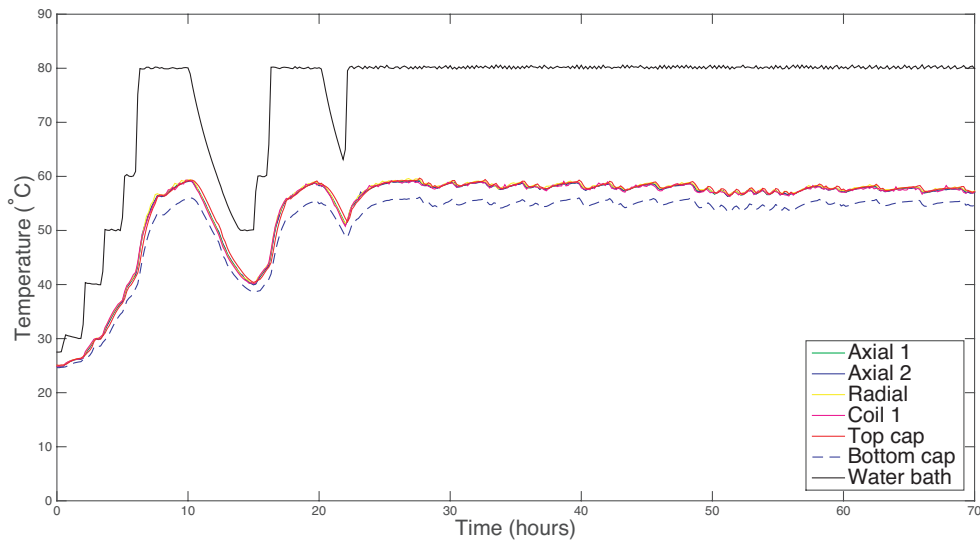


Figure A.33: Durham Clay 60 °C Temperature Profile. Test 14-DC-60

- Test 16-DC-10C: Figure A.34: The 10 cycle temperature profile was applied

using the same profile as the 5 cycle, with the water bath elevated to 80 °C during the heating stage and naturally cooled during the cooling stage.

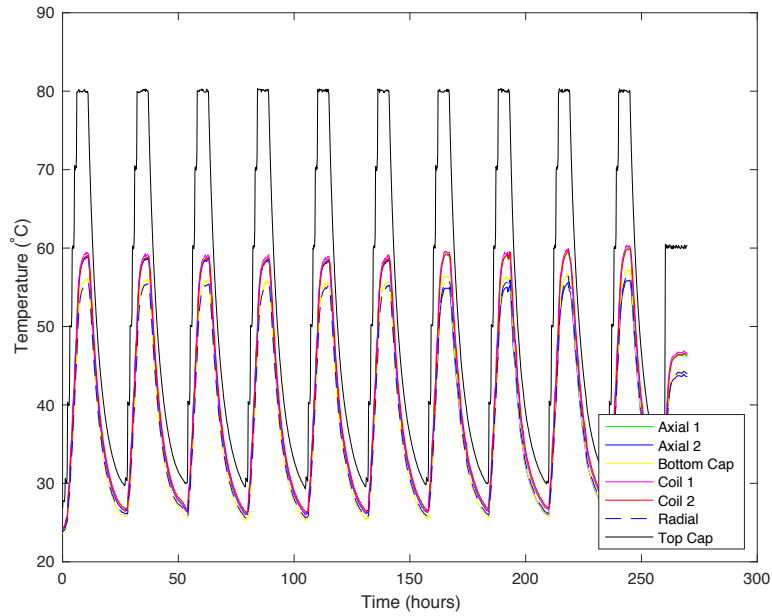


Figure A.34: Durham 10 cycles Temperature Profile. Test 16-DC-10C

- Test 21-DC-40: Figure A.35: During the application of the 40 °C temperature profile it can be seen that around the 20 - 40 hours period there was a small temperature increase in the sample. This temperature increase was due to a fault with the laboratory air conditioning system leading to a slight increase in the laboratory temperature, leading to a reduced heat loss across the system.

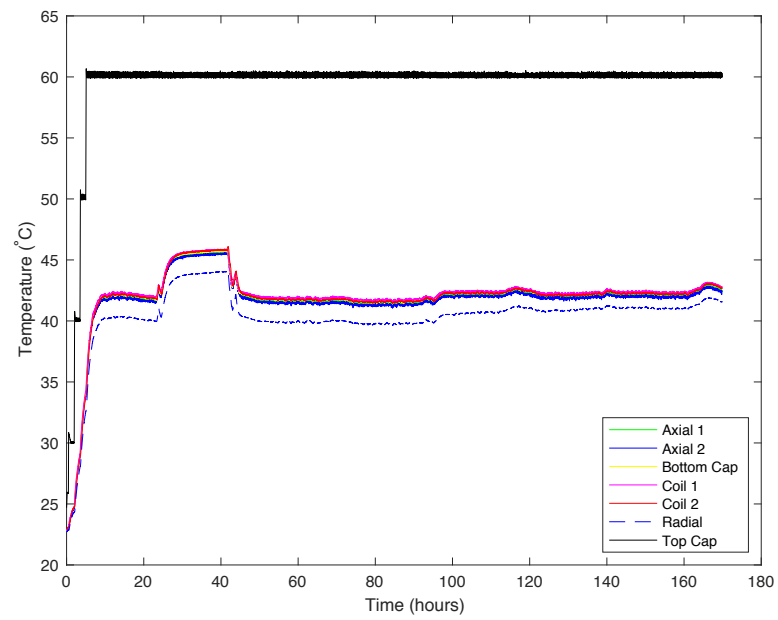


Figure A.35: Durham Clay 40 °C Temperature Profile. Test 21-DC-40

Appendix B

Lessons learnt

To aid future studies carried out on the temperature controlled triaxial developed as part of this study, this section details the problems faced and how these were overcome:

- GDS units reaching their maximum limits:

It was important to start testing with the GDS units three quarters empty. This left enough water within the unit to provide the increase in back pressure required for saturation, whilst accommodating the water expelled during consolidation and the later temperature increase. The most problematic stage of this was the heating stage as often this would bring the GDS unit to its limit. It was important to double check the volume of the GDS unit prior to the heating stage to ensure enough capacity. In the early test stages this was based on trial and error past experience, until the system was fully understood.

- LVDT peeling from the sample membrane:

During the testing of Durham clay, the LVDT's would peel from the membrane due to differential shrinkage of the membrane and the adhesive used to locate the LVDT's. This is the primary reason for the limited number of Durham clay tests. This issue was never fully overcome, as time pressures didn't allow for extensive testing. The intermediate solution was to inspect the LVDT reading post consolidation stage and heating stage to ensure the reading was still within

the LVDT range. If one of the rests had become unattached to the sample, the reading on the LVDT would be -5. If this was found on both LVDT's the test would be terminated. To improve this reliability of the LVDT adhesive, it would be recommended to consolidate the samples to a higher effective stress, so less consolidation is carried out within the triaxial system, thus less sample shrinkage. Another option would be to pin the LVDT's to the sample, through the membrane. This wasn't explored during the series of testing as this would add an additional pathway of water within the system.

- Leaks through thermocouple ports:

The thermocouples enter the cell through drilled blank connections. Following repeated heating and cooling of these connections, the adhesive sealing the thermocouples and the connection became weakened. During cell pressure increases and temperature increases, a water path would be found through the connection leading to a constant leak of cell volume. The solution to this was to visually inspect each of the connections prior to testing, and then again once the sample had been saturated and consolidated. The connections were then monitored during the heating stage. Going forward, the most ideal solution for this would be for the thermocouples to enter the cell through a compression fitting which could be maintained prior to testing.

The other area which caused an issue with leaks occurring through thermocouples was the top cap and bottom cap which had holes drilled and thermocouples sealed into. Over time, the seals were weakened with water leaking between the sample volume and cell volume. This was harder to determine as the leaks weren't outside of the cell. These leaks were determined through careful monitoring of the sample and cell volumes. A leak through the top cap occurred twice during the test period. This provided significant down time as due to the configuration the top and bottom cap, thermocouples had to be drilled out and replaced as they were through the sample blank connection. Going forward, it would be more practical to have these enter the cell through

separate blank connections, in addition to having a secondary top and bottom cap fabricated.

- Variation in temperature through testing:

Ensure the air conditioning within the laboratory is working correctly and plan laboratory testing around any maintenance. Ensure all other laboratory users are aware of the thermal testing being carried out in the laboratory and keep door opening to a minimum. Regular checking of the laboratory is recommended to ensure doors have not been left open. Where possible, access to the laboratory should be restricted to ensure temperature is maintained throughout testing. It is recommended that testing is not carried out when undergraduate laboratory sessions are running in the same period.